uOttawa

L'Université canadienne
Canada's university

FACULTÉ DES ÉTUDES SUPÉRIEURES ET POSTOCTORALES

uOttawa

L'Université canadienne
Canada's university

FACULTY OF GRADUATE AND POSDOCTORAL STUDIES

Norah Foy

AUTEUR DE LA THÈSE / AUTHOR OF THESIS

M.Sc. (Geography)

GRADE / DEGREE

Department of Geography

FACULTÉ, ÉCOLE, DÉPARTEMENT / FACULTY, SCHOOL, DEPARTMENT

Changes in Surface Elevation and Extent of the Kaskawulsh Glacier, Yukon Territory

TITRE DE LA THÈSE / TITLE OF THESIS

Luke Copland

DIRECTEUR (DIRECTRICE) DE LA THÈSE / THESIS SUPERVISOR

CO-DIRECTEUR (CO-DIRECTRICE) DE LA THÈSE / THESIS CO-SUPERVISOR

EXAMINATEURS (EXAMINATRICES) DE LA THÈSE / THESIS EXAMINERS

M. Sawada

C. Zdanowicz

Gary W. Slater

Le Doyen de la Faculté des études supérieures et postdoctorales / Dean of the Faculty of Graduate and Postdoctoral Studies

Thesis:

Changes in Surface Elevation and Extent of the Kaskawulsh Glacier, Yukon Territory

By: Norah Foy
Student # 3270427
Department of Geography
University of Ottawa

Submitted to: Dr. Luke Copland (Supervisor)
Dr. Mike Sawada
Dr. Christian Zdanowicz

August 31, 2009

Your file Votre référence
ISBN: 978-0-494-61315-3
Our file Notre référence
ISBN: 978-0-494-61315-3

Abstract

Between 1977 and 2007, the Kaskawulsh Glacier underwent an overall decrease in volume of between 2.76 km^3 water equivalent (we) and 4.60 km^3 we, and a decrease in area of 2.27%. Volume losses are consistent with changes observed at most glaciers in the Yukon/Alaska region which are thinning and/or retreating (Arendt et al. 2006; Chen et al. 2006a; Larsen et al. 2007; Molnia 2007). The rate of volume change over the periods 1977-1995 and 1995-2007 remained constant at -0.52 $km^3\ yr^{-1}$ we, while between 2000 and 2007 the glacier gained volume at a rate of 1.04 $km^3\ yr^{-1}$ we. Gains in the recent 2000-2007 period result from prominent thickening in the accumulation area above 1989 m (+16.9 m) and minor thickening in the ablation area (+0.5 m). The observed thickening pattern is similar to patterns observed in Greenland (Chen et al. 2006b; Johannessen et al. 2005; Luthcke et al. 2008b), Antarctica (Davis et al. 2005), the Karakoram Himalaya (Hewitt 2005), New Zealand (Chinn 1999; Hooker and Fitzharris 1999), Scandinavia (Bamber et al. 2004; Chinn et al. 2005, Nesje et al. 2000), and Alaska (Arendt et al. 2008; Muskett et al. 2003). Between 1956 and 2007, the glacier terminus retreated by an average of 655 m (13 m yr^{-1}). No scaling ratio between terminus retreat and volume change could be established for the Kaskawulsh Glacier for the period 1977-2007.

Acknowledgements

We wish to thank the Canadian Foundation for Innovation (CFI), the Ontario Research Fund (ORF), the Natural Science and Engineering Research Council of Canada (NSERC), the Northern Scientific Training Program (NSTP), and Parks Canada for financial support of this project. We would also like to thank the Arctic Institute of North America, Carmen Wong and Sierra Pope for contributions to fieldwork. Special thanks to Keith Echelmeyer, Anthony Arendt, and the University of Alaska Fairbanks, Chris Hopkinson and Mike Demuth (C-CLEAR consortium), and Christian Zdanowicz and the Geological Survey of Canada for supplying data.

Furthermore I would like to thank my supervisor, Luke Copland, for his academic guidance as well as for giving me the opportunity to travel. I would also like to thank Mike Sawada and Christian Zdanowicz for their helpful input throughout my studies, and Jim McGrath for continually fixing my computer. Members of the Laboratory for Cryospheric Research were also very supportive throughout the completion of this thesis, and for this I would like to thank Émilie Herdes, Colleen Mortimer, Amaris Page, Sierra Pope, Tyler Sylvestre and Wesley Van Wychen. I would also like to thank my good friends Michelle Cook, Josh Drummond, and Geneviève Piché.

Finally, I would like to thank my parents, Christine and James, for their continued support and encouragement over the course of my studies. I am also appreciative of the support I received from my sisters, Brigid, Fran and Kate.

Table of Contents

List of Figures

List of Tables

Chapter 1

1.0 Introduction

Mountain glaciers constitute about 3% of the glacierized surface on earth, but their small size makes them particularly vulnerable to climate change. Global sea level rose at an average rate of 1.8 +/- 0.5 mm yr^{-1} between 1961 and 2003, which increased to 3.1 +/- 0.7 mm yr^{-1} between 1993 and 2003 (IPCC 2007). After thermal expansion of the oceans, the loss of mass from mountain glaciers was the single most important component of this rise (0.77 mm yr^{-1} for 1993-2003), accounting for approximately double the sea level rise contribution from Greenland and Antarctica combined (0.42 mm yr^{-1} for 1993-2003). Over approximately the same period (1966-2003), land-surface air temperature north of 60°N rose by an average of 0.40°C $decade^{-1}$ (ACIA 2004). Models predict warming north of 60°N to continue into the future, with average annual temperatures reaching 4.9°C warmer than current by 2099 (IPCC 2007). Therefore, under the rapidly changing Arctic climate, melt from mountain glaciers is expected to have an increasingly large impact on sea level rise (Arendt et al. 2002).

Glaciers in the southwest Yukon and Alaska represent ~14% of Earth's glaciated area outside of Greenland and Antarctica (ACIA 2004), and like most mountain glaciers, they are thinning and retreating. Arendt et al. (2002) measured the average rate of thinning of glaciers in this area between the mid-1950s and mid-1990s to be ~0.52 m yr^{-1} (Arendt et al. 2002). Between the mid-1990s and 2001, the average rate of thinning had increased to ~1.8 m yr^{-1}. This change amounts to 96 km^3 (+/- 35 km^3) of water loss per year. This contribution raises sea level by 0.27 mm yr^{-1} (+/- 0.10 mm) or ~9% of the total observed rate in sea-level rise over the past 50 years (Arendt et al. 2002). These numbers are closely corroborated by a study conducted by Chen et al. (2006a), who studied mass changes in the Gulf of Alaska region using data from the GRACE (Gravity Recovery and Climate Experiment) satellite. Findings from this project reveal that glaciers in the region lost mass at an average rate of 101 km^3 yr^{-1} (+/- 22 km^3) between 2002 and 2005. Using mascon (mass concentration) corrections for GRACE, Luthcke et al. (2008) determined that glaciers in the Gulf of Alaska decreased by 84 km^3 yr^{-1} (+/-5 km^3 yr^{-1}) between 2003 and 2006. Arendt et al. (2008) narrowed GRACE mascon calculations to the St. Elias Mountains and by combining this data with laser altimetry measurements, losses were between 20.6 km^3 yr^{-1}

(+/- 3.0 km^3 yr^{-1}) and 21.1 km^3 yr^{-1} (+/- 3.8 km^3 yr^{-1}), a rate that had been approximately steady for several decades.

However, more recent work in the Western Chugach Mountains of Alaska suggests that these numbers are underestimated by a factor of two due to the omission during sampling of many rapidly retreating tidewater and lake calving glaciers (Arendt et al. 2006; Larsen et al. 2007). Given these recent sources of evidence, it is likely that the ice losses in this area are even greater than previously estimated, and that the meltwater contribution from this region is approximately twice as great as contributions by Greenland (ACIA 2004), making Alaskan/Yukon glaciers the world's largest contributors to eustatic sea level rise (IPCC 2007). Studies in Icy Bay, Alaska, show that much of this mass loss can be attributed to tidewater dynamics as well as climate warming (Muskett et al. 2008). These changes can be expected to accelerate as climate warming continues; many small glaciers are likely to disappear over the course of the 21st century (Meier et al. 2007). There is therefore a need for improved understanding of how climate change is affecting high altitude environments in the SW Yukon, particularly as most existing studies focus on the Alaskan side of the St. Elias Mountains. This study aims to address this need through calculations of changes in the elevation and areal extent of the Kaskawulsh Glacier located in the St. Elias Mountains, Yukon.

1.1 The St. Elias Mountains

The St. Elias Mountains are located in SW Yukon and extend into Alaska (Figure 1.1). The mean altitude in the Chugach/St Elias Ranges is ~1225 m, with 90% of the land area between 300 and 2200 m asl. Surface elevations above 3200 m occupy only ~2% of the land area. The St. Elias Range has a central plateau, bordered by steep slopes leading to increasingly high elevations. Slopes at low altitudes are generally low (<10°), while at higher altitudes (between 800 and 2800 m) the average slope angle is 20-30° (Meigs and Sauber 2000). Contained within this mountain range is Mt. Logan, the highest point in Canada, extending to 5959 m asl.

The cold climate and high altitudes in the St. Elias Mountains have allowed the development of extensive glacial cover. Areal coverage of glaciers in Alaska and SW Yukon amounts to approximately 90,000 km^2 (Arendt et al. 2002; Meier and Dyurgerov 2002). The

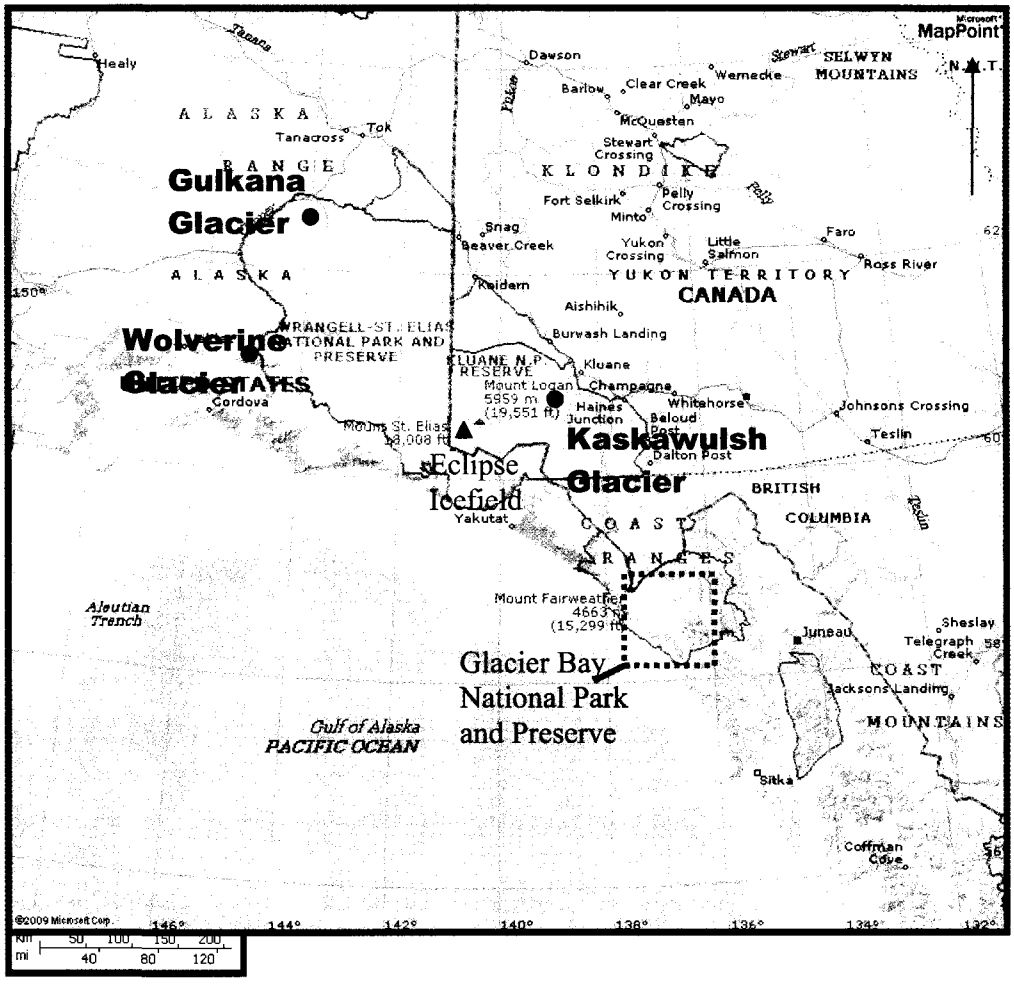

Figure 1.1: Map of the St. Elias Mountains, Yukon Territory
Source: MSN encarta, World Atlas,
http://encarta.msn.com/map_701583647/St_Elias_Mountains.html,
accessed Sept. 2, 2009

St. Elias Mountains contain the largest glaciers in the Canadian Cordillera (Reyes et al. 2006), and the Icefield represents the world's largest ice mass outside of the polar regions (Danby et al. 2003). The St. Elias Icefield is comprised of coalesced valley glaciers and piedmont lobes. Flow in the Icefield complex is influenced mainly by topography (Ward et al. 2007).

Tectonic rock uplift continues in the St. Elias Mountains (Sauber and Molnia 2004). A conservative estimate of average erosion rates in the St. Elias Mountains over the past 10,000 years is between ~5 and 8 mm yr^{-1} (Berger et al. 2008; Sheaf et al. 2003), however local erosion rates could be almost 100 mm yr^{-1} (Sheaf et al. 2003). Other estimates suggest that Alaskan Glaciers are responsible for the highest observed denudation rates in the world, and that short-term rates are in excess of 100 mm yr^{-1} (Spotila et al. 2004). These rates have increased in recent history, and the increase can be related to greater ice flux and a more variable equilibrium line altitude (ELA) (Sheaf et al. 2003; Spotila et al. 2004).

1.2 The Kaskawulsh Glacier

The Kaskawulsh Glacier is a large valley glacier located within Kluane National Park in the St. Elias Mountains (60°43'N, 138°51'W; Figure 1.2). Its thermal classification is temperate, which means that the ice is believed to be at the pressure melting point throughout (Macpherson and Krouse 1969). This glacier flows generally northeast and is about 70 km in length. The extensive Kluane Icefields, located to the west of the glacier, supply ice to the north and central arms of the Kaskawulsh. The south arm of the glacier is supplied by a catchment basin located to the southeast of the glacier (Macpherson and Krouse 1969). The terminus is currently at an elevation of ~830 m asl (Reyes et al. 2006).

Beginning in 1961, the Arctic Institute of North America and the American Geographical Society sponsored the Icefield Ranges Research Project (IRRP). The goal of this project was to increase understanding of the natural environment of the St. Elias Mountains. The study was multidisciplinary and geographical and addressed topics such as climate, snow and ice facies, crevasse formation, surface velocity patterns, supraglacial and proglacial drainage, historical glacier fluctuations, and biota in the region. Many studies from this project dealt specifically with the Kaskawulsh Glacier. This study was discontinued after publication of two volumes of papers in 1969, and little work has been

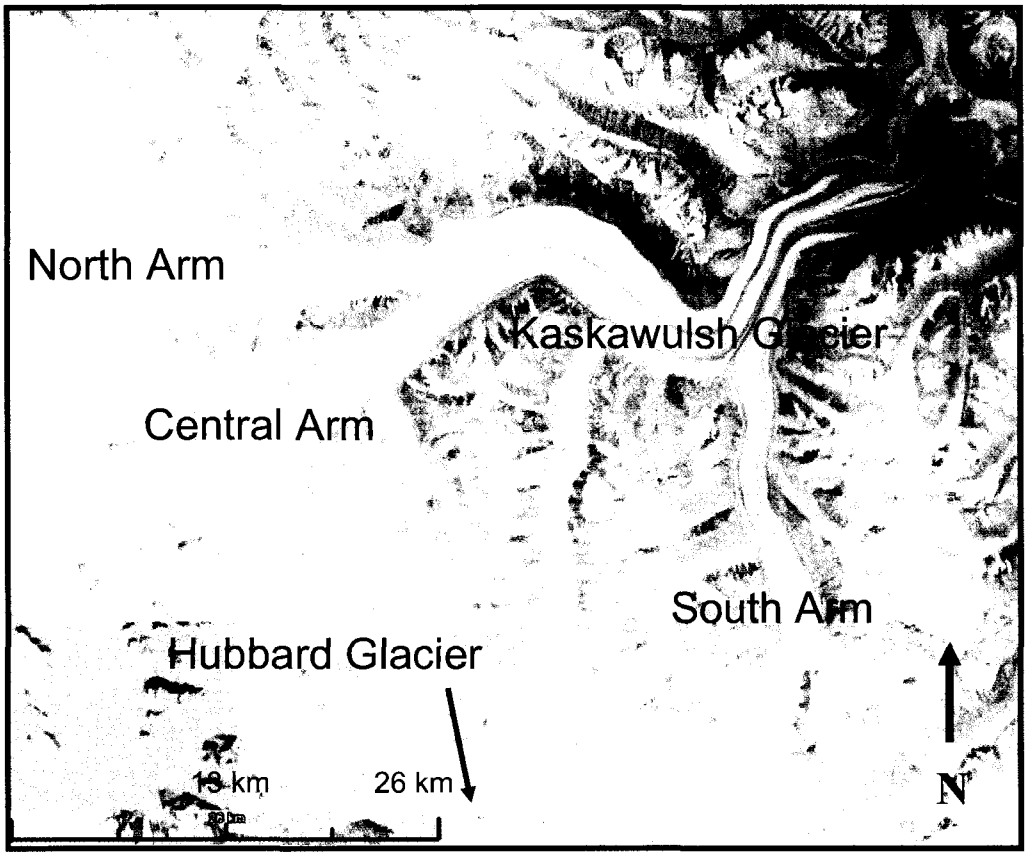

Figure 1.2: Kaskawulsh Glacier
Source: Google Earth; image acquisition 2002-2006

done since then concerning characteristics and change of the Kaskawulsh Glacier. Thus IRRP papers are an integral resource for understanding the context of change in the Kaskawulsh Glacier.

During the course of the IRRP (1961-1969) the firn line, which approximates the ELA, was estimated to lie between 1950 m and 2000 m asl (Denton and Stuiver 1969; Macpherson and Krouse 1969; Wagner 1969). In 1963, the Kaskawulsh Glacier was determined to be 778 m thick at ~1600 m elevation using seismic refraction methods (Figure 1.3; Clarke 1969). At the confluence of the north and central arms of the glacier (~1750 m elevation) the ice is known to be ~500 m thick (Dewart 1969a). This is the approximate thickness of the central arm above the convergence, while the north arm is thought to be thinner (Dewart 1969b). In the accumulation zone at the topographic divide between the Kaskawulsh and Hubbard Glaciers (at ~2500 m elevation), the depth of ice was determined to be 539 m (Clarke 1969). Nearby, at an elevation of 2608 m, GPR traces from July 2006 in this area place the glacier thickness at ~350 m (Copland 2009, personal communication). Maximum thicknesses of ice in the upper reaches of the Kaskawulsh Glacier are in excess of 820 m (Havens and Saarela 1969).

The central arm of the Kaskawulsh Glacier can be divided into three snow facies (Wagner 1969); the ablation facies extends from the terminus at 830 m to ~1990 m (the 1963 budget year firn line) (Figure 1.3). Between 1990 m and 2330 m, the wetted facies exists. The saturation line for snow exists somewhere between 2220 m and 2430 m. Above 2420 m is the percolation facies, while no dry snow facies occurs on the Kaskawulsh Glacier. The Kaskawulsh is well-drained during the melt season, with countless supraglacial streams visible at the surface, moulins extending to depths as great as 65 m (Dewart 1969b), and over 30 glacier dammed lakes (Johnson 1986). The supraglacial drainage networks display high annual variability (Dewart 1969a). Crevasses supply water to englacial channels, but are confined to the near-surface. Water-spouts have also been observed on the glacier (Ewing et al. 1969).

The Kaskawulsh Glacier has two main water outlets; the Slims River to the north and the Kaskawulsh River to the southeast (Figure 1.4). The Slims River is the primary outlet, and it drains to Kluane Lake. The lake drains to the Yukon River system, and eventually supplies water to the Bering Sea (Bostock 1969; Reyes et al. 2006). The greatest meltwater

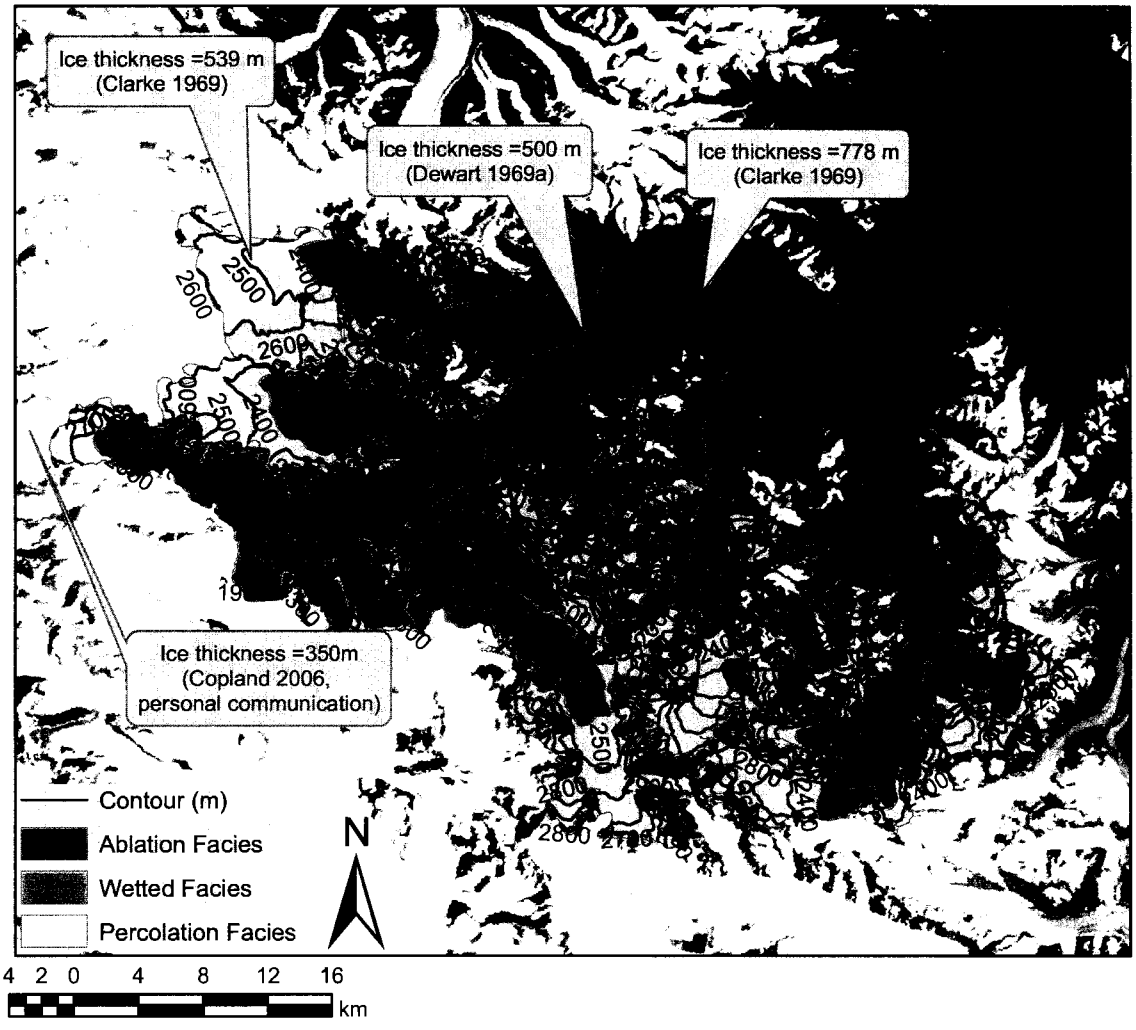

Figure 1.3: Snow facies and ice thicknesses of the Kaskawulsh Glacier. Although snow facies observations were only made for the central arm of the glacier, this figure indicates where these facies would be expected on all arms of the glacier, given constant elevation gradients. The image is displayed over the 1977 Landsat image, and includes contours from the 1977 DEM

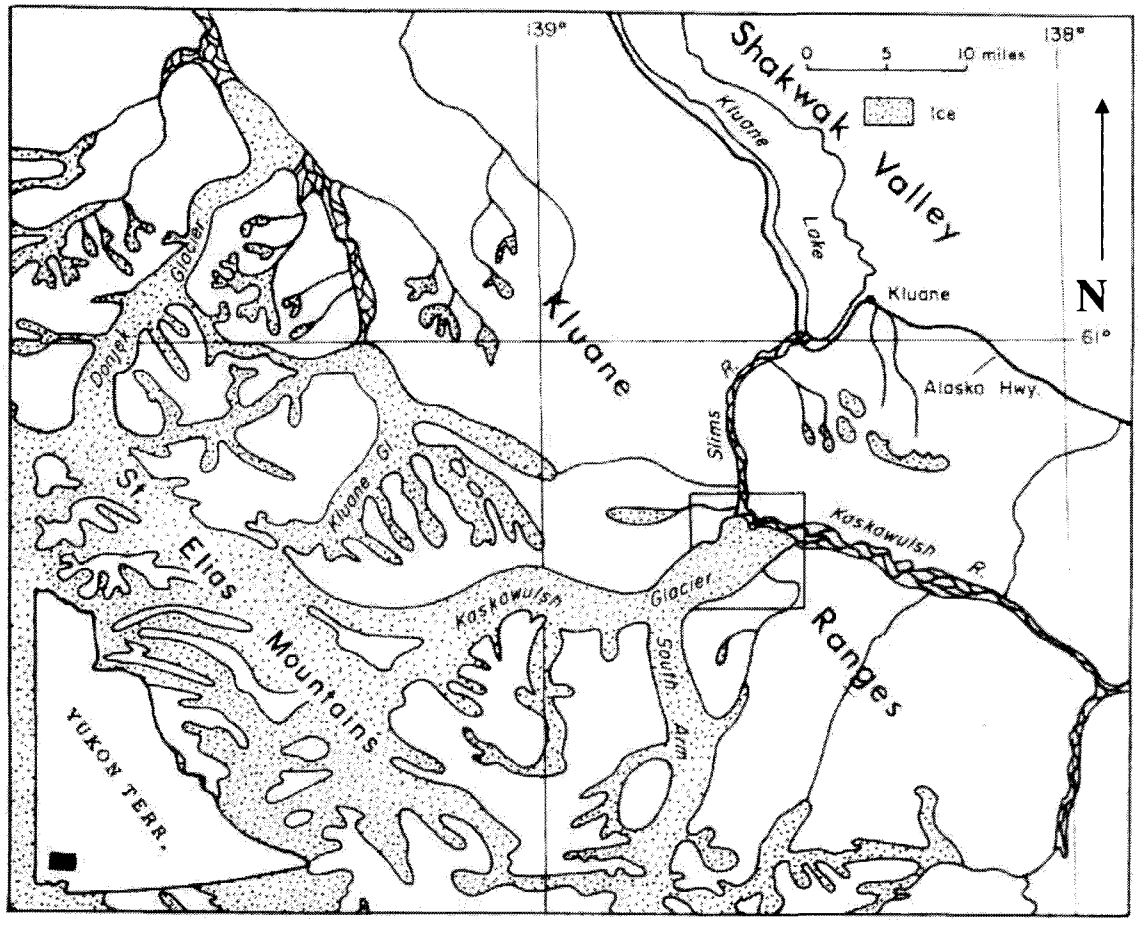

Figure 1.4: Index map of the drainage system of the Kaskawulsh Glacier
Source: Borns and Goldthwait (1966)

contribution to the Slims River comes from two subglacial streams, with the water issuing from sub- or englacial channels under hydrostatic pressure (Borns and Goldthwait 1966). The secondary meltwater flow path is through the Kaskawulsh River system which flows southeast, contributing to the Alsek River and finally the Gulf of Alaska (Bostock 1969; Bryan 1972). This drainage system has not been constant through time (Bostock 1969; Bryan 1972; Clague et al. 2006; Johnson 1985; Reyes et al. 2006), as discussed in more detail below.

1.3 History of the Kaskawulsh Glacier

The extent of the Kaskawulsh Glacier has fluctuated greatly over time. Expansion into the Shakwak Valley (Figure 1.4) occurred almost 30,000 years ago during the Wisconsin Glaciation. Evidence of this expansion was discovered through carbon dating of the Shakwak Drift; the lowest drift sheet to be found in the northeastern St. Elias Mountains (Denton and Stuiver 1969). By 12,500 years ago, the glacier had receded ~48 km, leaving alluvial fans in the Slims River and till along the valley walls (Borns and Goldthwait 1966). As the climate warmed and became drier, vegetation and species composition in the southwest Yukon changed (Borns and Goldthwait 1966). About 2700-1500 years ago there was a readvance of the Kaskawulsh Glacier caused by a shift towards cooler, moister climatic conditions. Moraines from this advance are found up to ~1.6 km from the current terminal position in the direction of the Slims River, or 0.8 km from the glacier edge in the direction of the Kaskawulsh River (Borns and Goldthwait 1966). Other similar advances occurred in ~300 AD and 1200 AD (Borns and Goldthwait 1966; Wiles et al. 2002). These advances are known to have occurred in the nearby Wrangell Mountains, and are therefore inferred to have occurred in the Kaskawulsh Glacier as well (Borns and Goldthwait 1966). The extent of advance of the Kaskawulsh Glacier during these periods is, however, unknown.

The most recent advance of the Kaskawulsh Glacier corresponds with the Little Ice Age and began in the early 1600s. Tree ring dating indicates that it reached its maximum extent between 1670 and 1750 (Borns and Goldthwait 1966; Reyes et al. 2006; Wiles et al. 2002), ~1.6 km ahead of its current terminal position of 60°50'21"N, 138°35'55."W.

During the Pleistocene advance of the Kaskawulsh Glacier, the current drainage system started to establish; while the Kluane Lake basin was still filled with ice, a proglacial stream initiated the formation of the Kluane River. As the ice within what would become Kluane Lake began to melt, water drained through the Slims and Kaskawulsh Rivers via an outlet developed in the valley fork. This drainage pattern persisted until the Neoglacial when the Kaskawulsh Glacier again advanced (Bostock 1969). Advances of the glacier were accompanied by increased sediment delivery to the Slims-Kaskawulsh valley. A low-angle fan began to aggrade and impeded the flow of a southward draining river at the outlet of Kluane Lake (Bostock 1969; Clague et al. 2006; Reyes et al. 2006). This caused a progressive rise in the lake level; by the late 17th century, the lake was ~12 m above its present level. Eventually this caused an overflow which caused a moraine dam at the north end of Kluane Lake to be breached, allowing the water to drain into the White and Yukon River Systems (Bryan 1972; Clague et al. 2006; Johnson 1985). This allowed the lake level to drop to its current level (Clague et al. 2006).

The Kaskawulsh Glacier continues to be an important control on the level of Kluane Lake. Between July and early August, meltwater discharge reaches its annual maximum and causes a 1-2 m increase in lake level compared to its winter level (Brahney et al. 2008a; Brahney et al. 2008b; Bryan 1972). The lake level reaches its winter level in autumn prior to the lake's freeze-up. Additionally the Slims River is the primary source of sediment in southern Kluane Lake (Brahney et al. 2008a; Bryan 1972). Periodically the point of main glacier drainage switches from the Slims to the Kaskawulsh River due to internal glaciological conditions (this occurred in 1957 and 1971). When this occurs the level of Kluane Lake does not increase during the summer months, which in turn reduces outflow from Kluane Lake (Johnson 1986).

The Kaskawulsh Glacier began its current retreat in 1836 (Borns and Goldthwait 1966; Reyes et al. 2006; Wiles et al. 2002). In general, ice in this region has been retreating over the 20th century, with increased wastage since 1980 that is consistent with regional warming. According to the study by Arendt et al. (2002), the Kaskawulsh Glacier thinned by an average of ~1.5 m yr^{-1} between 1950 and 1995. Between 1995 and 2001, there is evidence that the rate of thinning decreased to ~0.5 m yr^{-1} (Arendt et al. 2002). This thinning is approximately equal to the current global rate of thinning for all glaciers and ice caps

(excluding Greenland and Antarctica) of 0.55 m yr^{-1} for the period ~1996-2006 (Meier et al. 2007). The present study updates these figures by extending analysis of the Kaskawulsh Glacier to 2007 and adding another interval of observation in 1977. In addition, data with increased spatial coverage of the glacier is used in order to more accurately quantify thinning.

1.4 Climate and Climate Change

The average temperature for the study area, as measured at the Burwash Landing meteorological station (61°22'11"N 139°03'00"W, 806 m asl) between 1971 and 2000, is -3.8°C. This station is located ~228 km northwest of Whitehorse, and ~63 km northwest of the base of the Kaskawulsh Glacier. The average annual precipitation is 321 mm (Environment Canada 2009a). These measurements cannot, however, be generalized and applied throughout the mountain range.

Spatial climatological variability throughout the mountains arises from complex topography, elevation, radiative properties of the surface, distance from the ocean as well as the variable incursion of air masses (Anderson et al. 2005; Taylor-Barge 1969). For the eastern slope of the St. Elias Mountains, the mean environmental lapse rate is 0.72°C per 100 m (Havens and Saarela 1969). Because of the large altitudinal variation throughout the St. Elias Mountains, different portions of the mountains may be affected by different air masses, despite geographical proximity. For instance, Eclipse Icefield and Mount Logan are separated by only ~51 km, yet these sites are under the influence of different air masses due to the 2 km vertical separation between them (Yalcin and Wake 2001; Yalcin et al. 2007).

The position and intensity of the Aleutian Low is the main determinant for moisture received in the St. Elias Mountains because it controls the trajectory of air masses. The Gulf of Alaska is the primary source of precipitation received in the Yukon, although air masses originating from the Arctic and Bering Sea can also transport moisture into this region (Figure 1.5) (Anderson et al. 2005; Benjey 1969). When the Aleutian Low is located in a relatively eastern position it is intensified (Figure 1.6a) and strong southerly winds transport moisture toward mountain ranges along the Alaskan coast, causing intense precipitation in coastal regions. In general, the orographic obstacle presented by the St. Elias Mountains (and the nearby Wrangell Mountains) intercepts westerly airflow from the North Pacific

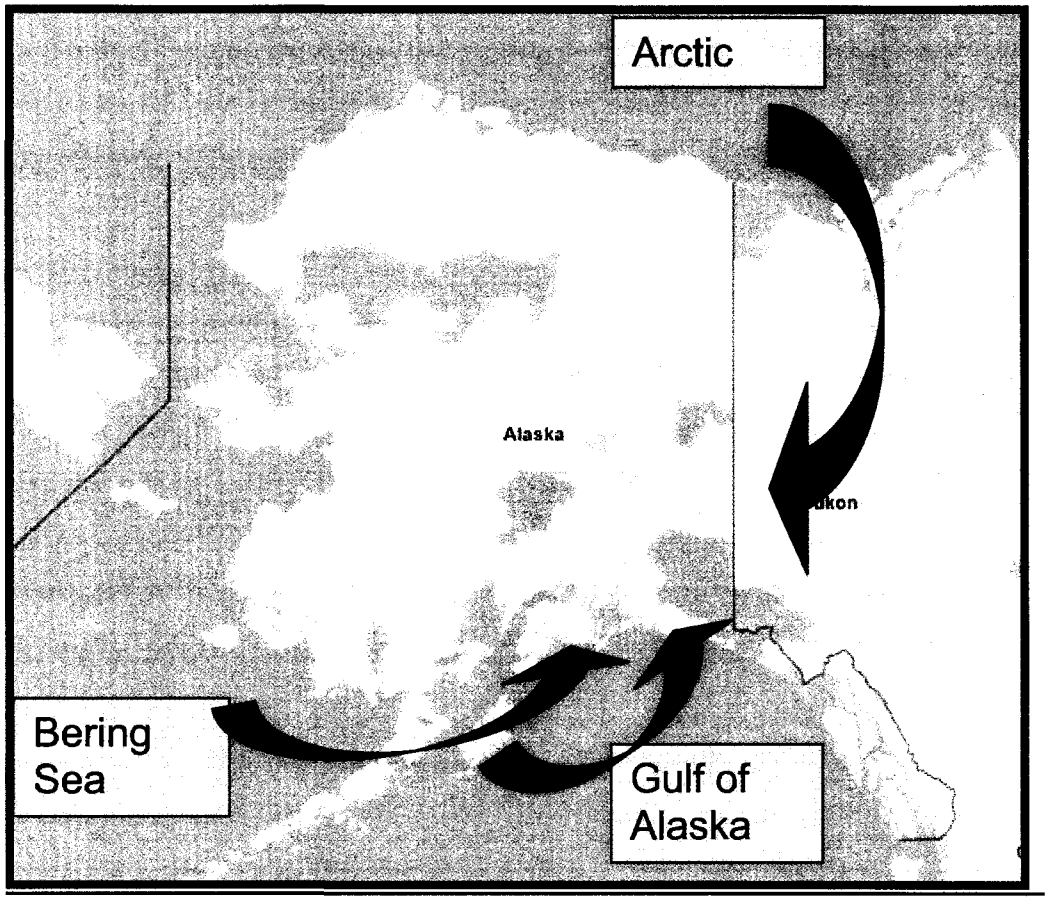

Figure 1.5: Provenance of air masses for the SW Yukon
Source: Google Maps, http://maps.google.com/, accessed Sept. 2, 2009

a

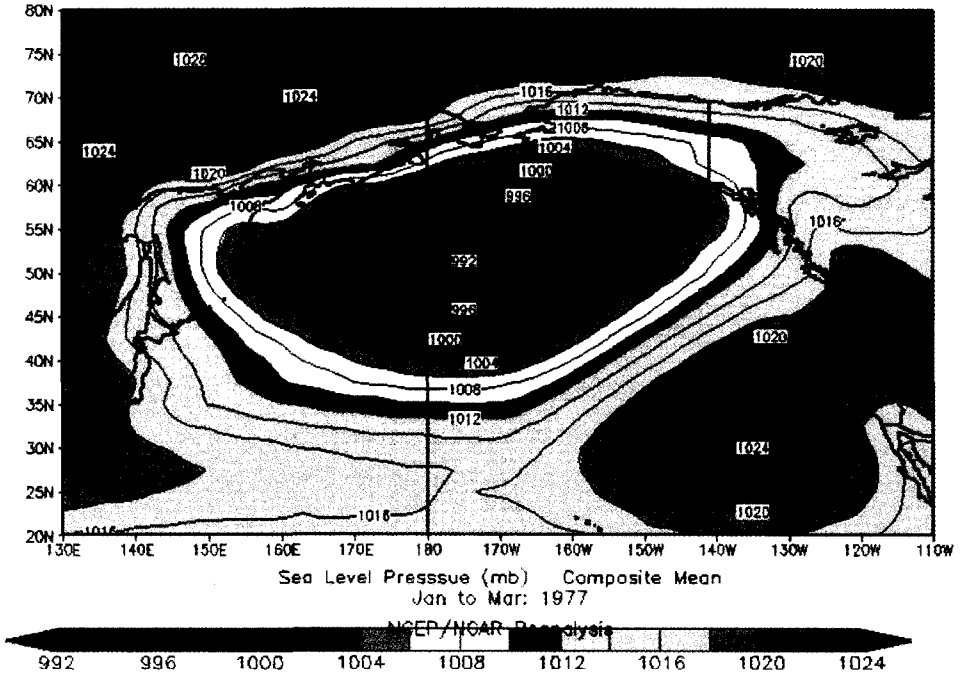

b

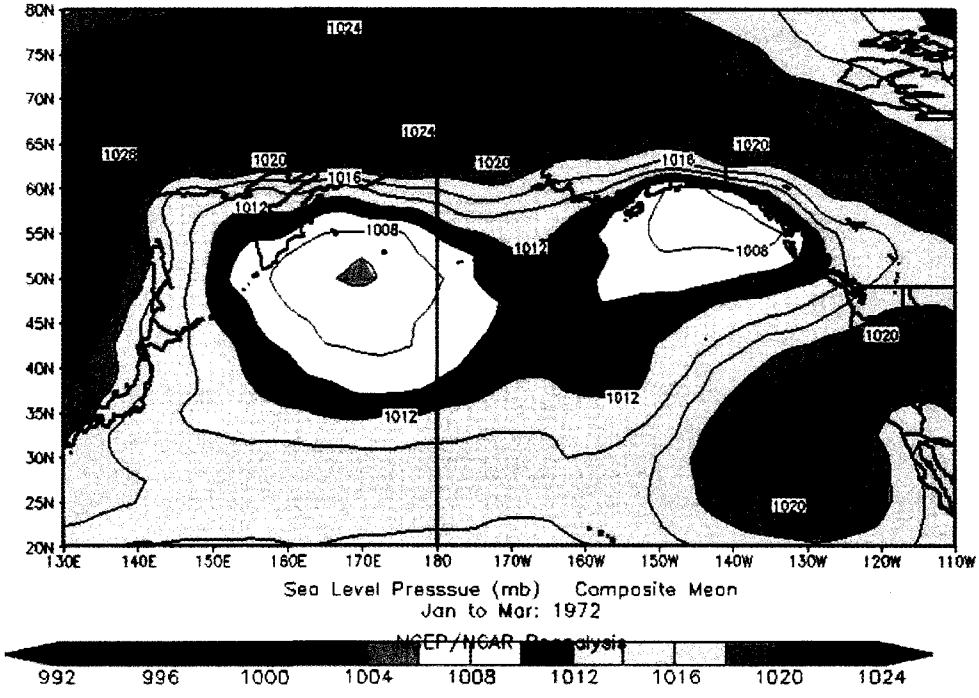

Figure 1.6: Position of the Aleutian Low detected using average pressure patterns over a 3 month period

a: Strong, eastern position (January 1977- March 1977)

b: Weak , westward position (January 1972- March 1972)

Source: Tim Lopes, The Aleutian Low: Trends and Cycles, http://apollo.lsc.vsc.edu/classes/met430/lopest/pres3/aleutian.htm, accessed Sept. 2, 2009

rendering the Yukon interior a semi-arid environment. Thus hydrological regimes in the area are dominated by snowmelt and ablation from the glaciers (Anderson et al. 2005; Johnson, 1986). The Aleutian Low is much weaker when located in a relatively westward position (Figure 1.6b), with more moisture originating from the Bering Sea under such conditions. This flow occurs more or less parallel to the coastal mountain barriers, and moisture is able to reach more interior regions of the Yukon and Alaska (Anderson et al. 2005; Marcus and Ragle 1970). During the early to middle Holocene, the Aleutian Low was weaker and situated in a more westward position. The current climate in the St. Elias Mountains is therefore drier than observed through much of the Holocene (Anderson et al. 2005).

ENSO (El Niño Southern Oscillation), the PNA pattern (Pacific North America) and the PDO (Pacific Decadal Oscillation) are thought to have important effects on snow accumulation in the St. Elias Mountains (Moore et al. 2001). ENSO increases moisture in the Mount Logan region. The PNA pattern involves monthly fluctuation in circulation patterns and has two phases: the positive phase involves an eastward shift of the East Asian jet stream, while the negative phase redirects the jet stream towards eastern Asia. The positive phase is associated with warmer temperatures over western Canada, and tends to coincide with El Niño conditions. Finally, the PDO describes an abrupt shift in surface temperatures in the Pacific Ocean that occurs every 20 to 30 years. The PDO has a warm phase during which surface temperatures are high in the eastern tropical Pacific and low in the northern and western parts of the Pacific Ocean. During the cold phase of the PDO, surface patterns are the opposite. When the PDO is in a warm phase, the effects of ENSO are intensified (Aguado and Burt 2004).

Based on ice core records from an elevation of 5340 m asl on Mt. Logan, snow accumulation in the North Pacific region has increased in general since 1736 (despite interannual variability), coincident with a long-term intensification of the PNA (Moore et al. 2002; Figure 1.7). Between 1736 and 1851, the observed increase of 0.003 m water equivalent (we) decade^{-1} is not statistically significant. However increases in snow accumulation of 0.008 m we decade^{-1} since 1851 are statistically significant at a 95% confidence level. Beginning in the middle of the 20th century the PDO intensified and there is evidence for a recent acceleration in the rate of snow accumulation. Between 1976 and 2000 increases in accumulation of 0.12 m we decade^{-1} were measured and determined as

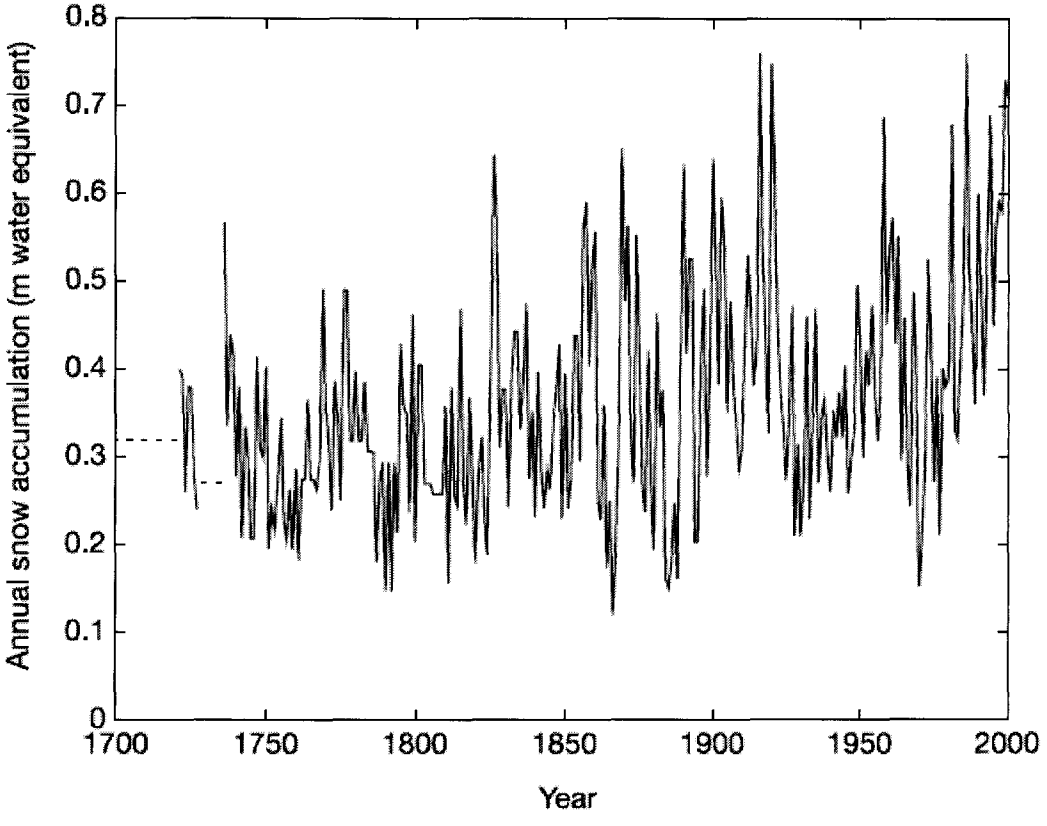

Figure 1.7: Annual snow accumulation (m water equivalent) at Mount Logan, 5340 m asl (1700-2000)
Source: Moore et al. (2002)

statistically significant to a 99% confidence level (Moore et al. 2002). These oceanic climatic controls are being reflected in ice cores and signify that the higher altitudes of the St. Elias Icefields are influenced by these systems through increased precipitation (Moore et al. 2001).

In comparison, an ice core taken from Eclipse Icefield (situated 3017 m asl, more than 2 km lower than the Mt. Logan ice core and situated 45 km to the northeast; Figure 1.1), demonstrates significantly different precipitation sources than the Mt. Logan ice core (Wake et al. 2002, Yalcin and Wake 2001). There is also little correlation between the precipitation data from low-altitude instrumental precipitation data and the record from the Eclipse ice core (Wake et al. 2002). Thus precipitation distribution is variable and highly dependent on altitude throughout the St. Elias Mountains, and it is still unclear as to how changes in these systems are impacting snow accumulation in the Kaskawulsh Glacier catchment. Furthermore, there is also no clear indication of how climate change will affect El Niño (IPCC 2007).

During the summers of 1963-1965, Taylor-Barge (1969) monitored climate on the Kaskawulsh Glacier using a series of meteorological stations. Along the central arm of the glacier, climate regimes were continental (with low temperatures, stable conditions, and clear skies or some cumulus clouds). The average summer temperature near the equilibrium line (~1750 m) was ~4°C, and on any given day there was a 50% chance of precipitation. Katabatic winds (average speed of 5.14 m s^{-1}) are present approximately 70% of the time (Benjey 1969). These are thermally induced through nocturnal radiative cooling or by daytime conduction of heat away from the air to the ice surface. These winds can occur at any time of day and are funneled downglacier between the mountains bordering the north and central glacier arms. Warm up-glacier winds are less frequent and tend to bring more precipitation, but less cloud, than downglacier winds. A climatological divide exists in a zone between the central arm of the Kaskawulsh Glacier, and the topographic divide between the Kaskawulsh and Hubbard Glaciers (Figure 1.2). In the accumulation zone at ~2650 m, the average summer temperature was between -4°C and -1°C and varied ~8°C diurnally. The average wind speed was 2.52 m s^{-1} originating dominantly from the west. The probability of precipitation of a given day was 65%, and snow was the only form of precipitation observed.

The position of the St. Elias Mountains provides a barrier to westerly air flow in the subpolar low pressure belt. This orographic obstacle is thus of primary importance in terms of climatic influences (Benjey 1969). However, orographic effects on the distribution of precipitation on the Kaskawulsh Glacier are of limited importance. Between 1000 m and 2500 m, a precipitation gradient of 0.65 m km^{-1} (in units of mean annual precipitation) exists, however above 2500 m elevation orographic effects do not exert an important control on precipitation amounts (Macpherson and Krouse 1969; Keeler 1969). Other important controls on received precipitation include redistribution by wind, and frontal processes. The Kaskawulsh Glacier lies to the southeast of Mount Logan which acts as a barrier to storms tracking through the region from the Gulf of Alaska; the large mountain causes orographic uplift of the storms which results in a large amount of local precipitation in the upper reaches of the Kaskawulsh Glacier system (Alford and Keeler 1969). At the divide between the Kaskawulsh and Hubbard Glaciers (which serves as a common accumulation area for the two glaciers) there is an annual net accumulation on the order of 3-4 m yr^{-1} (Grew and Mellor 1969; Havens and Saarela 1969; Wagner 1969; Zdanowicz 2009, personal communication). Little net change in snowpack volume occurs in the accumulation area over the summer, although surface lowering does occur as low density snow from the surface melts and refreezes as high density firn at depth (Wagner 1969).

Recently, temperatures in SW Yukon have been increasing. Between 1976 and 2005, a climatic shift occurred in the North Pacific region known to be coincident with a shift in the PDO. Compared to 1950-1975, there was an increase in average annual surface air temperature of 1.1°C in SE Alaska, with a 1.7°C increase during the winter months, a 1.4°C increase during the spring months, a 0.7°C increase during the summer months, and a 0.4°C increase during the fall months (Hartmann and Wendler 2005). Furthermore, between 1948 and 2008, the Yukon displayed a warming of 2.0°C (Environment Canada 2009b). Warming is predicted to continue, with Figure 1.8 showing the projections for North America by 2099 (IPCC 2007). This figure shows that the mean annual temperature in the SW Yukon is expected to increase by ~3 to 3.5°C. As a consequence of the temperature increase and a projected intensification of the Aleutian Low (IPCC 2007), there is expected to be an increase in precipitation; increases may be as high as 20% in the study area with up to a 30% increase in the winter (IPCC 2007).

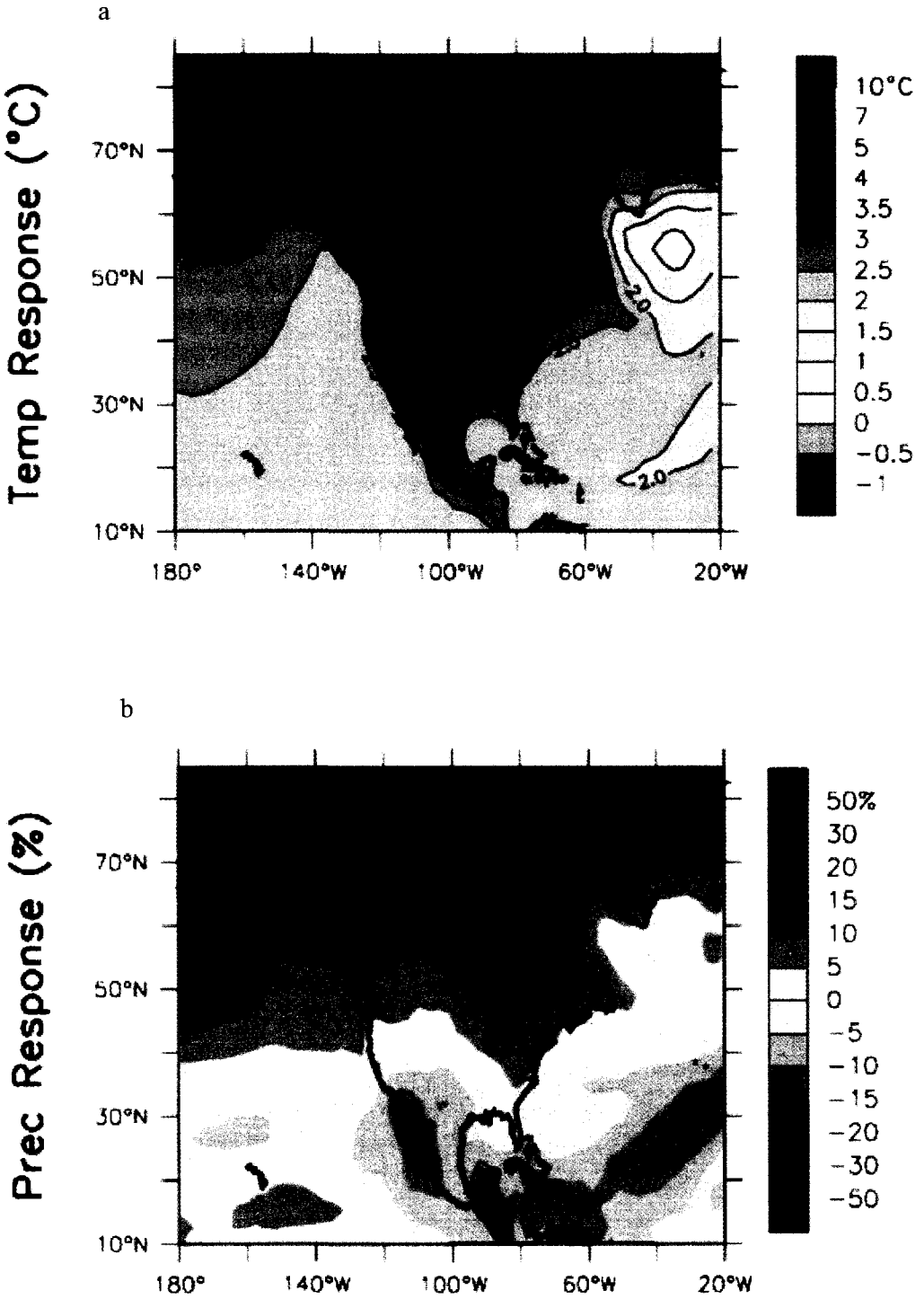

Figure 1.8: Predicted temperature and precipitation changes over North America from the MMD-A1B simulations. a: Annual mean temperature change between 1980 and 1999 to 2099, averaged over 21 models.
b: Same, but for fractional change in precipitation. Source: IPCC (2007).

The St. Elias Mountains are unlikely to respond to climate change in the same manner as nearby low-altitude environments. The largest warming is likely to occur over elevated areas as a result of the snow-albedo feedback (IPCC 2007). Furthermore, climate models have resolutions that are too coarse to adequately model high altitude terrain. Therefore, monitoring of the Kaskawulsh Glacier provides an opportunity to gain insight into how these ongoing changes are affecting high altitude environments in this region.

1.5 Changes in Glaciers of the St. Elias Mountains

Recent climate changes in the SW Yukon have resulted in enhanced melt in the St. Elias Mountains. The GRACE satellite infers changes in mass on the earth's surface from changes in gravity. The output data is a spatial average of the surface-mass anomaly (Swenson and Wahr 2002). Trends can be observed for continental sites with an optimal averaging radius of 500 km or smaller (King et al. 2006). Here a 250 km averaging radius is used. Satellite measurement errors include noise error in the intersatellite range, accelerometer error, error in the oscillator, and error in the orbits, while other errors include truncation during smoothing/averaging of data, and leakage of mass data from outside the basin under consideration. Nonetheless, measured changes are accurate to better than 1 cm water equivalent (Swenson and Wahr 2002).

Satellite data from the GRACE program show the broad downward trend in mass balance for the mountain range (Figure 1.9a). Figure 1.9b shows the seasonal changes in mass measured over the St. Elias Mountains since 2003, expressed in units of mm of water. Seasonal patterns of snow accumulation and snow melt are clearly evident, and are superimposed on a prominent downward trend in mass which is statistically significant at a confidence interval of >99%. GRACE data indicates an average water equivalent mass loss of ~64 mm yr^{-1} in the study region, which translates into a vertical loss of ~71 mm yr^{-1} of ice. However, GRACE examines changes in more than just glaciers; it also measures water redistribution, changes in biomass, fluctuations in atmospheric mass, postglacial rebound, and snow accumulation (Swenson and Wahr 2002). When correction for such factors are made, GRACE satellite data displays ice losses of 101 km^3 yr^{-1} we (+/- 22 km^3) over the Gulf of Alaska region since 2002 (Chen et al. 2006a) or 84 km^3 yr^{-1} we (+/-5 km^3 yr^{-1})

a.

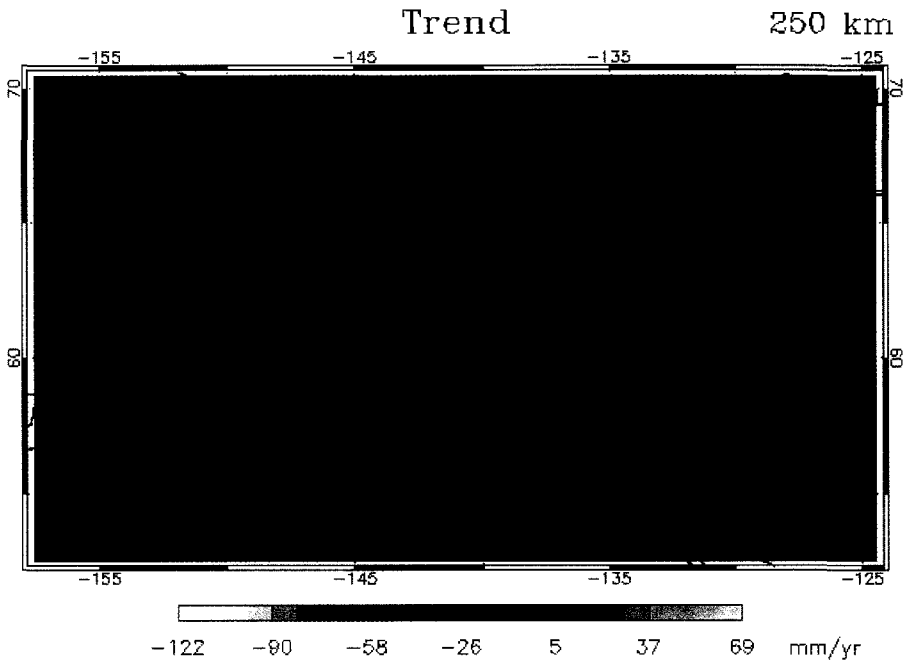

b.

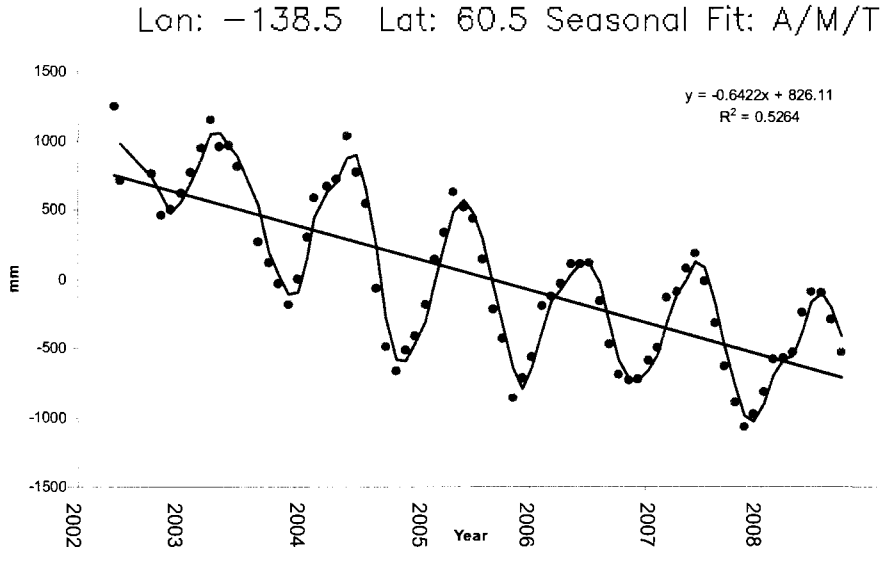

Figure 1.9: Trends in mass change (2003-2008) measured by GRACE Satellite
a: Trends in mass change in mm we in Yukon Territory and Alaska (2003-2008); CSR RL04 solution, 250 km averaging radius.
b: Seasonal time series centered on 60°5'N, 138°5'W (Kaskawulsh Glacier) showing monthly deviations in water equivalent mass from the long-term mean, as well as the trend
Source: NASA Research, Education, and applications Solution Network, GRACE, http://geoid.colorado.edu/grace/grace.php, accessed Sept. 2, 2009.

between 2003 and 2006 (Luthcke et al. 2008). These numbers agree very well with the thinning of 96 km^3 yr^{-1} (+/- 35 km^3) of water loss observed by Arendt et al. (2002).

Arendt et al. (2002) used airborne laser altimetry to measure the change in volume of 67 glaciers in Alaska and the SW Yukon and found volumetric changes to be highly variable between glaciers (Figure 1.10). Globally, the relative retreat of a glacier varies depending on factors such as maximum thickness, mass balance, area-altitude distribution, orientation, slope, thermal conditions and rate of terminus melting (Kulkarni et al. 2007). In Alaska/Yukon, distance from the coast is also important as this determines the relative amount of precipitation received on a given glacier (Arendt et al. 2002). The terminal condition of glaciers is also of primary importance in the region, with tidewater glaciers thinning up to 2-3 times more quickly than valley glaciers (Molnia 2007). About 10% of glaciers sampled by Arendt et al. (2002) thinned while advancing, and still other glaciers thickened while retreating, although these showed very low correlation between change in length and change in thickness (Sapiano et al. 1998). These findings highlight the importance of taking into account both thickness and extent when estimating changes in volume.

Long-term mass balance estimates are currently only available for Gulkana, Wolverine and Lemon Creek Glaciers (Figure 1.1). These account for only 53 km^2 of the 90,000 km^2 glaciated area in Alaska and southwest Yukon, although comparison with the laser altimetry data of Arendt et al. (2002) shows that these glaciers can be considered representative for the region (Figure 1.11a) (Meier and Dyurgerov 2002). Because these representative glaciers follow a global trend of accelerated melting since about 1990, Meier and Dyurgerov (2002) were able to calculate the impact of glaciers in the region on global sea level rise. Figure 1.11 shows that the estimated sea level rise due to melt from glaciers of the St. Elias Mountains accounts for about half of the total measured change in global sea level resultant from glacier melt between 1965 and 2000 (Meier and Dyurgerov 2002).

Most (though not all) thinning glaciers in Alaska have demonstrated similar spatial trends: in general thinning at higher elevations is minimal or non-existent, and thinning increases to a maximum at the terminus (Arendt et al. 2006). Examples of glaciers that exhibit different patterns of thinning include Colony, Knik South, Matanuska East and West, Tonsina, and Woodward Glaciers which displayed moderate increases in thickness above

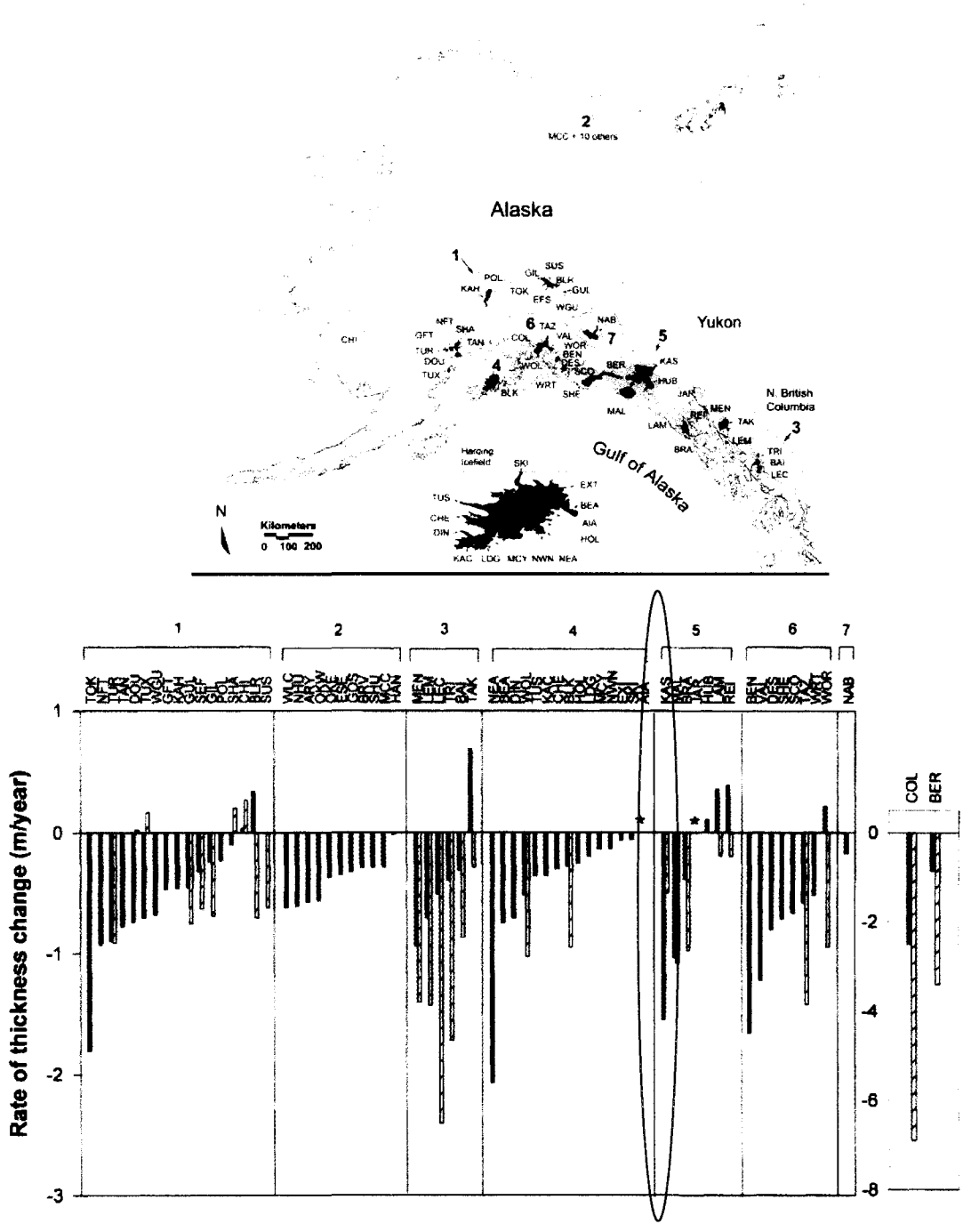

Figure 1.10: Changes in Alaskan glaciers (1950-2001)
a: Location of glaciers surveyed
b: Rate of glacier-wide average thickness change of 67 glaciers in Alaska during the early period (~1950 to 1995; solid black bars) and 28 glaciers during the recent period (~1995 to 2001; hatched bars). The red circle indicates rate of thickness change on the Kaskawulsh Glacier. Source: Arendt et al. (2002)

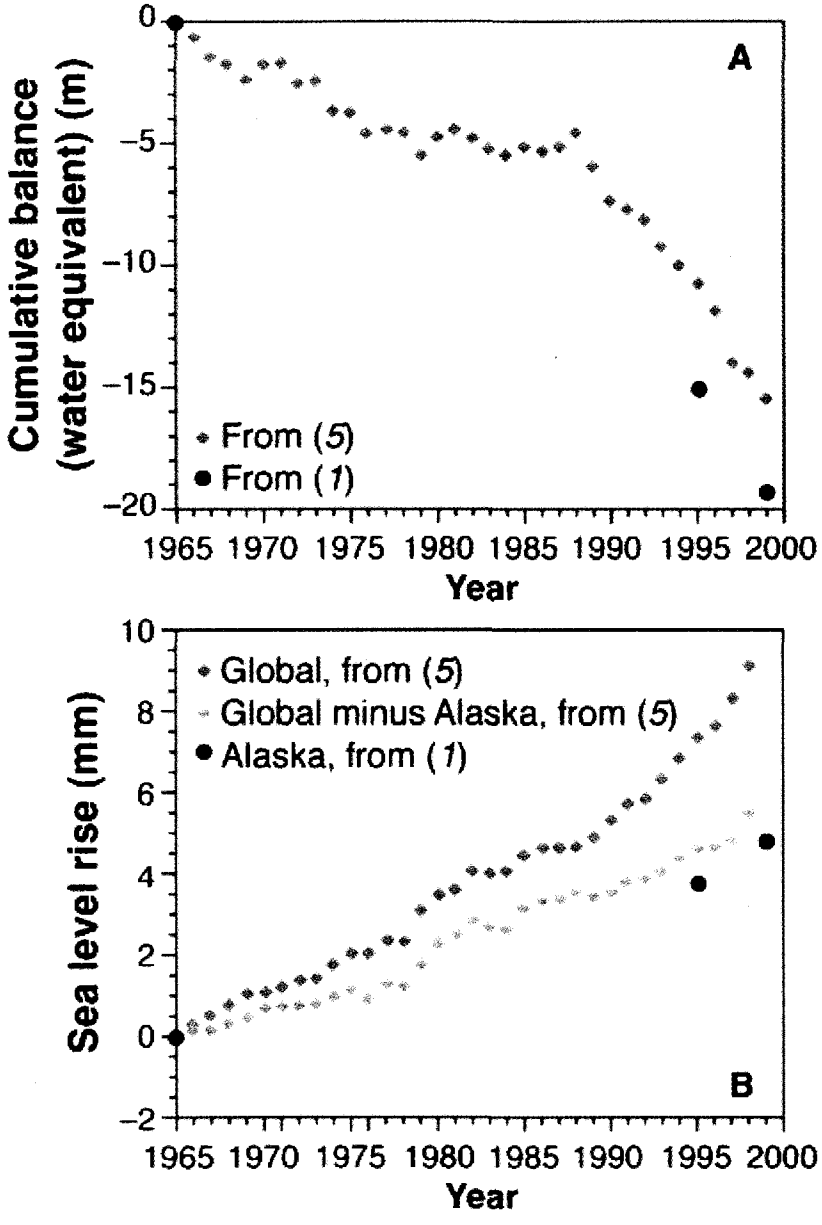

Figure 1.11: Global and Alaskan glacier melt and their relative contributions to sea level rise.
a. Surface mass-balance observations on Alaskan Glaciers (Gulkana, Wolverine, and Lemon Creek) by Dyurgerov (2002) (5) and laser altimeter measurements by Arendt et al. (2002) (1)
b. Sea level rise due to glacier wastage, including area-weighted global total based on mass balance (5), and Alaskan glacier total from laser-altimetry (1).
In figure 1.11b, the orange dots show the global sea level rise resultant from glacier melt worldwide. The green dots represent the global sea level rise due to the melt of glaciers besides those located in Alaska. The pink dots show the contribution to global sea level rise resultant from the melt of Alaskan glaciers. The green curve and the pink dots are approximately equal; thus glaciers of the St. Elias Mountains are responsible for approximately the same amount of sea level rise as all other glaciers between 1965 and 2000.
Source: Meier and Dyurgerov (2002)

1000 m, Bench Glacier, whose entire surface experienced thinning, Harvard Glacier which thickened due to its tidewater dynamics, and Sherman Glacier which maintained its thickness due to debris cover recently afforded by a landslide (Arendt et al. 2006). Optimally, more glacier monitoring stations are needed to improve understanding of climate related changes on glaciers (Molnia 2007). The proposed study addresses this need as it forms the basis of a new project to establish long-term monitoring of the Kaskawulsh Glacier.

1.6 Consequences of Glacier Retreat/Thinning/Disappearance

Thinning and retreat of the Kaskawulsh Glacier is likely to have various environmental impacts. For instance, the level of Kluane Lake is sensitive to climate-induced changes to the Kaskawulsh Glacier. At ~23 m above the present level of Kluane Lake, a valley fork exists that is important to the maintenance of the current drainage pattern (Bryan 1972). The gradient of the Kaskawulsh River is greater than the gradient of the Slims River, meaning that a retreat in the position of the glacier terminus would cause the Kaskawulsh River to pirate the Slims River water. This event would result in a decrease in the level of Kluane Lake of ~2 m, and the discharge of Kluane River would be greatly reduced (Bostock 1969; Brahney et al. 2008a; Brahney et al. 2008b; Bryan 1972; Clague et al. 2006). In the past there have been periods during which more meltwater was discharged to the Kaskawulsh River system rather than the Slims River system. For instance, in 1967, drainage of the Kaskawulsh Glacier meltwater occurred preferentially through the Kaskawulsh River for an extended period of time. As a result the level of Kluane Lake fell by 0.6 m (Johnson 1986).

Glacier retreat can also affect the rate of erosion and exhumation in the mountains; rapid surge and retreat can cause an erosion rate of up to 100 mm yr^{-1} (Sheaf et al 2003). Increased ablation can be expected to encourage more rapid ice flux, and thus promote erosion (Spotila et al. 2004). This, in turn, can affect the frequency and magnitude of mass movements. In August 2007 a landslide with a transport zone measuring 1350 m occurred on Mount Steele, Yukon, located ~96 km northwest of the terminus of the Kaskawulsh Glacier (Lipovsky et al. 2008). The causes of the Mount Steele landslide are still being evaluated, and it is possible that thinning of Steele Glacier was a contributor since increased

erosion in conjunction with a decrease in ice mass is known to increase landsliding (Sheaf et al. 2003).

Finally, the southern portions of Alaska and Yukon are subject to earthquakes associated with continued mountain building in the region. Although tectonic forces control deformation, fluctuation of glaciers in the region may influence the timing of earthquakes. A large decrease in ice load may cause a local increase in seismic activity (Sauber and Molnia 2004). Larsen et al. (2005) completed a study in nearby Glacier Bay, Alaska (Figure 1.1) where an icefield containing 3030 km^3 of ice existed in the Little Ice Age (LIA). After the LIA, the icefield melted and drained in the largest known post-LIA deglaciation. This has resulted in a glacio-isostatic uplift rate of 32 mm yr^{-1}, one of the fastest present day rates on earth. Models indicate that the area has regained about half of its LIA subsidence and that a further rebound of 6-8 m can be expected to occur over the next 700-800 years. This rebound has increased seismicity in southern Alaska (Larsen et al. 2005).

1.7 Objectives

The primary objective of this study is to quantify recent changes in the volume and area of the Kaskawulsh Glacier. Most previous studies of mountain glaciers have focused on changes in extent or terminus displacement to monitor change, whereas this study combines accurate area and thickness change measurements to calculate of the volumetric changes of the Kaskawulsh Glacier over the period 1977-2007. Through differencing digital elevation models (DEMs) from various years, the total change in surface elevation over time can be calculated. Changes in the extent of the Kaskawulsh Glacier since 1956 are also explored through the use of multi-temporal aerial photography and remote sensing imagery. Finally, the potential for a volume/area scaling ratio is examined via comparison of the elevation, extent and volume variables over time. This ratio would enable improved up-scaling of area changes measured on other glaciers in this region to true volume changes

The broader purpose of this project is to contribute to the long-term monitoring of the Kaskawulsh Glacier, as part of a collaborative project between the University of Ottawa, Geological Survey of Canada and Parks Canada. This project also expands upon the work of Arendt et al. (2002) who studied changes in the volume of all Alaskan glaciers; this study

helps to assess the accuracy of Arendt's work through in-depth focus on one of the glaciers studied in his project, and it extends the time period of his study.

Chapter 2

2.0 Data and Methods

2.1 Introduction

This study examines changes in the Kaskawulsh Glacier over the period 1956-2007, and ultimately quantifies the volumetric changes of the glacier between 1977 and 2007. Changes in the areal extent of the glacier are determined via the use of aerial photography and visible satellite imagery. Changes in the surface elevation of the glacier are calculated using differences between historical digital elevation models (DEMs) derived from stereo aerial photography and modern DEMs derived from airborne laser altimetry profiles. The DEMs and satellite imagery are checked and georectified using ground control points (GCPs) collected with a high resolution differential Global Positioning System (dGPS) system during a 2008 field campaign. Changes in the volume of the Kaskawulsh Glacier are then calculated by multiplying the changes in areal extent by the changes in surface elevation.

2.2 Image Sources

As described in Sections 2.2.1 and 2.2.2 below, various media were used to examine changes in elevation and extent of the Kaskawulsh Glacier. Criteria used for image selection include:

- Acquisition from the summer season (late May to early September). This is to minimize the influence of seasonal snowfall on the findings.
- Limited or no cloud cover (<20%). This facilitates accurate digitization and georectification.
- Extensive coverage (at least 50%) of the Kaskawulsh Glacier. An exception was made for the 1959 DEM, as this allowed extension of the period of analysis when no other elevation data sources are available.

2.2.1 Elevation Data

Elevation data for the Kaskawulsh Glacier was obtained for five periods between 1959 and 2007 from stereo aerial photography and airborne laser altimetry (Table 2.1). In particular, the following datasets were used:

Table 2.1: Elevation and area data used to calculated changes along the Kaskawulsh Glacier. The source, date, image ID and resolution of each dataset is provided.

Elevation Data				
Type	**Source**	**Date**	**ID**	**Resolution**
Topographic Map	USGS*	1959	AK B Mt. St. Elias A-3	1:62 500
Topographic Map	USGS	1959	AK B Mt. St. Elias A-4	1:62 500
Topographic Map	USGS	1959	AK B Mt. St. Elias A-5	1:62 500
Topographic Map	USGS	1959	AK B Mt. St. Elias B-3	1:62 500
Topographic Map	USGS	1959	AK B Mt. St. Elias B-4	1:62 500
Topographic Map	USGS	1959	AK B Mt. St. Elias B-5	1:62 500
DEM (Level 1)	CDED**	1976	NTS 115b06	1:50 000
DEM (Level 1)	CDED	1976	NTS 115b07	1:50 000
DEM (Level 1)	CDED	1976	NTS 115b10	1:50 000
DEM (Level 1)	CDED	1976	NTS 115b11	1:50 000
DEM (Level 1)	CDED	1977	NTS 115b12	1:50 000
DEM (Level 1)	CDED	1977	NTS 115b14	1:50 000
DEM (Level 1)	CDED	1977	NTS 115b15	1:50 000
Non-scanning LIDAR profile	University of Alaska Fairbanks	20-May-95	n/a	0.18 m
Non-scanning LIDAR profile	University of Alaska Fairbanks	29-May-00	n/a	0.18 m
Scanning LIDAR profile	C-CLEAR consortium	12-Aug-07	n/a	0.18 m
Extent Data				
Air photo	NAPL***	11-Sep-56	A15517 #20	10 m
Air photo	NAPL	11-Sep-56	A15517#22	10 m
Air photo	NAPL	11-Sep-56	A15517#24	10 m
Air photo	NAPL	11-Sep-56	A15517#42	10 m
Air photo	NAPL	11-Sep-56	A15517#44	10 m
Air photo	NAPL	11-Sep-56	A15517#48	10 m
Air photo	NAPL	11-Sep-56	A15517#50	10 m
Air photo	NAPL	11-Sep-56	A15517#52	10 m
Air photo	NAPL	11-Sep-56	A15517#54	10 m
Air photo	NAPL	11-Sep-56	A15517#56	10 m
Air photo	NAPL	9-Aug-57	A15739#10	10 m
Satellite image	Landsat 2 (GLCF)	3-Sep-77	p067r17_2m19770903	60 m
Satellite image	Landsat 5 (GLCF)	29-Oct-86	L5062017_01719861029	30 m
Satellite image	Landsat 5 (GLCF)	12-Aug-90	p063r17_5t900812	30 m
Satellite image	Landsat 5 (GLCF)	16-Aug-94	p062r17_5t940816	30 m
Satellite image	Landsat 5 (GLCF)	19-Jul-01	p061r018_7t20010719	30 m
Satellite image	Landsat 7 (USGS)	9-Jun-07	L71062018_01820070609	30 m
Satellite image	Landsat 7 (USGS)	12-Aug-07	L71062018_01820070812	30 m
Satellite image	Landsat 7 (USGS)	28-Aug-07	L71062017_01720070828	30 m
Satellite image	ASTER (LP DAAC)	10-Jun-01	L1B_00306102001204453	15 m
Satellite image	ASTER (LP DAAC)	20-May-03	L1B_00305202003205442	15 m
Satellite image	ASTER (LP DAAC)	7-Jun-03	L1B_00306072003204217	15 m
Satellite image	ASTER (LP DAAC)	2-Mar-06	L1B_00303022006204717	15 m
Satellite image	SPOT (SPIRIT)	3-Sep-07	5474226070903	5 m

*USGS: United States Geological Survey
**CDED: Canadian Digital Elevation Data Centre
***NAPL: National Air Photo Library

a. 1959 DEM from USGS (US Geological Survey)

This DEM was produced from topographic maps created by the U.S. National Imagery and Mapping Agency (NIMA) from stereo matching of aerial photographs collected in 1959. Because this is an American dataset and the Kaskawulsh Glacier is located entirely within Canada, only partial coverage of the glacier is provided (Figure 2.1). The data is projected in UTM zone 7, with the NAD 27 datum and Clarke 1866 ellipsoid. The pixel resolution is 60 m. A complication associated with this dataset is the possibility of large vertical errors, particularly since it covers an icefield where there are few distinctive features that can be used as match points in the DEM creation process. For its DEMs, the USGS quotes a 30 m vertical accuracy (USGS, Standards for Digital Elevation Models, http://rockyweb.cr.usgs.gov/nmpstds/acrodocs/dem/1DEM0897.PDF, accessed Sept. 4, 2009).

b. 1977 DEM from CDED (Canadian Digital Elevation Data)

This raster file was derived from stereo matching of aerial photographs collected in 1976 and 1977 (Figure 2.2). The original DEM was produced by the Centre for Topographic Information (a division of Natural Resources Canada) jointly with the Yukon territorial government and private sector, and was downloaded in tiles from GeoBase (http://www.geobase.ca/geobase/en/index.html, accessed Sept. 4, 2009). The data is projected in UTM zone 7N, with a NAD83 datum and GRS 80 ellipsoid. It has a resolution of 1:50,000 and pixel size of 22 m. Figure 2.3 shows how these tiles are distributed geographically, and the year represented by each tile. This dataset is considered to be the 1977 glacier surface.

According to the Geobase website, cumulative vertical errors in the CDED files result from horizontal errors and errors inherent in the source data. Thus, for elevations below the ELA an uncertainty of +/-15 m may be assumed (Larsen et al. 2007), while above the ELA errors between 30 and 45 m are possible (Echelmeyer et al. 1996; Larsen et al. 2007). Comparison of the 1977 CDED DEM with GCPs collected in summer of 2008 (see section 2.3.1) as well as the 2007 LIDAR DEM (section 2.2.1d) gives an average vertical error of 15 m. Above the ELA, the average error was slightly higher (~19 m). These errors

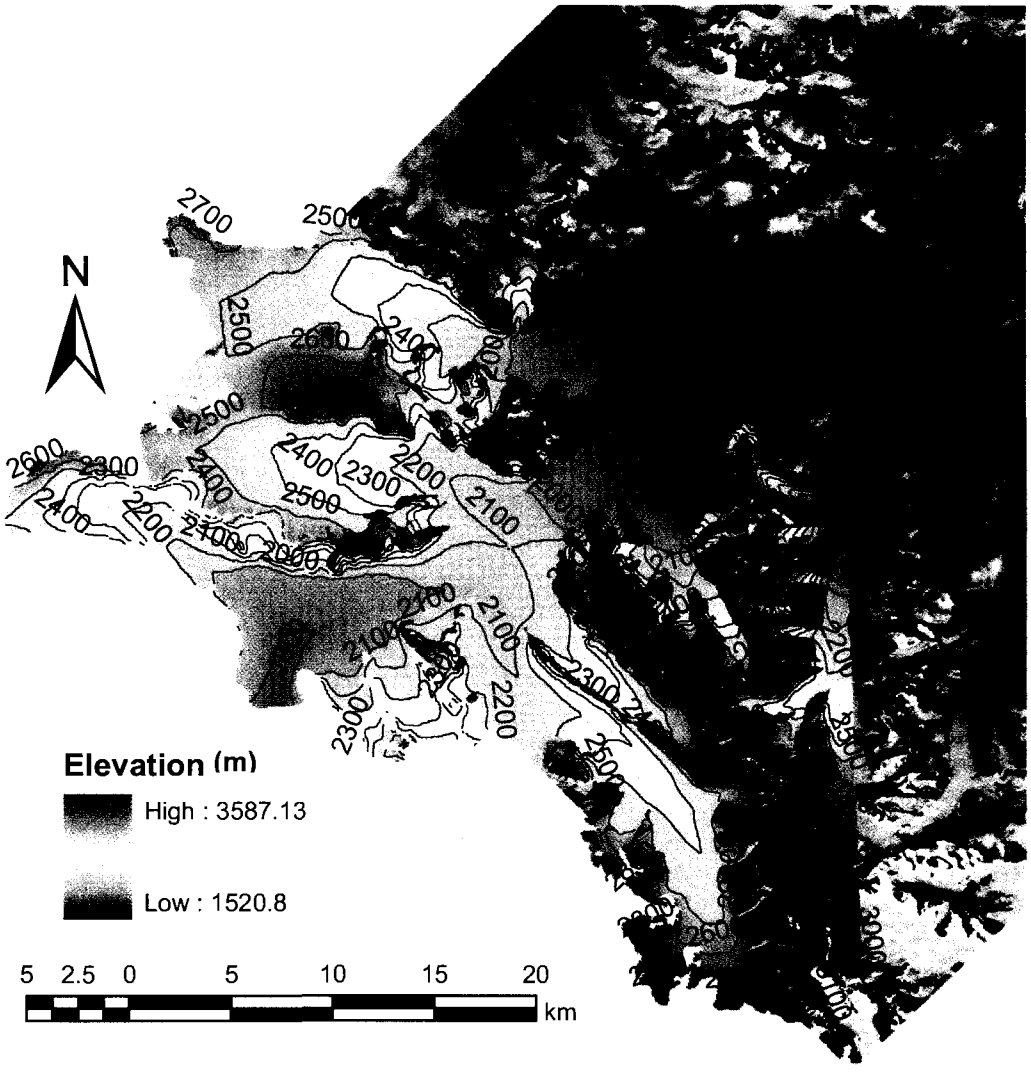

Figure 2.1: 1959 DEM of the Kaskawulsh Glacier with contours displayed over a 2007 SPOT-5 image.

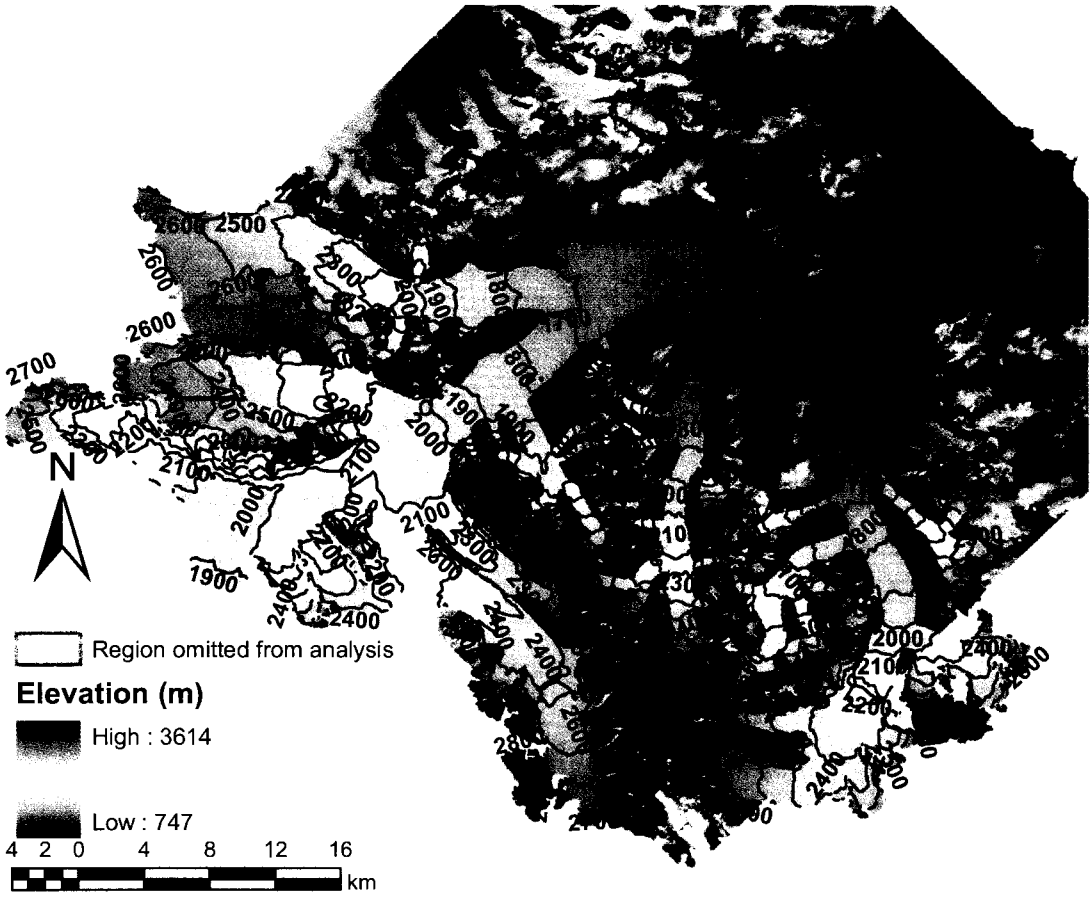

Figure 2.2: 1977 DEM of the Kaskawulsh Glacier with contours displayed over a 2007 SPOT-5 image. The area indicated by the green outline represents a suspected low-level cloud interpreted by cartographers mistakenly as the glacier surface. This region is therefore omitted when comparative analyses are conducted against the 1977 DEM

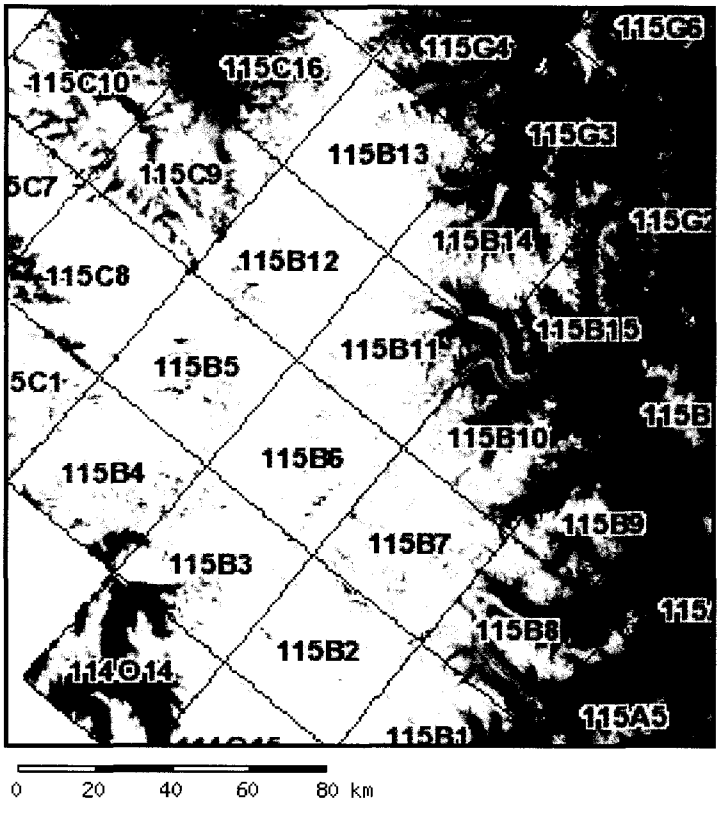

Tile	Year
115b06	1976
115b07	1976
115b10	1976
115b11	1976
115b12	1977
115b14	1977
115b15	1977

Figure 2.3: Location and date of DEM tiles for 1977 glacier surface.
Source: Natural Resources Canada, The Atlas of Canada,
http://atlas.nrcan.gc.ca/site/english/maps/topo/map, accessed Sept. 2, 2009.

were calculated using 50 randomly selected points in areas of low relief bedrock where the DEMs overlap (25 near the glacier terminus, 25 along the nunatak separating the north and south glacier arms).

In addition to potential errors created by DEM production in snow-covered areas, the use of photographs from various dates to create a single contour may also introduce error; changes in the glacier between aerial photographs could be interpreted as changes in slope at a single moment in time by the cartographer (Echelmeyer et al. 1996). These complications generally introduce error of about 5 m (Sapiano et al. 1998). One area of anomalously high elevation was observed in this dataset, where the slope increases by 126 m over a distance of 2 km. Although this slope is not uncommon in this environment, when this DEM is compared to all other DEMs, a prominent depression is observed, the shape and size of which suggested that a low-level cloud may have been interpreted locally as the glacier surface. This region was removed from consideration for all analytical purposes whenever the 1977 DEM is concerned, and is outlined in green in Figure 2.2.

c. 1995 and 2000 Glacier Profiles collected by University of Alaska Fairbanks

These datasets were created from flightlines collected using an airborne non-scanning laser altimeter. Laser altimetry is currently one of the best methods to monitor mass balance of glaciers in mountainous areas (Echelmeyer et al. 1996) as current technology allows relatively good accuracy over larger areas, and even small changes can be quantified (Etzelmüller 2000). Furthermore, over icefields, where derivation of topographic information from aerial photography is unreliable, laser altimetry provides the best accuracy (Hopkinson et al. 2001).

Laser altimetry profiling measures the absolute surface elevation along a flightline over a glacier surface (Figure 2.4). In order to obtain an absolute elevation, the position of the surface relative to the aircraft, as well as the absolute position of the aircraft, must be known at all times. In light of this, an accurate IMU (Inertial Measurement Unit) must be operational in the aircraft that detects its rate of motion, direction, and change in orientation (pitch, roll and yaw). A kinematic dGPS must also be constantly recording the position of the aircraft. The surface elevation of the glacier is then calculated relative to the recorded

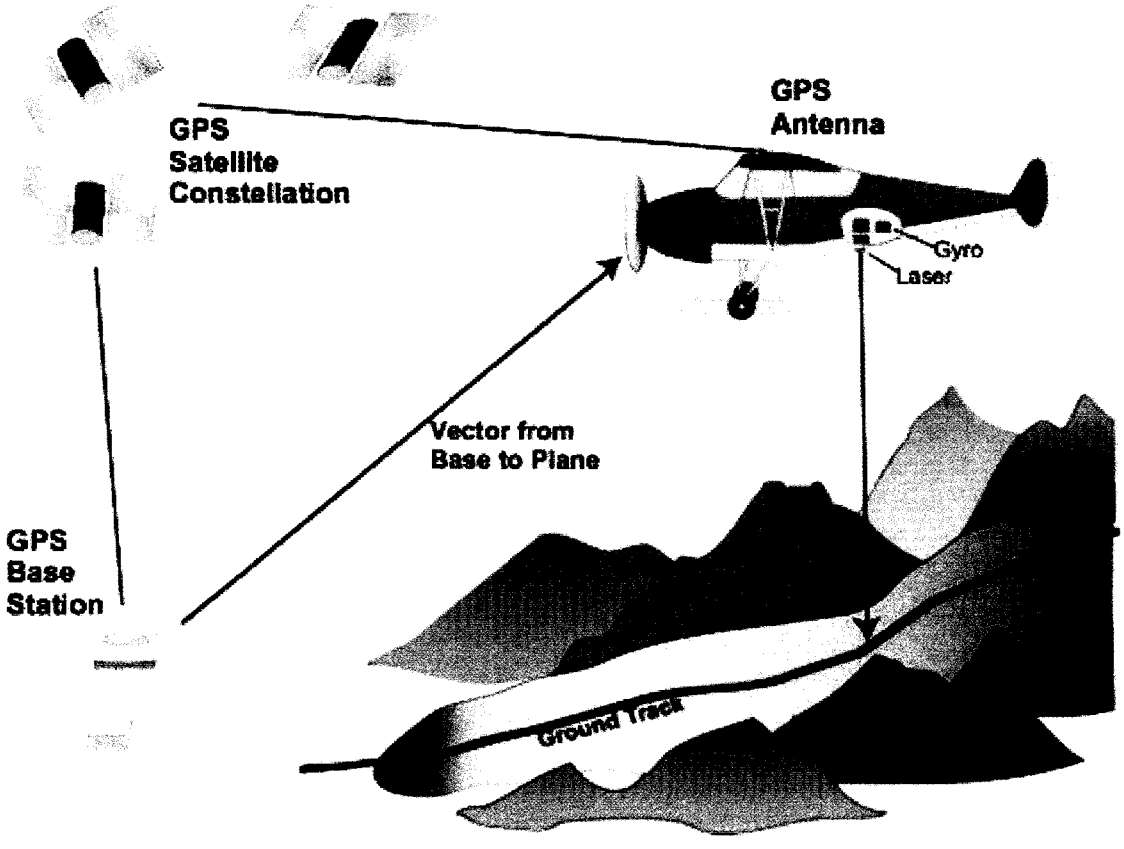

Figure 2.4: Sketch of the non-scanning laser altimetry system. An IMU on board the aircraft detects the plane's rate of motion, direction, and change in orientation, while a kinematic dGPS records the position of the aircraft. The measured elevation of the aircraft (as determined by the GPS) is corrected according to the positioning calculated (as determined by the IMU). The result is a narrow profile of the absolute surface elevation.
Source: Geophysical Institute, University of Alaska Fairbanks, Alaskan Glacier Laser Altimetry, http://gps.alaska.edu/chris/altimetry_text.html, accessed Sept. 2, 2009.

positioning calculated using orientation and acceleration variables (a_{xs}, a_{ys} and a_{zs}) (as determined by the IMU).

Fixed laser altimetry uses a non-scanning head which samples only the points directly beneath the aircraft. Thus the surveyed area is only as large as the extent of the footprint of the laser pulse, which is largely dependent on the altitude that the aircraft is flown at. The diameter of the laser pulse used in this study is 0.18 m. The vertical accuracy of laser altimetry measurement techniques is on the order of 30 cm, and the horizontal accuracy is even better (Arendt et al. 2002). Errors increase with increasing slope (Echelmeyer et al. 1996). Using a fixed laser altimeter introduces error because data is only collected in a single line over the glacier surface, whereas changes in elevation are not constant over the width of the glacier. This introduces a possible error of 1-3 m at the margins (Arendt et al. 2008; Echelmeyer et al. 1996).

Two narrow DEMs up the centre line of the Kaskawulsh Glacier were created from this data source: one collected on May 20, 1995 (Figure 2.5a), and the second on May 29, 2000 (Figure 2.5b).The data created from these laser altimetry profiles is in the NAD83 datum and GRS 80 ellipsoid, and projected in UTM zone 7N. The raw elevation data was imported into ESRI ArcMap 9.2 and converted into a DEM through an IDW (Inverse Distance Weighting) interpolation in the 'Interpolate to Raster" function (using a power of 2, a variable search radius of 12 points, and an output cell size of 10 m).

d. 2007 Glacier Profile collected by the C-CLEAR consortium (Dr. Chris Hopkinson and Dr. Michael Demuth, NSCC)

This dataset was created from a flightline collected using an airborne scanning laser altimeter. Acquisition of this data was much the same as the 1995 and 2000 flightlines, with the exception that the laser altimeter had scanning capabilities (Figure 2.6). Scanning laser altimeters have nutating heads that scan in a left-right zigzag pattern over the earth's surface (Hopkinson et al. 2001). This pattern of data collection is called swath mapping. In scanning laser altimetry, the width of the flightline is defined by the swath width (Abdalati et al. 2004), which is mainly defined by flight altitude. Thus scanning laser altimetry has the potential for coverage over the full width of a glacier, which reduces error at the glacier margins associated with non-scanning laser altimeters. For this study the swath width was

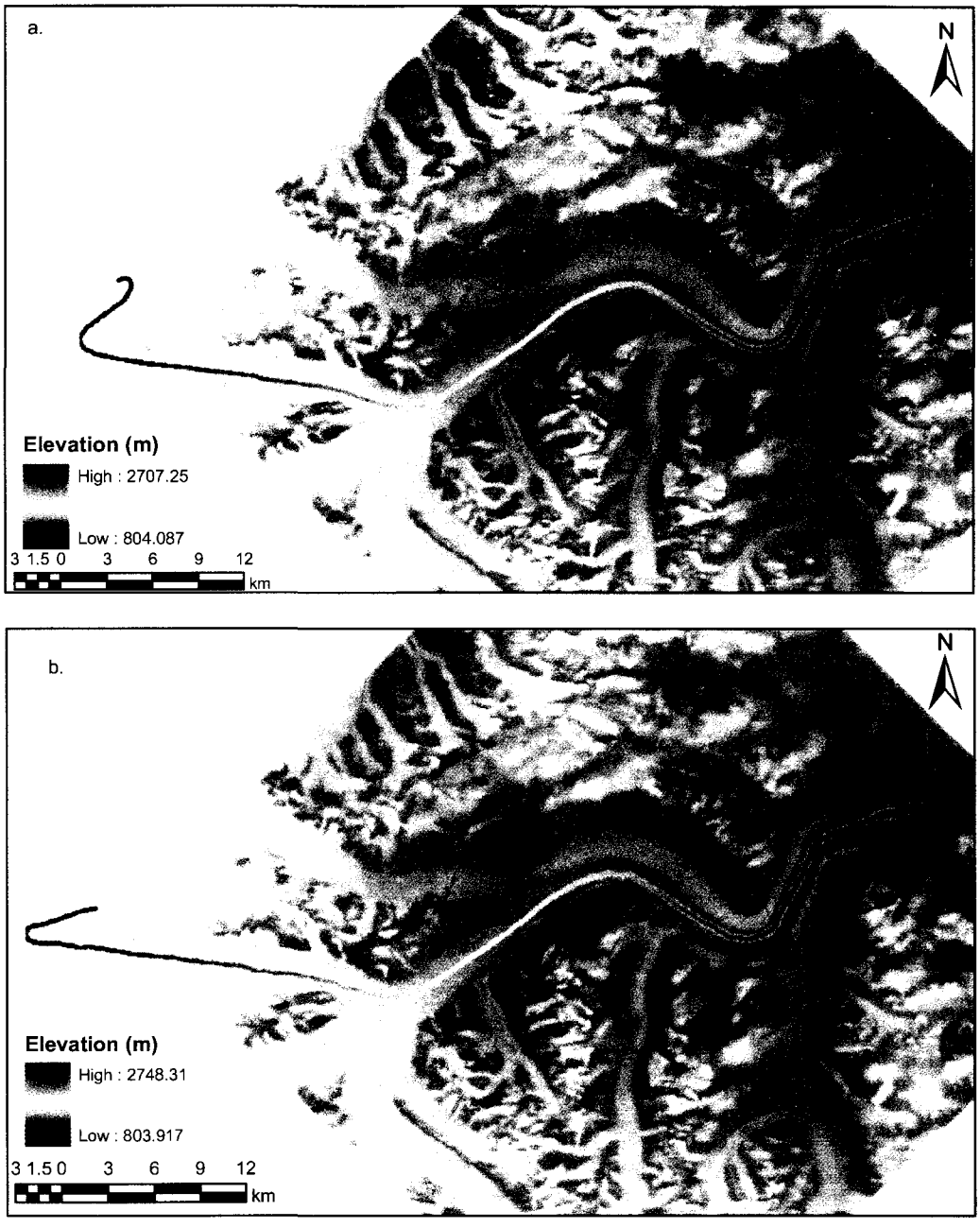

Figure 2.5: DEMs created from non-scanning laser altimetry flightlines displayed over 2007 SPOT-5 image a: 1995 DEM (May 20, 1995) ; b: 2000 DEM (May 29, 2000)

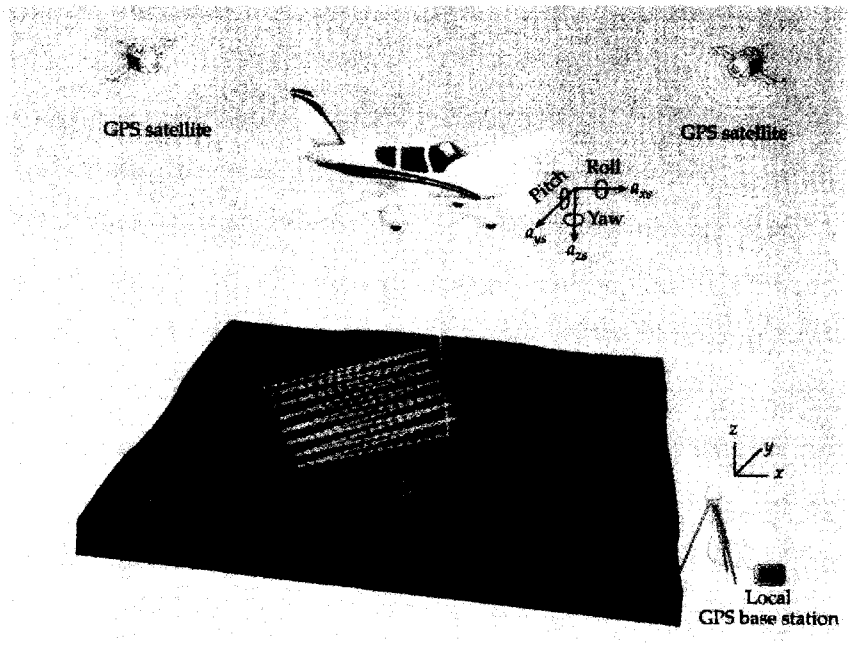

Figure 2.6: Airborne laser swath mapping by a small aircraft. GPS configuration for determining the absolute position of the aircraft is shown; orientation and acceleration parameters are used to calculate the coordinates and elevation of surface using the GPS data Source: Carter et al. 2007.

~2.3 km, and near complete coverage of the main glacier was achieved via data collected along two flightlines: one flown in an upglacier direction, and the other in a downglacier direction.

This dataset is in the NAD83 datum, uses the GRS 80 ellipsoid, and is projected in UTM zone 7 (Figure 2.7). Data represents the elevations on August 12, 2007. A subset of the data was created so that point spacing was never denser than 5 m. A DEM was then created using a nearest neighbour routine, and the data was resampled to 10 m resolution. This DEM was ground-truthed against GCPs collected along the central moraine at altitudes between 1321 m and 1353 m between June 28, 2008 and July 10, 2008. Because these GCPs were collected on the ice, some change in elevation would be expected over the intervening 11 months between collection of the two datasets. Nonetheless, the two datasets agree very well, and based on the GCPs the maximum estimated vertical error for the 2007 DEM is 2.5 m.

One of the 2007 flightlines deviated moderately from the original LIDAR lines from 1995 and 2000, so comparisons were only made where there was direct data overlap. To facilitate comparison between the 2000 and 2007 glacier surfaces, the raw 2007 data was used to interpolate a DEM of the entire terminus. This was necessary as the original 2007 did not overlap with the 2000 flightline for most of the length of the terminus. Therefore original data was converted to a DEM using an IDW in the 'Interpolate to Raster' function (using a power of 2, a variable search radius of 12 points, and an output cell size of 10 m). The interpolation covers the entire area of the terminus to an altitude of 1353 m (Figure 2.8).

e. DEMs created from ASTER scenes

The ASTER (Advanced Spaceborne Thermal Emission and Reflection Radiometer) sensor was launched on the Terra satellite in 1999. ASTER is an optical satellite sensor that collects information in visible and near-infrared (VNIR), shortwave infrared (SWIR) and thermal infrared (TIR) bands, and is additionally equipped with a backward facing telescope designed to collect stereoscopic VNIR information (Fujisada et al. 2005). Due to the collection of stereoscopic images, DEMs can be derived from Level-1A ASTER scenes (scenes that are reconstructed, unprocessed, and at full resolution). Scenes covering the entirety of the Kaskawulsh Glacier were downloaded for June 10, 2001 and March 2, 2006

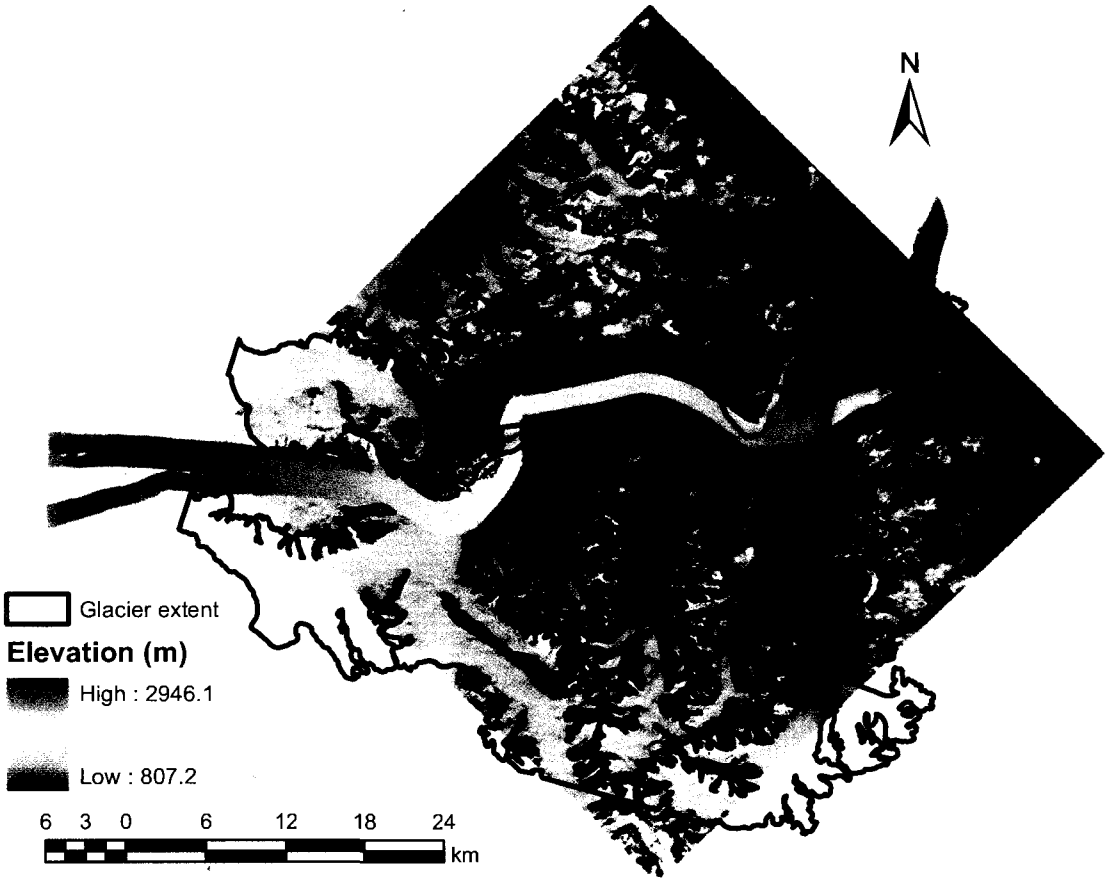

Figure 2.7: 2007 DEM created from scanning laser altimetry flightline displayed over 2007 SPOT-5 image.

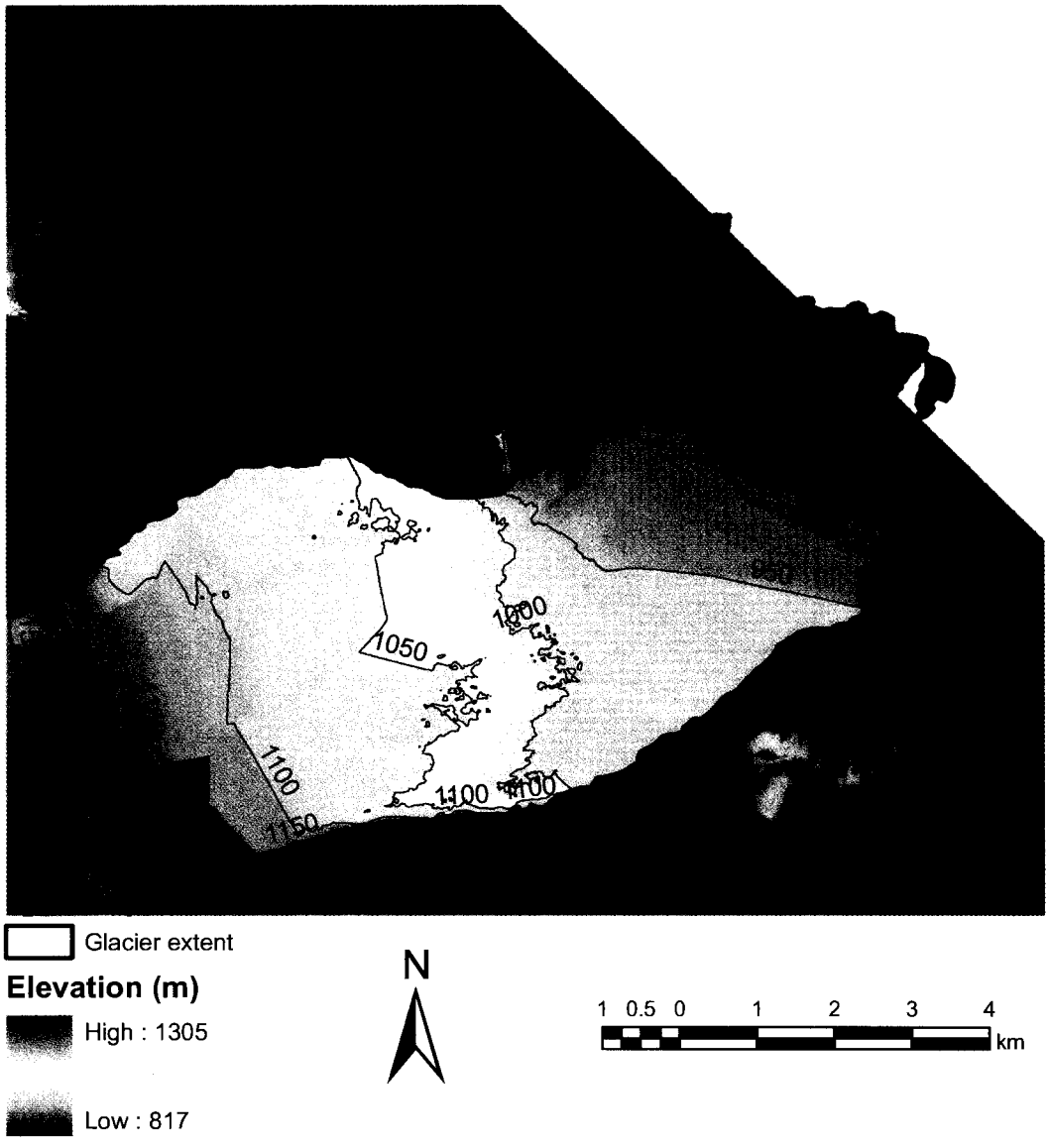

Figure 2.8: 2007 DEM of the glacier terminus interpolated from scanning laser altimetry flightlines displayed over 2007 SPOT-5 image.

via the LP DAAC (Land Processes Distributed Active Archive Center), which is a division of NASA (https://lpdaac.usgs.gov/, accessed Sept. 4, 2009).

A pre-made DEM can be ordered from the LP DAAC, which is created from Level-1A ASTER scenes. However, because no ground-control is used in this processing, the product created for the Kaskawulsh Glacier was inadequate. Elevation values were reasonable in both DEMs (Figure 2.9a and b), but comparison against one another reveals unrealistically large changes in elevation for a 5-year period (Figure 2.10). Further comparison against GCPs collected in summer 2008 suggest that these ASTER DEMs underestimate elevation by as much as 40 m locally, while other elevations are overestimated by as much as 30 m. A well-known and documented shortcoming of automated ASTER DEMS is that areas of high relief tend to be exaggerated (Fujisada et al. 2005). Therefore the LP DAAC DEMs were not used in analysis.

Manual creation of DEMs from ASTER images was performed in ITT Visual Information Solutions ENVI 4.4 software to attempt to correct the shortcomings of the automated DEMs. Interactively defined GCPs, a mathematical model, and satellite ephemeris information were used to calculate elevation data (Fujisada et al. 2005). For DEM creation, a minimum of 9 GCPs and 20 tie points were used per image. The resultant ASTER DEMs have pixel sizes of 15 m, and theoretically have a vertical accuracy of 10-30 m.

Scenes were georectified using GCPs collected in the field and a high resolution SPOT image. Initial observation of the ASTER DEMs yielded promising results; the range of elevations as well as the slope patterns seemed realistic (Figure 2.11). However, when these DEMs were compared to one another or to other DEMs, the apparent changes in elevation were highly unrealistic. For instance, some areas exhibited apparent losses of up to 374 m yr^{-1} (Figure 2.12). Thus these DEMs were deemed to be of too poor quality to use in this study. The discrepancies in the ASTER DEMs are likely due to the high relief in this area (making interpolation over any distance difficult), a paucity of GCPs (particularly in the accumulation area), a reliance on a small number of ground-truthed elevation points, and a reliance on older inaccurate DEMs to supplement the ground-truthed GCPs. This corroborates other studies that found ASTER DEMs ineffective for detecting elevation

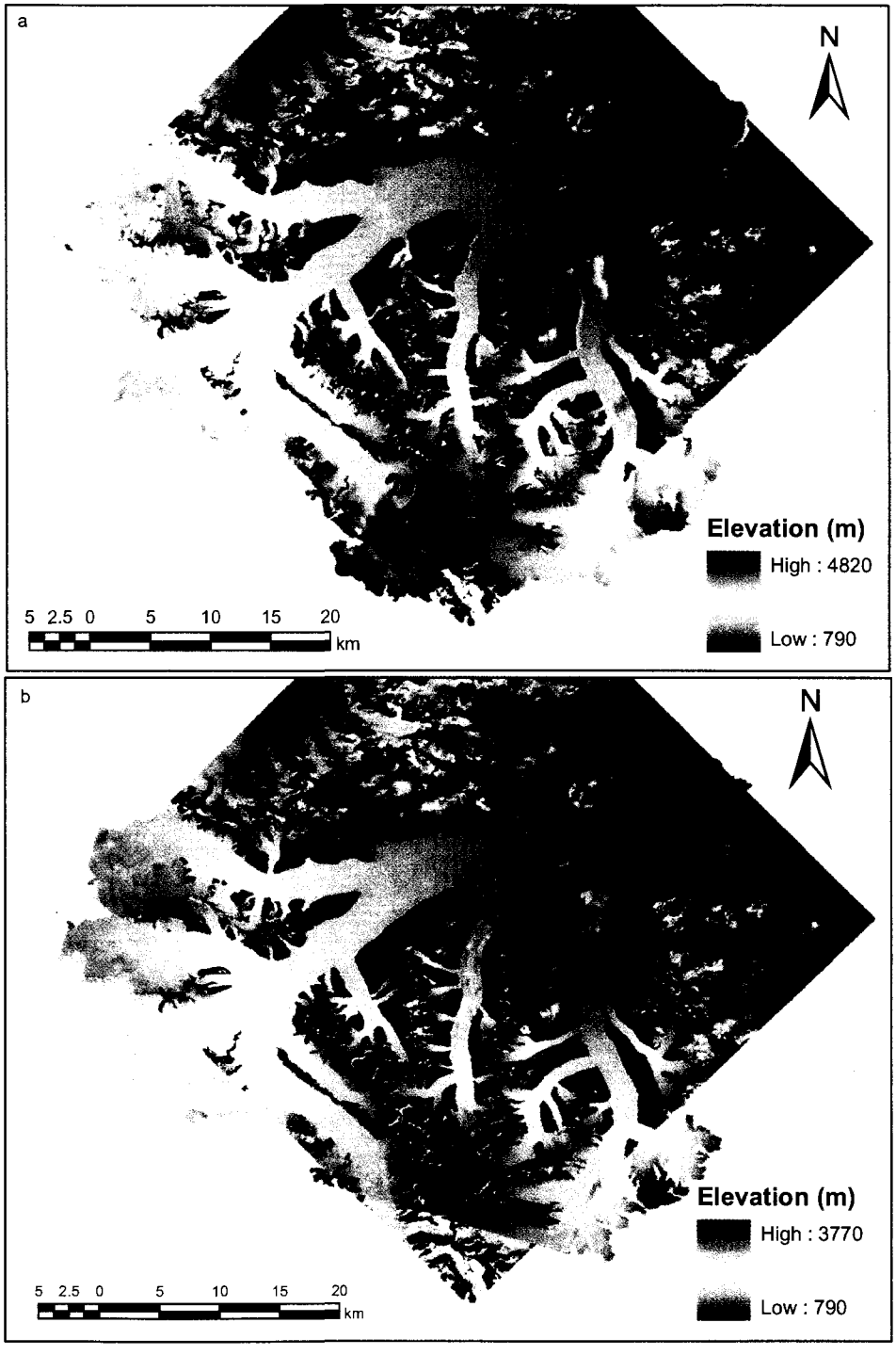

Figure 2.9: DEMs created from ASTER images by the LP DAAC. a: June 10, 2001; b: March 2, 2006.

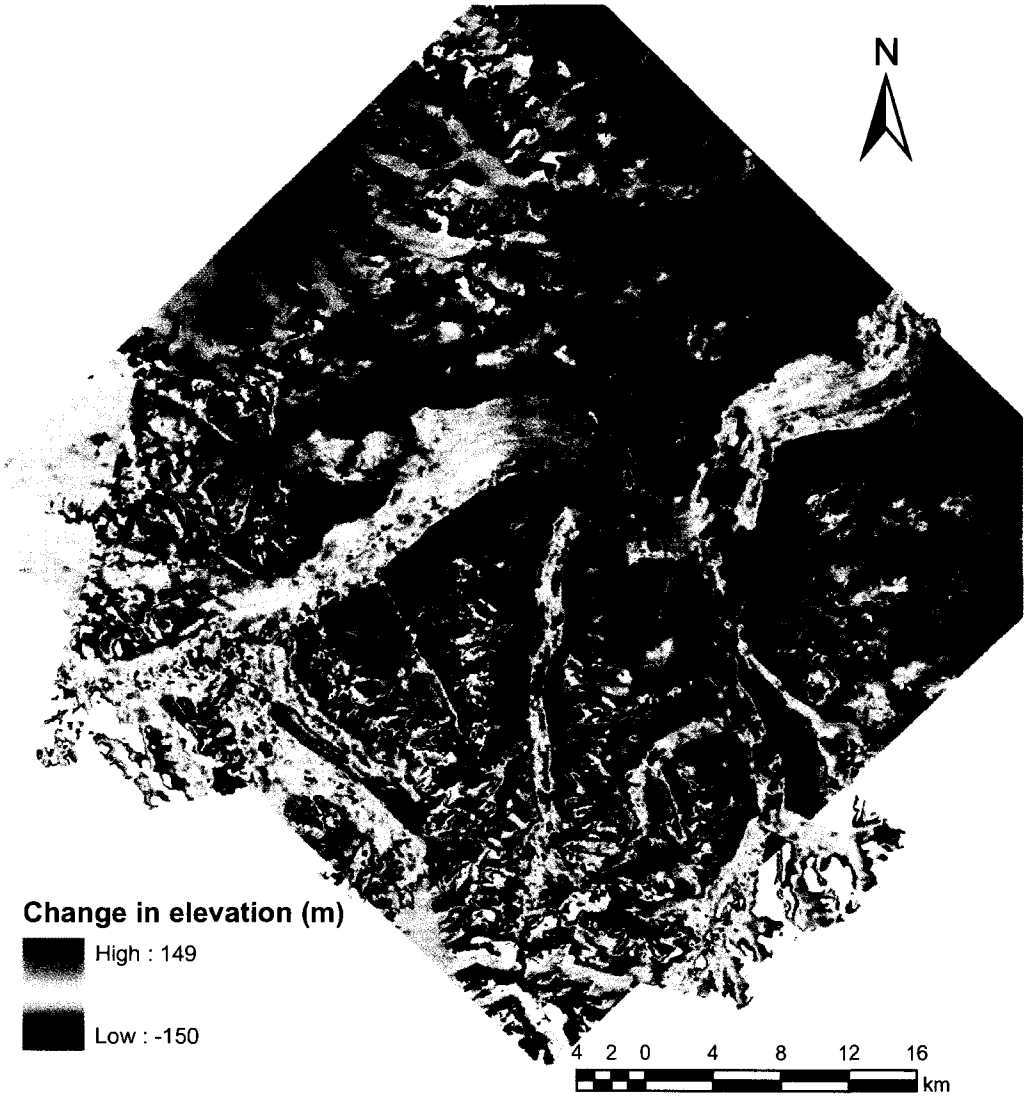

Figure 2.10: Difference in elevation between 2001 ASTER DEM created by the LP DAAC and the 2006 ASTER DEM created by the LP DAAC. Note that the changes in elevation are highly unrealistic over a 5- year period. Thus these data sources were deemed inadequate for quantifying changes in the surface elevation of the Kaskawulsh Glacier.

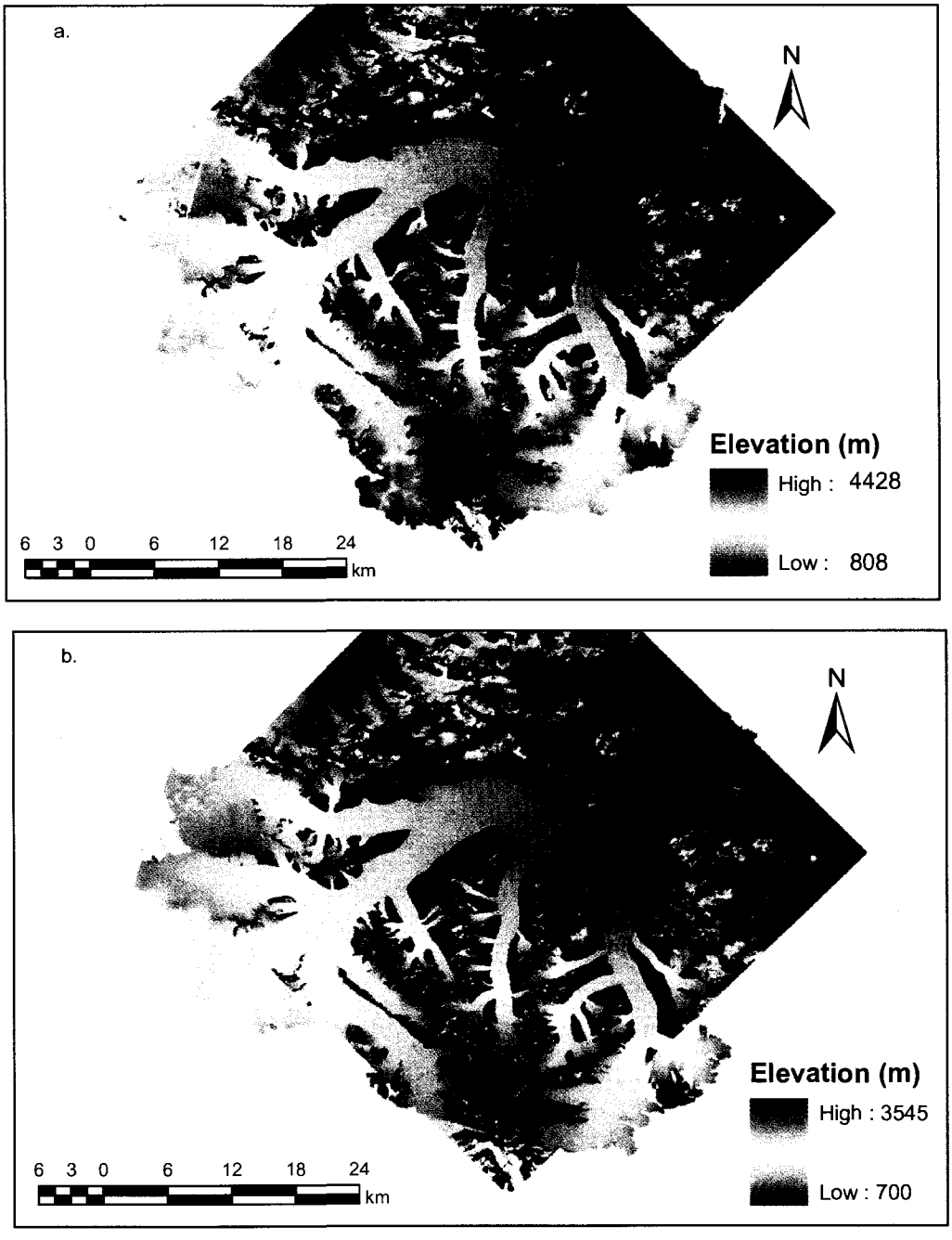

Figure 2.11: DEMs created from ASTER images in ENVI using interactively defined GCPs. a: June 10, 2001; b: March 2, 2006.

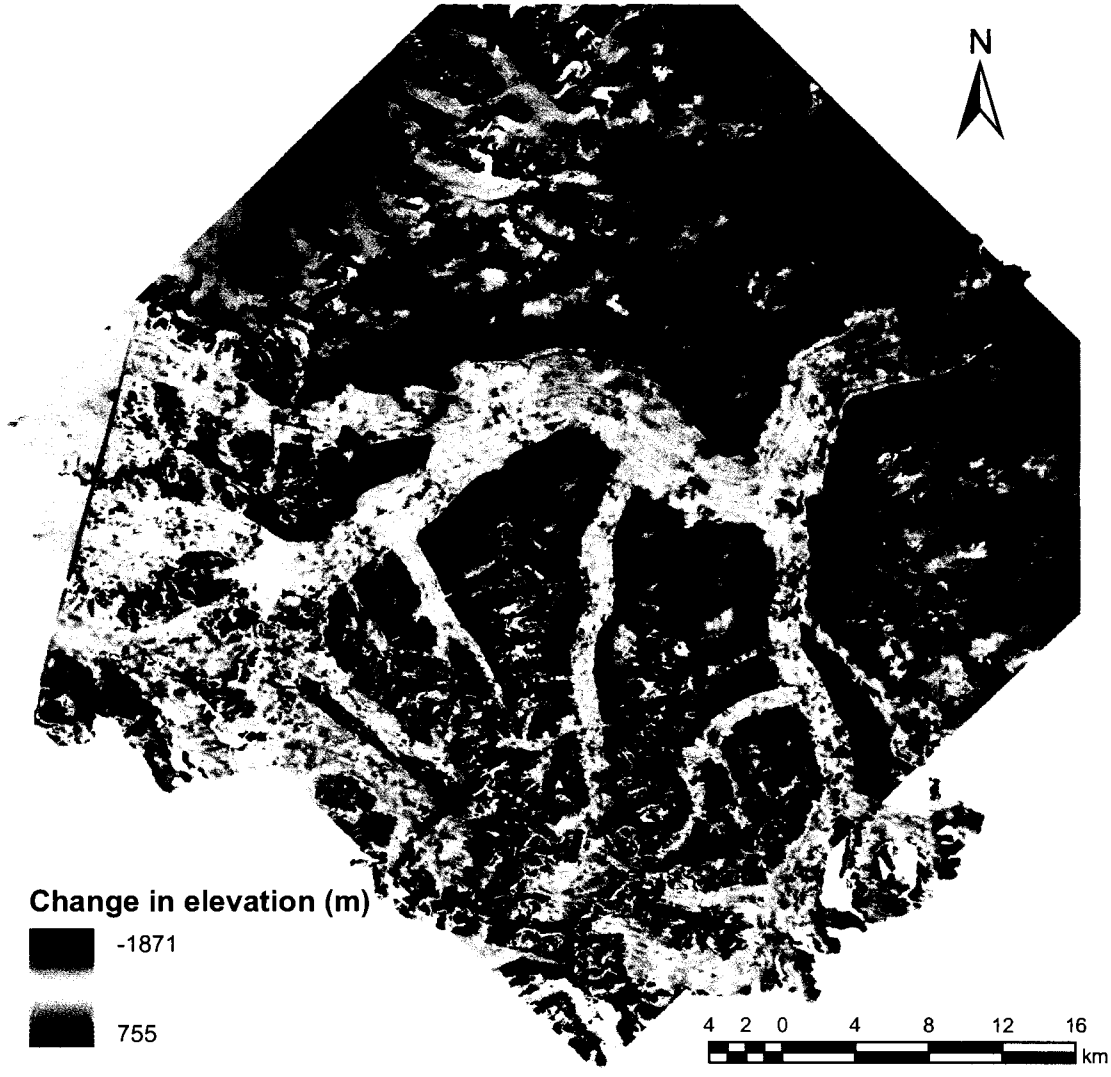

Figure 2.12: Difference in elevation between 2001 ASTER DEM created in ITT Visual Information Solutions ENVI 4.4 using interactively defined GCPs and the 2006 ASTER DEM created in ITT Visual Information Solutions ENVI 4.4 using interactively defined GCPs. Note that the changes in elevation are highly unrealistic over a 5-year period. Thus these data sources were deemed inadequate for quantifying changes in the surface elevation of the Kaskawulsh Glacier.

changes on the order of 1 m yr^{-1} (Kääb 2002; Toutin 2008). Given these limitations, no further use or discussion of the ASTER DEMs will be provided here.

2.2.2 Areal Data

Areal data for the Kaskawulsh Glacier was obtained for 1956, 1977, 1986, 1990, 1994, 2001, 2003, 2006, and 2007 from aerial photographs and various satellite sensors including Landsat, ASTER and SPOT-5 (Table 2.1). The following datasets were used:

a. Air Photo mosaic

Partial coverage of the Kaskawulsh Glacier is available for 1956 using aerial photographs from the National Air Photo Library (NAPL), available via the University of Ottawa GSG (Geographic, Statistical and Government Information) Library. The air photo mosaic (Figure 2.13) consists of 11 aerial photographs, each covering an area of ~230 km^2 (~15.2 km by ~15.2 km). The images were acquired from flight altitudes ranging between 3,400 m and 4,900 m, all during the summer season. Monochrome photographs cover the entire south arm of the glacier as well as the central arm of the glacier almost up to the ablation zone. The photographs were scanned at 150 dpi, which yielded a resolution of 10 m. The images were then imported into ESRI ArcMap 9.2, georeferenced, and the perimeter of the glacier was digitized.

b. Landsat images

The Landsat satellite is part of NASA's Earth observation program, and supplies imagery in the visible, infrared, and thermal spectra. In this project, multi-temporal images were used at a variety of resolutions. Landsat MSS (multi-spectral scanner) images are available at 60 m resolution, Landsat TM (thematic mapper) images are available at 30 m resolution, and Landsat ETM+ (enhanced thematic mapper plus) images are available at 15 and 30 m resolution.

Free Landsat images since 1977 were downloaded from the Global Land Cover Facility (GLCF) (http://glcfapp.umiacs.umd.edu:8080/esdi/index.jsp, accessed Sept. 4, 2009) and the U.S. Geological Survey (USGS) (http://edcsns17.cr.usgs.gov/EarthExplorer/, accessed Sept. 4, 2009). Images were acquired for September 3, 1977, August 12, 1990,

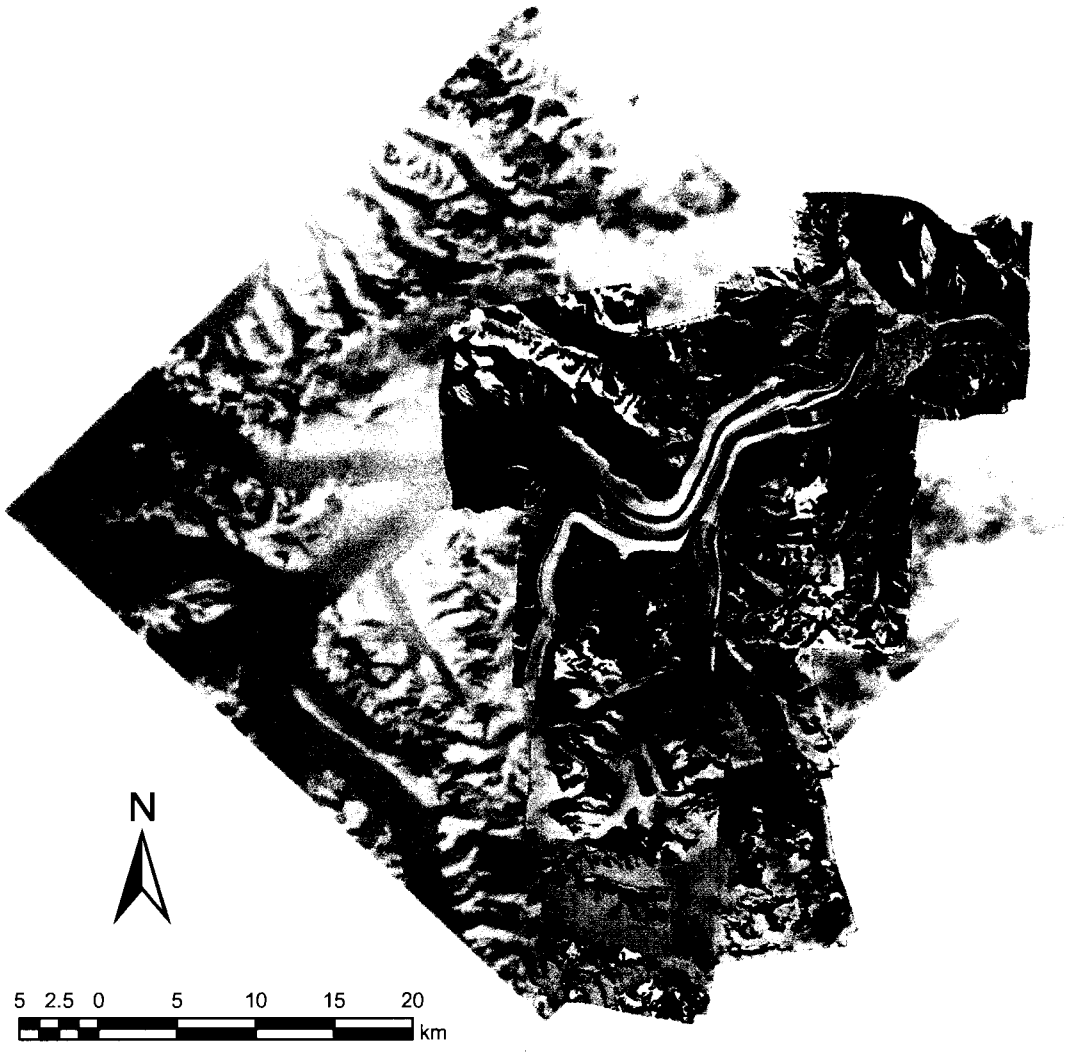

Figure 2.13: Mosaic of registered aerial photographs from 1956 displayed over the 2007 SPOT-5 image.

August 16, 1994, July 19, 2001, June 9, 2007, August 12, 2007, and August 28, 2007 (Figure 2.14; Table 2.1), which enabled the creation of digitized perimeters of the Kaskawulsh Glacier for these dates.

Images from 2007 have bands with missing data due to a damaged sensor on the Landsat-7 satellite. Data gaps alternate for varying acquisition dates, therefore data in one image may be used to fill bands of missing data in another image. In the accumulation zone, bands of missing data in the June 9, 2007 image are supplemented with the August 12, 2007 image. Therefore between the two images, full coverage of the accumulation area of the Kaskawulsh Glacier is available. At the terminus, the August 28, 2007 image uses the June 9, 2007 image to supplement the bands of missing data to allow full coverage of the glacier terminus.

c. ASTER images

Information on the acquisition of ASTER scenes is provided in Section 2.2.1e and Table 2.1. The georectified ASTER images were used to digitize the glacier extent for June 10, 2001, summer 2003 (through use of scenes acquired on May 20, 2003 and June 7, 2003) and March 2, 2006 (Figure 2.15).

d. SPOT-5 image

SPOT-5 (Satellite Pour l'Observation de la Terre) was launched in 2002 by CNES (Centre national d'études spatiales- the French space agency). This satellite offers multispectral (visible and infrared) images acquired by two high-resolution geometrical (HRG) instruments at 10 m resolution, as well as panchromatic images collected through the use of a high resolution stereo (HRS) instrument at a resolution of 2.5 m or 5 m. A SPOT image of the Kaskawulsh Glacier was acquired on September 3, 2007 (Figure 2.16) via a collaborative agreement with SPIRIT (Spot 5 stereoscopic survey of Polar Ices: Reference Images and Topographies). The image is panchromatic with a 5 m resolution.

2.3 Image Correction

In order to accurately quantify changes in areal extent and elevation of glacier ice, all data sources must be well aligned with each other. This ensures that true changes in the

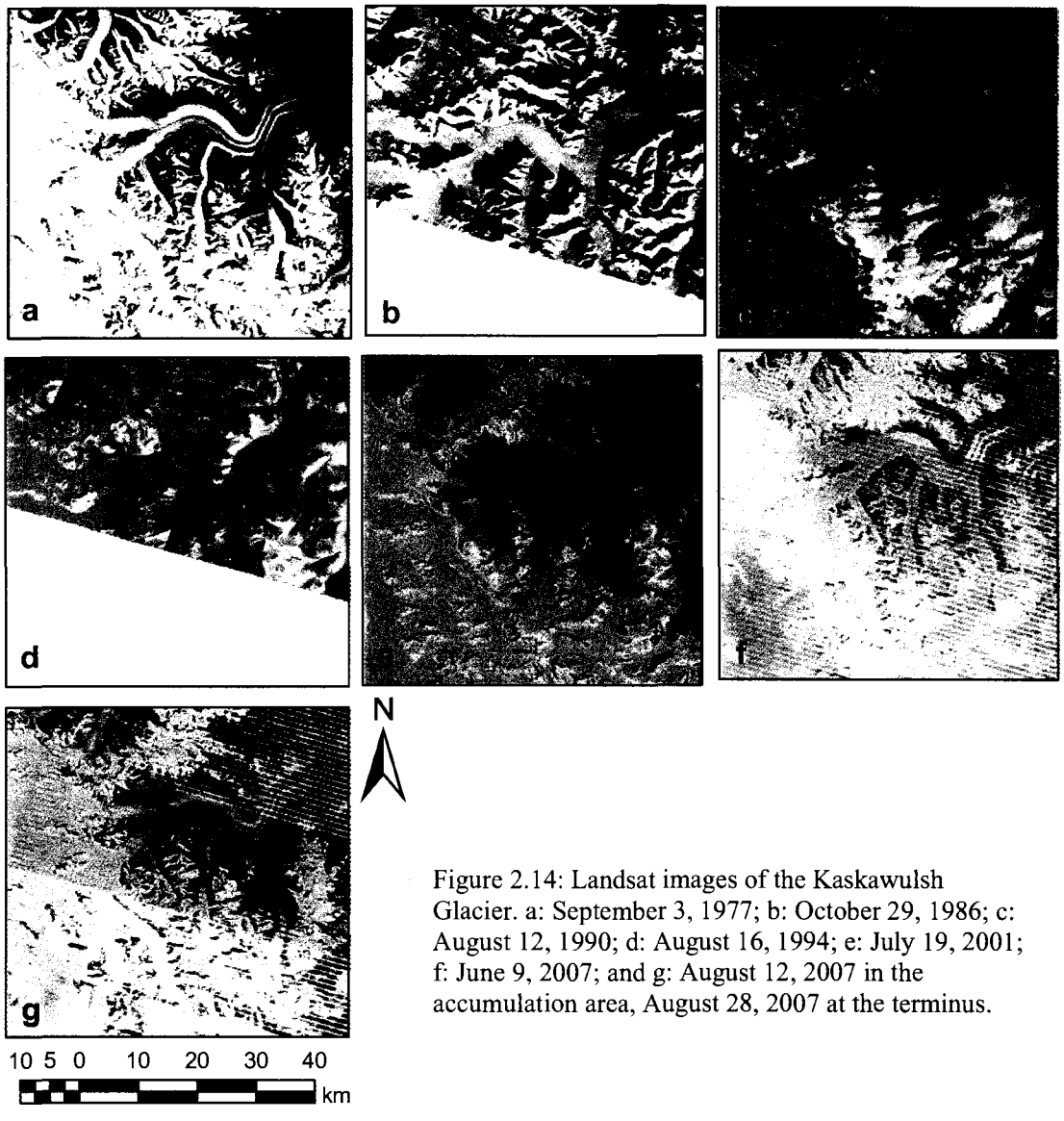

Figure 2.14: Landsat images of the Kaskawulsh Glacier. a: September 3, 1977; b: October 29, 1986; c: August 12, 1990; d: August 16, 1994; e: July 19, 2001; f: June 9, 2007; and g: August 12, 2007 in the accumulation area, August 28, 2007 at the terminus.

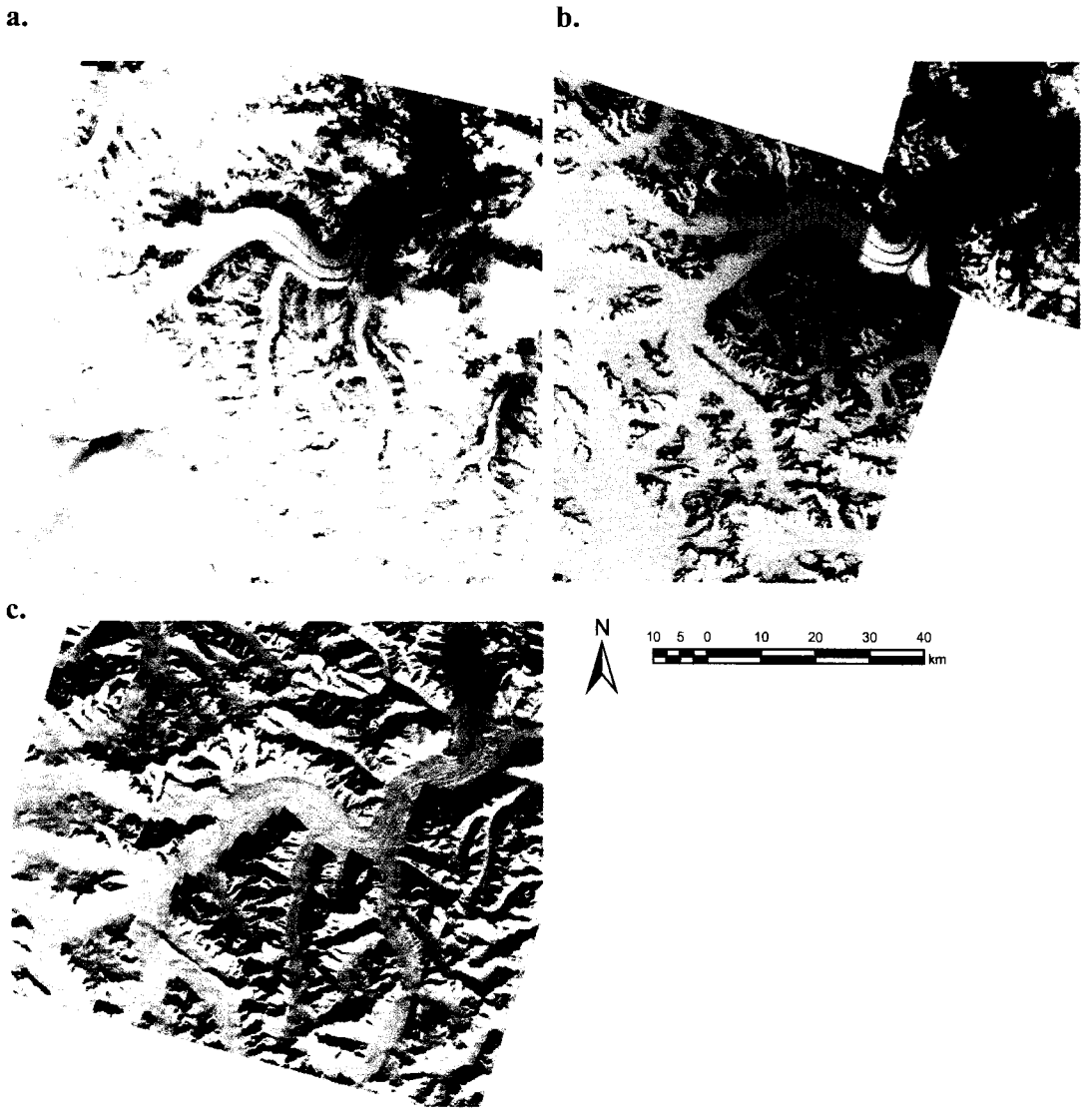

Figure 2.15: ASTER images of the Kaskawulsh Glacier. a: June 10, 2001; b: summer 2003 (through use of scenes acquired on May 20, 2003 and June 7, 2003); and c: March 2, 2006.

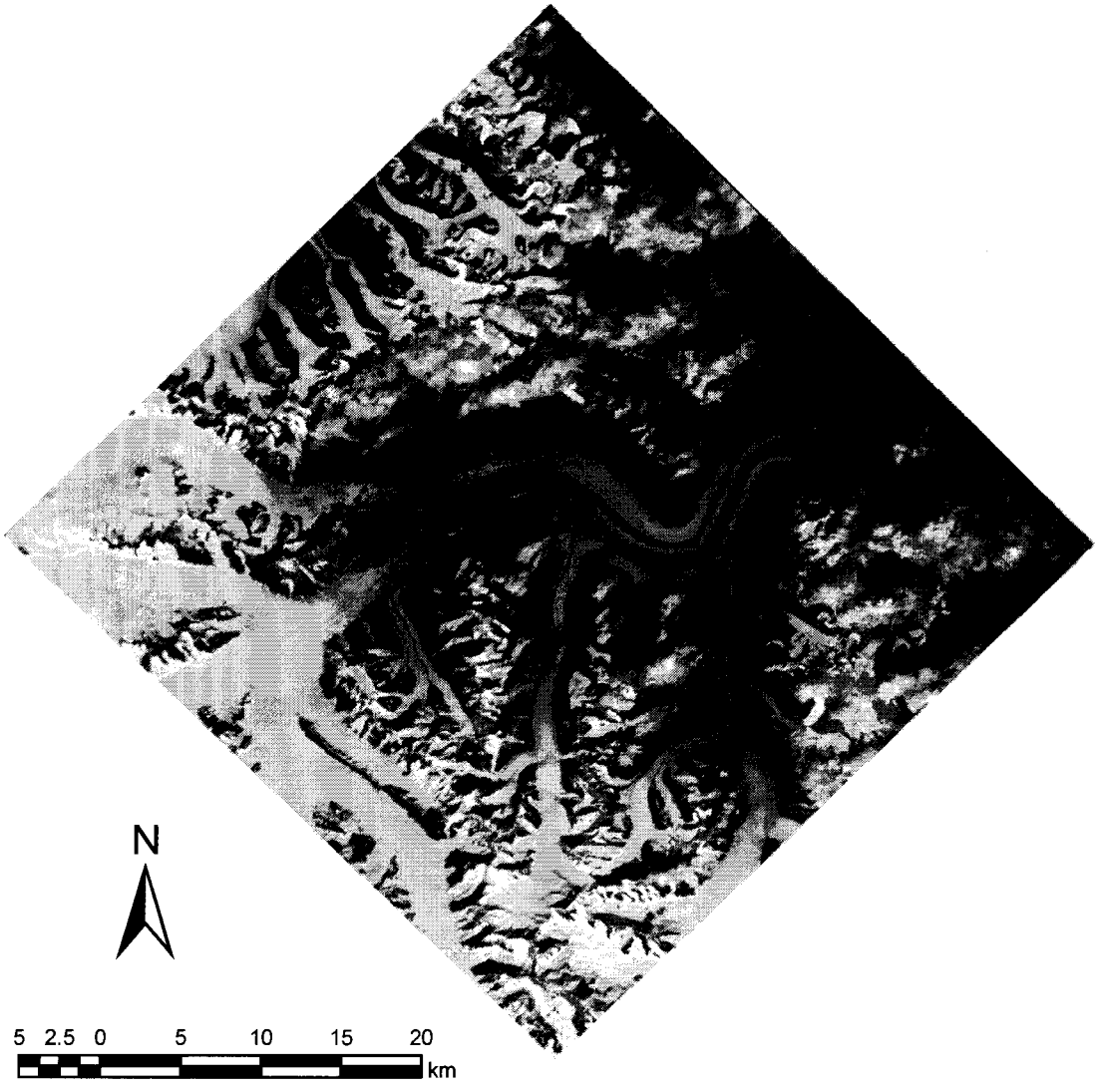

Figure 2.16: SPOT-5 image (5 m resolution) of the Kaskawulsh Glacier from September 3, 2007.

glacier are being measured, rather than artifacts created by inaccuracy in the relative positioning of images.

Besides inaccuracies associated with the x (longitudinal) and y (latitudinal) position of images, DEMs may contain errors in their z (elevation) values. For instance, when a cartographer creates a DEM from stereo satellite images, ground control points (GCPs) are required to match the scenes. GCPs are points of a known location which are easily recognizable on a map or a satellite image. In the accumulation area of glaciers, nearly continuous snow cover typically results in poor surface contrast and few exposed rock locations, which makes the identification of fixed reference points difficult. This makes relative changes in elevation very hard to determine, and vertical errors of 30-45 m are possible (Echelmeyer et al. 1996; Larsen et al. 2007). These errors tend to be lower below the equilibrium line where more reference points are available, where accuracies of +/-15 m may be assumed (Larsen et al. 2007).

When data sources are compared, the error becomes cumulative, which means that every effort needs to be made to minimize errors prior to comparative analysis. To help with this, fieldwork was conducted in 2008 to collect accurate GCPs. These GCPs were then used to register the xy position of all images used in this study, thereby ensuring that they overlaid one another properly. The GCPs were also used to verify the accuracy of the elevation values in the DEMs discussed in Section 2.2.1.

2.3.1 Fieldwork

When selecting a GCP in a glaciated region, it is important to select features which will not change in position (x, y) or elevation (z) over time; nothing located on or within ice or snow should be used as melt and ice flow will affect the position of these features. Thus the best GCPs are rock nunataks that are directly adjacent to glacier ice. Unfortunately nunataks may be sparsely distributed over a study region, which means that the use of other features is often required. For instance, a curving moraine may be used for horizontal (x, y) GCPs despite the fact that melting will cause the elevation (z) to change over time.

For this study, both nunatak and moraine GCPs were collected in July 2008 at sites that were accessible from camping locations. A Trimble R7 dGPS was used to determine the xyz position of GCPs. These positions are accurate to a few centimeters both horizontally

and vertically. The raw data was converted into RINEX files that were processed using Precise Point Positioning (PPP), a service provided by NRCan (http://www.geod.nrcan.gc.ca/products-produits/ppp_e.php, accessed Sept. 4, 2009). PPP uses highly accurate GPS orbital (ephemeris) and clock information to adjust the position of dGPS points without the use of a base station. The precise orbits are made publicly available 7 days after the date of observation by the International Geodynamics GPS Service (IGS). The PPP processing method is well suited to studies on glaciers where fixed bedrock locations are not available and/or easily accessible for the establishment of dGPS base stations.

The returned latitude/longitude .csv files were converted to UTM zone 7 coordinates in ITT Visual Information Solutions ENVI 4.4. These points were then imported into ESRI ArcMap 9.2 where they were compared against the 2007 SPOT-5 image. This image was georeferenced by Spot Image Corporation using GCPs obtained from a map and topographic surveys, and was projected into UTM Zone 7. The two datasets aligned very well, with an estimated error of +/- 2 pixels (10 m) (Figure 2.17). Therefore both the GCPs from the field and the 2007 SPOT-5 image were used to register all other satellite images and aerial photographs.

2.3.2 Registration of Images

When images did not align properly with the field sampled GCPs and the SPOT-5 image, georectification was required. Georectification is the process of matching image data to a set of geographical coordinates.

Satellite images and aerial photographs were imported into ESRI ArcMap 9.2 and registered using both the 2008 GCPs and the 2007 SPOT-5 satellite image. Because all datasets used have a defined coordinate system, each dataset was reprojected and integrated on the fly by ESRI ArcGIS 9.2 (ESRI ArcGIS 9.2 Desktop Help). For satellite images, between 20 and 70 tie points were selected across the image. The central moraine GCPs (Figure 2.17b) were used for ~6 tie points on average, while tie points on the SPOT-5 image were selected based on features that were stationary in time (not located on the ice or snow surface) and were easily recognizable on the corresponding satellite image or aerial photograph. An "adjust" transformation was then applied, which optimizes for local

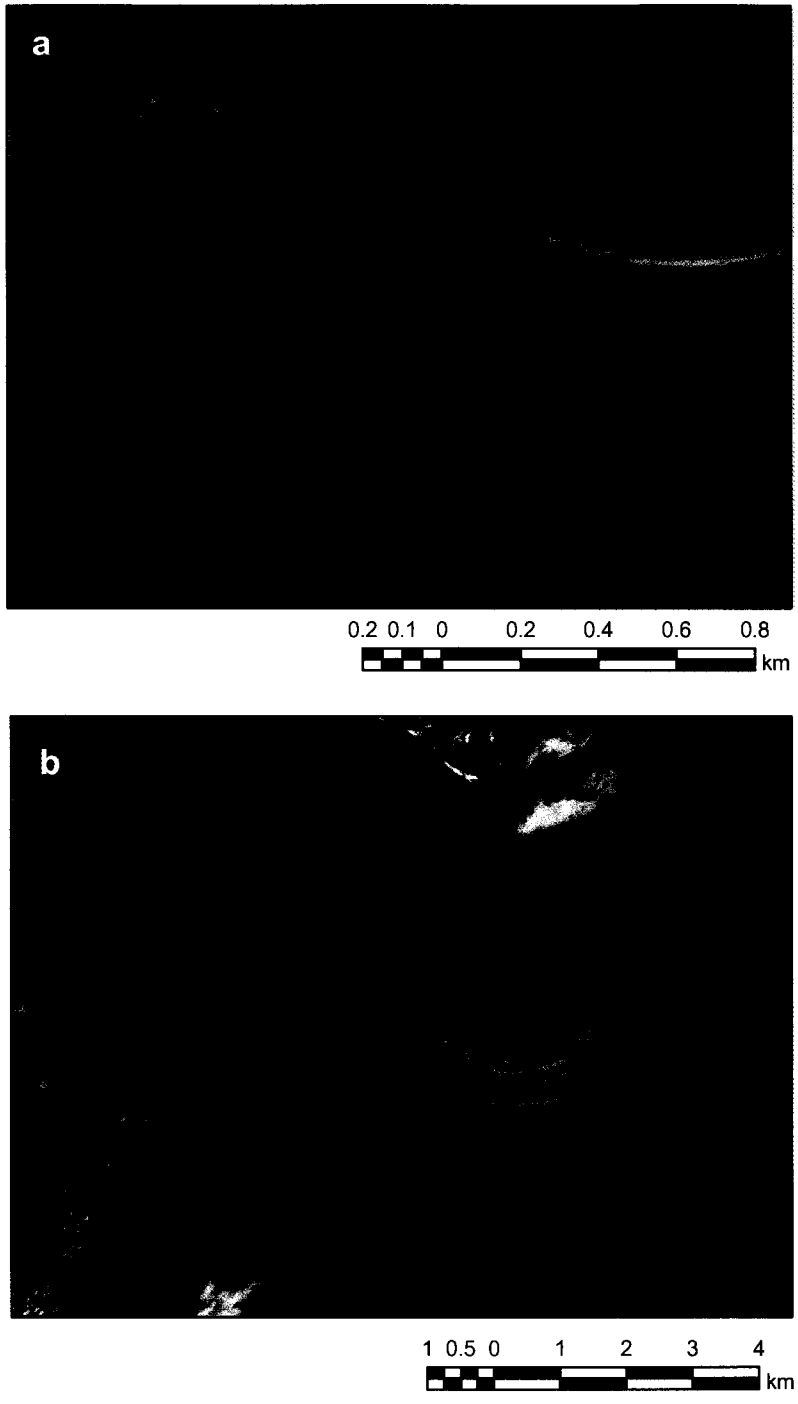

Figure 2.17: GCPs collected in summer 2008 superimposed on the 2007 SPOT-5 image from September 3, 2007
a: GCPs collected on the nunatak at the confluence between the north and central glacier arms
b: GCPs collected along the central glacier moraine

accuracy and the global least square fitting by using polynomial transformation and triangular irregular network (TIN) interpolation techniques. This transformation thus warps and/or shifts the image depending on how well the image initially aligns with the GCPs. This process creates a matrix of empty cells using map coordinates. These empty cells are not assigned values until they are resampled (ESRI ArcGIS 9.2 Desktop Help).

The warped images were saved when visual investigation revealed pixel alignment of all major features within the area of interest (the Kaskawulsh Glacier and its immediate surroundings), and the RMSE (root mean squared error) was <10 m, which is smaller than the resolution of any of the satellite images being registered (Table 2.1). The images were then resampled to make the files permanent. A cubic convolution interpolation was used for resampling as it tends to sharpen the data and is considered most appropriate for satellite imagery and aerial photographs; this interpolation calculates a weighted average value for each cell based on the cell centre values from the 16 nearest neighbours (ESRI ArcGIS 9.2 Desktop Help).

Registering of the aerial photographs followed the same general process. Although these files cover less geographic space (~230 km^2) than the satellite images (~29,650 km^2; the full extent of the glacier and its surroundings), they required more warping as the initial georeferencing was inaccurate. Therefore more tie points were selected (between 35 and 80 points were used for each photograph), and a spline transformation was applied to warp the images. A spline transformation optimizes for local accuracy by transforming the source control points exactly to the target control points. Pixels not used as tie points are not guaranteed to be accurate, which means that the more tie points used, the more accurate the transformation is. Like the adjust transformation, this process creates a matrix of empty cells using map coordinates which are not assigned values until the data is resampled (ESRI ArcGIS 9.2 Desktop Help). Resampling was performed using cubic convolution. An RMSE of <2 m was deemed acceptable for registration of the aerial photographs as the resolution of these images is 10 m. The registered aerial photographs were then mosaiced together in ESRI ArcMap 9.2 to provide the best available coverage of the Kaskawulsh Glacier (Figure 2.13).

The DEMs were not registered after their initial creation. Comparison of the 1959 USGS DEM to the digitized extent of the registered 1977 Landsat image reveals good

relative accuracy, with an approximate error of +/-4 pixels. Further correction could not be made to the 1959 DEM due to its position entirely within the accumulation area and the corresponding lack of control points. Comparison of the 1977 CDED DEM with the digitized extent of the georectified 1977 Landsat image reveals an approximate error of +/- 1 pixel. Therefore no warping of the 1977 DEM was required. Finally, the laser altimetry-derived DEMs did not require any warping due to the use of an IMU and dGPS during data acquisition.

2.4 Quantification of Glacier Changes

2.4.1 Determination of temporal changes in elevation along the glacier surface

Elevation data for the Kaskawulsh Glacier was obtained for five periods between 1959 and 2007 from a variety of techniques including stereo aerial photography, stereo satellite imagery and airborne laser altimetry. A DEM (digital elevation model) was created for each dataset. By differencing DEMs collected in different years, the spatial distribution of ice thinning/thickening along the Kaskawulsh Glacier was obtained.

2.4.2 Determination of temporal changes in areal extent

The terminal position of the Kaskawulsh Glacier was digitized for all areal datasets (Table 2.1), and a shapefile was created for each terminus position. For the 2001 digitized terminus, the ASTER image was primarily used due to its higher resolution. However due to cloud over the eastern terminus lobe, the 2001 Landsat image was also used to determine the terminal position for this year. For 2007 the position of the terminus for August 28 was digitized using the June 9 image to supplement data gaps. For all other terminus positions, only one image was used.

To determine temporal changes in terminus position, measurements were taken along 27 planes in the direction of ice flow between the old and new glacier front (Figure 2.18). The average of these measurements was then used to quantify the displacement of the terminus over time (Arendt et al. 2006).

In the accumulation area of the Kaskawulsh Glacier, changes in extent are examined through changes in the area of exposed rock (nunataks). Due to difficulties in georeferencing of images over an icefield, as well as intermittent cloud cover, only five different complexes

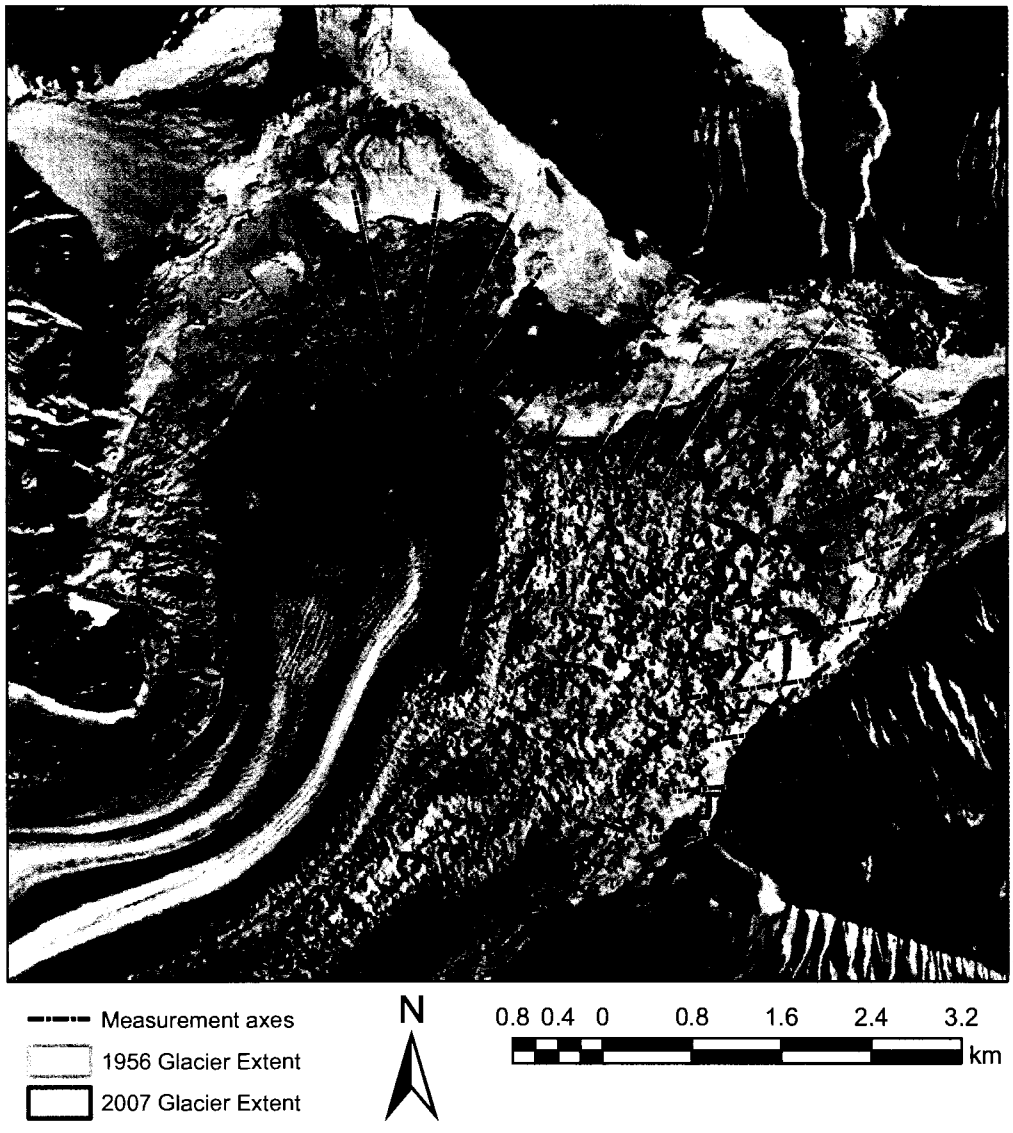

Figure 2.18: Planes along which change in terminus position were measured displayed over the 1956 air photo mosaic.

of exposed rock were examined (Figure 2.19). An effort was made to select rock complexes on each of the glacier arms to maximize representativeness of the findings in the accumulation zone. Furthermore, in order to avoid the impact of seasonal snowfall skewing results, only images from late summer and early fall were selected for this portion of the analysis. The outlines of the exposed rock complexes were stored as shapefiles, and the field calculator in ESRI ArcMap 9.2 was used to calculate their areas using the following:

```
Dim dblArea as double
Dim pArea as IArea
Set pArea = [shape]
dblArea = pArea.area
```

This routine outputs a field in the attribute table indicating the area of the polygon in square metres. When a shapefile consisted of more than one polygon, the areas of all polygons were added together. The changes in exposed rock area over time were then compared.

To calculate the total area of exposed rock in the accumulation zone, the 1977 shapefile of the glacier was clipped to create a polygon of only the upper glacier. Another polygon was created to cover areas of both exposed rock and the glacier accumulation zone above the glacier's equilibrium line. The differences in area between these polygons then yielded the total area of exposed rock in the accumulation zone of the glacier for 1977.

A simple ratio between changes in area of the five rock complexes studied and the total exposed rock in the accumulation zone could then be established. This allowed calculation of the periodic area change in exposed rock in the accumulation zone of the Kaskawulsh Glacier. Because the exposed rock enlarges at the expense of glacier ice, this change in exposed rock can be taken as proportional to the periodic change in area of the accumulation zone. This method incurs high potential errors as it assumes that all areas of exposed rock within the accumulation zone will respond uniformly to climatic perturbations. Nonetheless, in the absence of accurate ground control in the icefield ranges, this method provides the best available areal data for the accumulation zone.

Figure 2.19: Areas of exposed rock digitized in order to determine changes in glacier extent in the accumulation zone displayed over the 2007 SPOT-5 image.

2.4.3 Determination of changes in volume

Once changes in the surface elevation and area of the glacier have been calculated, the volume of ice loss over a given time interval can be calculated from:

$$\Delta v = (a_1 * \Delta h_1 + \Delta a_2 * h_2)_{acc} + (a_1 * \Delta h_1 + \Delta a_2 * h_2)_{abl} \quad (1)$$

where a_1 is the area of remaining glacier ice, Δh_1 is the change in elevation of the remaining glacier ice, Δa_2 is the change in area of the glacier, and h_2 is the former thickness of the ice that was removed. To determine spatial variability in volume changes, the glacier is subdivided into elevation regions, and the average ice loss in each region is calculated. The term with subscript "acc" represents values from above the ELA (equilibrium line altitude) in the accumulation zone, and the term with subscript "abl" represents values from below the ELA in the ablation zone. The change in ice volume in each region is added together to yield the total change in ice volume.

The equilibrium line is the plane along which annual snowmelt balances annual snow accumulation. For the period 1977-2007, the change in surface height is graphed against altitude. The y-intercept indicates where the change in surface height for this period is zero; above this line the glacier has experienced net accumulation, while below this line, the glacier has experienced net loss. The y-intercept can therefore be interpreted as the ELA for this period. For the period 1977-2007 the ELA is calculated at 1989 m, so in this study the glaciated area above 1989 m is considered the accumulation area, while the glaciated area below 1989 m is the ablation area .

The change in volume of the glacier is calculated for the time intervals over which elevation data is available (1977-1995, 1995-2000, 2000-2007 and 1977-2007). Note that these intervals are not exactly the same intervals over which data on changes in area is available (Table 2.1). However, for periods when an area measurement is available close to an elevation measurement (e.g., area is available for 1994, elevation for 1995), then by assuming a linear rate of change over the measurement period it is possible to adjust the area calculations to better match the elevation calculations. For example, using the known glacier areas in 1994 and 2000, the approximate area in 1995 can be calculated from:

$$a_{acc(1995)} = a_{acc(1994)} + (\Delta r * n) \quad (2)$$

where $\Delta a_{acc(1995)}$ is the area of the accumulation zone in 1995, $a_{acc(1994)}$ is the area of the accumulation zone in 1994, Δr is the average rate of change in area from 1994-2000 of the accumulation zone, and n is number of years of elapsed time. Using this adjustment method, the area of the glacier for 1995, 2000 and 2007 is calculated.

2.4.4 Determination of changes in water volume

To determine the change in water equivalent volume, the change in glacier volume must be multiplied by the ice/snow density. However, densities are not constant along the length of the glacier; glacier ice dominates the ablation zone and has a typical density of 0.90 g cm^{-3}. Densities are lower in the accumulation zone, where new snow accumulation gradually becomes compressed as it is buried and turns to firn and then ice. Using an 8.1 m deep density profile collected in a snowpit at an elevation of 2606 m in July 2007, the average density of snow at the surface of the accumulation area was determined to be 0.51 g cm^{-3}. The maximum density in the profile was 0.74 g cm^{-3}, measured at 8.1 m depth. The minimum density was 0.40 g cm^{-3}, measured at 5.1 m depth. Densities fluctuate randomly around the mean throughout the profile with a standard deviation of 0.11 g cm^{-3}. This depth (8.1 m) is generally representative of the order of thickness changes observed with the DEM data (Chapter 3), and was therefore used as a mean value for the accumulation area. By using these densities, the change in water equivalent for the glacier is therefore calculated from:

$$\Delta v_{we} = (a_1 * \Delta h_1 + \Delta a_2 * h_2)_{acc} * (d_1) \quad + (a_1 * \Delta h_1 + \Delta a_2 * h_2)_{abl} * (d_2) \quad (3)$$

where d_1 is the mean density of ice in the accumulation zone (0.51) and d_2 is the mean density of ice in the ablation zone (0.90).

2.4.5 Determination of a ratio between change in volume and change in terminal position

One of the simplest means of estimating changes in glacier mass balance is to monitor the position of the glacier's terminus (Paterson 1994). An advance of the terminus is

interpreted as an increase in mass balance, while a retreat of the terminus suggests a negative mass balance. From this a volume-area scaling ratio can be used to calculate the mass lost or gained from the glacier using these areal changes. However, traditional volume-area scaling ratios typically rely on simplistic models to calculate ice geometry, which assume flat beds, perfectly plastic solids, uniform accumulation and ablation rates, and one-dimensional surfaces on valley glaciers. The assumption that the extension of a glacier results in a correspondingly larger mass balance and vice versa can also be erroneous because the length, width and thickness of a glacier cannot be expected to scale in a constant manner (Bahr et al. 1997). Thus current volume-area scaling ratios are often inadequate.

At the moment, labour intensive remote sensing studies and/or expensive repeat field campaigns in remote regions are required to accurately determine whether a glacier has changed in volume (as is the case with the current study). However, once a detailed measure of glacier volume changes has been made, it should be possible to calculate a much improved area-volume scaling relationship for that region. The change in terminus position and elevation/volume for each observation interval in this study are therefore compared to determine whether such a relationship can be derived for the Kaskawulsh Glacier. If a robust relationship can be found it would greatly facilitate calculation of ice volume loss in Alaskan/Yukon glaciers from changes in area alone (which can be quickly and easily derived from repeat satellite imagery).

Chapter 3

3.0 Results

Changes in the Kaskawulsh Glacier, YT, are examined via changes in surface height, area and volume. Section 3.1 examines changes in surface height of the glacier for 5 separate intervals over the period 1959-2007. Section 3.2 investigates changes in the area of the glacier via changes in the area of the ablation zone and the accumulation zone. The ablation zone is defined as the area below the long-term ELA of 1989 m and is monitored via measurements of terminus displacement over 8 intervals over the period 1956-2007. Changes in the area of the accumulation zone are examined via changes in the area of exposed rock above the ELA for 5 intervals between 1956 and 2007.

Section 3.3 combines the changes in surface height and area to determine the changes in volume of the Kaskawulsh Glacier. Changes in volume are examined for 3 intervals between 1977 and 2007, and over the study period as a whole. Finally, the potential for a ratio relating terminus displacement, area, and volume change is evaluated statistically in Section 3.4.

3.1 Changes in Elevation

Since the 1950s the Kaskawulsh Glacier has thinned in general, which is broadly consistent with losses measured on other glaciers and ice caps both within this region (Arendt et al. 2002; Arendt et al. 2006; Chen et al. 2006a; Larsen et al. 2007) and globally (ACIA 2004; IPCC 2007; Meier et al. 2007; Meier and Dyurgerov 2002). However, the changes on the Kaskawulsh are not consistent through space or time, so here the patterns and rates of thinning/thickening are examined in detail. Between 1959 and 2007, four different time intervals are examined (1959-1977, 1977-1995, 1995-2000, 2000-2007), together with changes over the longest period for which data covering the entire glacier is available (1977-2007).

3.1.1 Elevation changes over 1959-1977

During the first observation interval, only the accumulation zone was observed as the 1959 DEM only covered this area (Figure 3.1). Due to significant errors in the 1959 DEM, elevation changes for this time period appear to be exaggerated. For instance, large areas

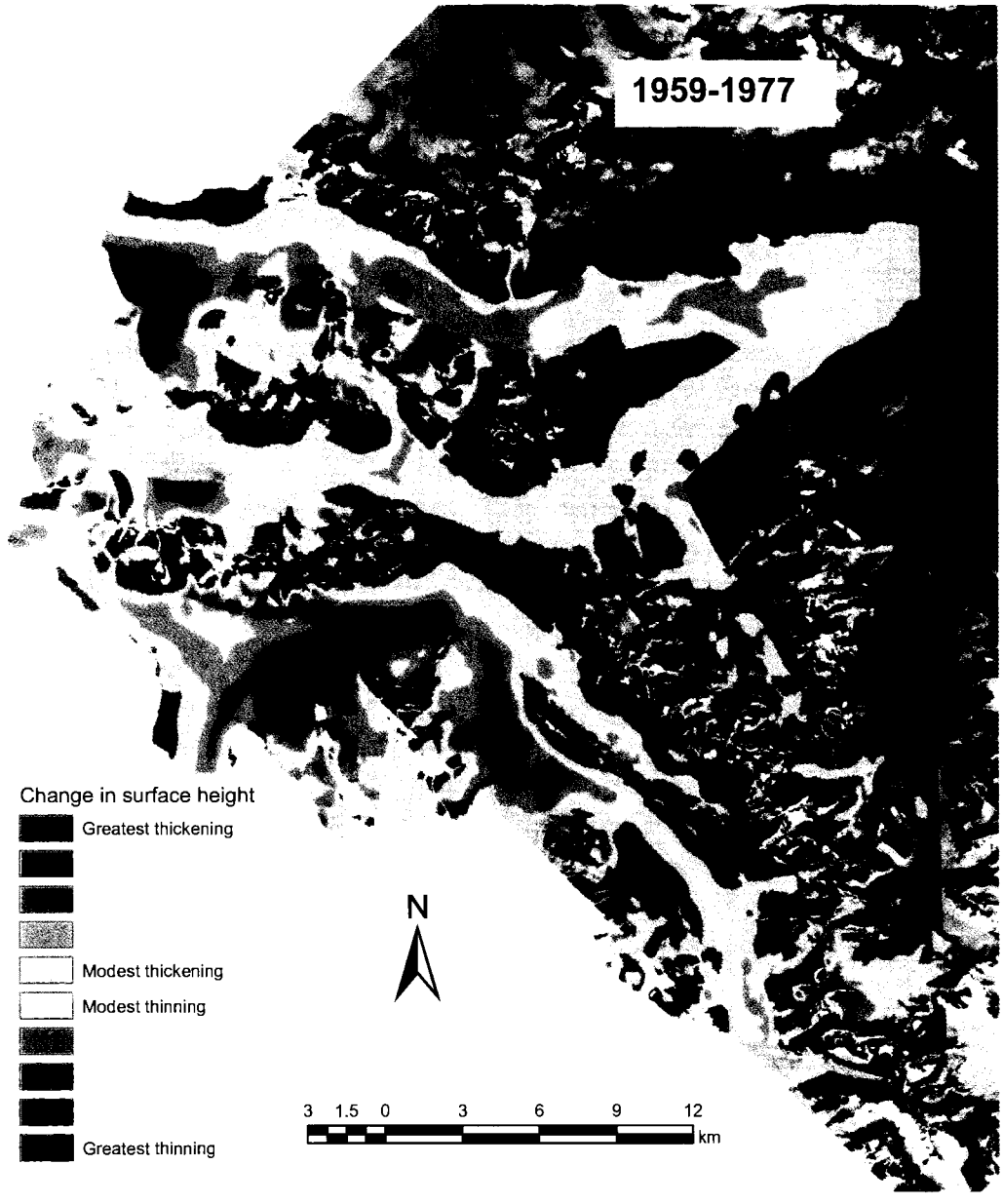

Figure 3.1: Surface elevation changes from 1959-1977 (1959 USGS DEM subtracted from the 1977 CDED DEM) displayed over the 2007 SPOT-5 image.

indicated thinning of up to 200 m, which would translate to a thinning of 11.1 m yr^{-1}. Various other areas appeared to undergo local thickening of up to 149.7 m, which represents a thickening rate of 8.3 m yr^{-1}. Thickness changes at these rates are not possible, and for this reason an absolute scale of thinning/thickening is not presented. Although the USGS quotes a vertical accuracy of +/-30 m, errors in the 1959 DEM are likely higher. Inaccuracy in this DEM likely arises from difficulties in extracting elevation data in an area with low contrast and an absence of GCPs for pair matching (Echelmeyer et al. 1996; Larsen et al. 2007).

The mean reduction in surface height for this time period, however, is 5.5 m, which translates to a rate of thinning of 0.3 m yr^{-1}. This thinning rate is plausible for the accumulation area of the Kaskawulsh Glacier. Most areas undergo this modest change, so while it is problematic to provide specific values for thinning, a general trend of modest glacial thinning seems reasonable. Because this data only covers the accumulation area of the glacier, glacier-wide thickness calculations cannot be made accurately for the period 1959-1977, nor can calculations of volume change.

In general, a positive relationship between change in surface height and altitude is observed and the relationship is statistically significant at the 99.9% confidence interval (Figure 3.2). The slope of the line (10.943) indicates that the change in surface height increases by 91.4 m km^{-1}, suggesting that thinning was greatest at lower elevations over this 18-year period. The y-intercept indicates where the change in elevation for this period is zero; above this line the glacier has experienced net accumulation, while below this line, the glacier has experienced net loss. The y-intercept can therefore be interpreted as the ELA, which in this case is 1970 m. However, the lack of data from the ablation area as well as the errors in the DEM means that this estimate should be treated with caution.

Graphs relating surface height change and altitude are displayed here with a superimposed linear regression line despite the fact that the data does not always meet the assumption of a normal distribution of residuals. Using other best-fit lines (e.g., polynomial) does not, however, resolve this problem. Thus, linear regression lines are useful for understanding existing data, although they cannot be used for predictive purposes. It is for this reason that low-elevation ice thinning over the period 1959-1977 cannot be calculated.

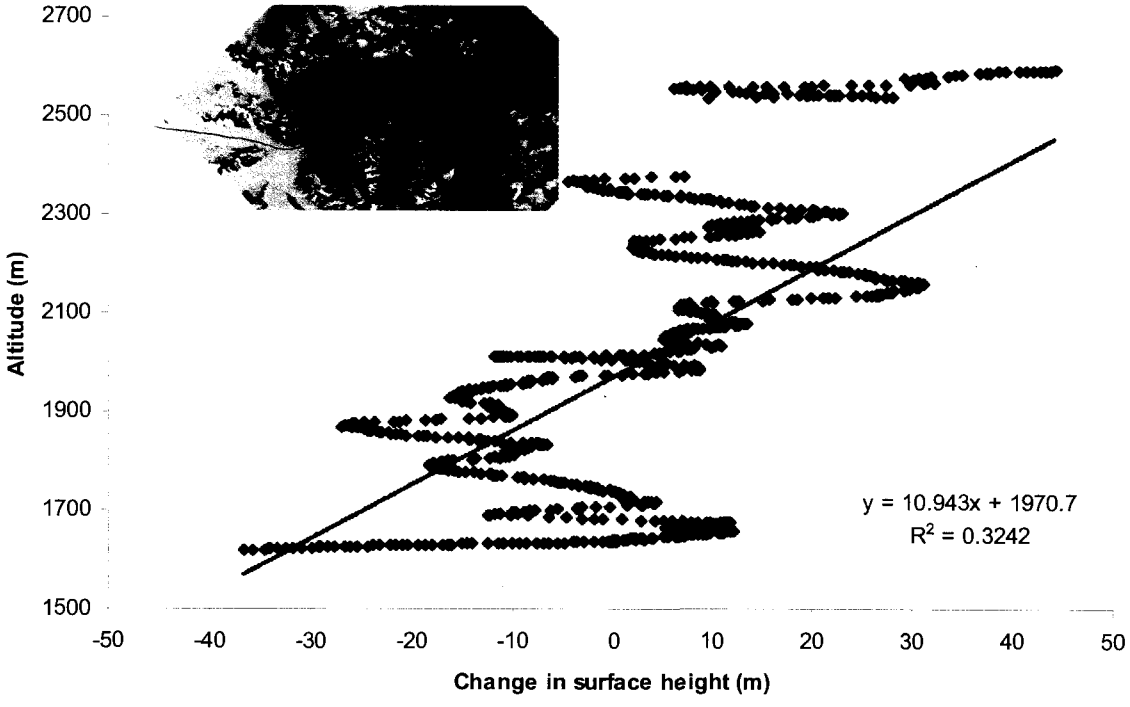

Figure 3.2: Relationship between changes in surface height and altitude (1959-1977) sampled from the profile shown in the inset map.

3.1.2 Elevation changes over 1977-1995

Figure 3.3 maps the change in elevation along the central arm of the Kaskawulsh Glacier between 1977 and 1995. Change measurements are limited by the areal coverage of the 1995 DEM; this DEM consists of a narrow center-line profile because it was acquired using a non-scanning laser altimeter. The maximum thinning experienced is 39.4 m, and this occurs in the ablation zone, primarily near the terminus. Thinning is prominent throughout the ablation zone, with only one area at an elevation of 1688 m asl that appears to have thickened (by ~17 m). Within the ablation zone the average change in surface elevation is a thinning of 15.6 m (Table 3.1), while the mean change in the accumulation zone is a thinning of 12.4 m (with only a few localized areas of apparent thickening). For the entire length of the glacier the mean thinning is 14.5 m, which constitutes an average rate of 0.8 m yr^{-1} for this 18-year period.

In general, the change in surface height increases at a rate of 54.6 m km^{-1} altitude, meaning that thinning is greatest at lower elevations (Figure 3.4). This relationship is statistically significant at a >99.9% confidence level. The ELA for this period (1977-1995) is located at 1878 m altitude (Figure 3.5). This calculated ELA approximates the ELAs derived from satellite images. On temperate glaciers, the snow line at the end of the summer season coincides roughly with the ELA and is visible in satellite imagery (Paterson 1994). Visual estimates using snow lines along the central arm of the glacier taken from Landsat images indicate an ELA of ~1813 m in 1977, and an ELA of ~1852 m in 1994 (Figure 3.6). ELAs derived from Landsat images must, however, be treated as approximations as they will be artificially low if image capture did not occur at the true end of the summer ablation season.

3.1.3 Elevation changes over 1995-2000

Between 1995 and 2000 thinning of the glacier continued, with maximum losses of 24.6 m occurring near the terminus (Figure 3.7). There are some small, isolated areas within the ablation zone that appear to undergo thickening of up to 3.4 m, although the localized nature of these changes suggests that they could be due to measurement error. For the ablation zone as a whole, the mean change in surface height is a thinning of 5.8 m (Table 3.1). In the accumulation zone, the mean change in elevation is a thinning of 2.7 m, although

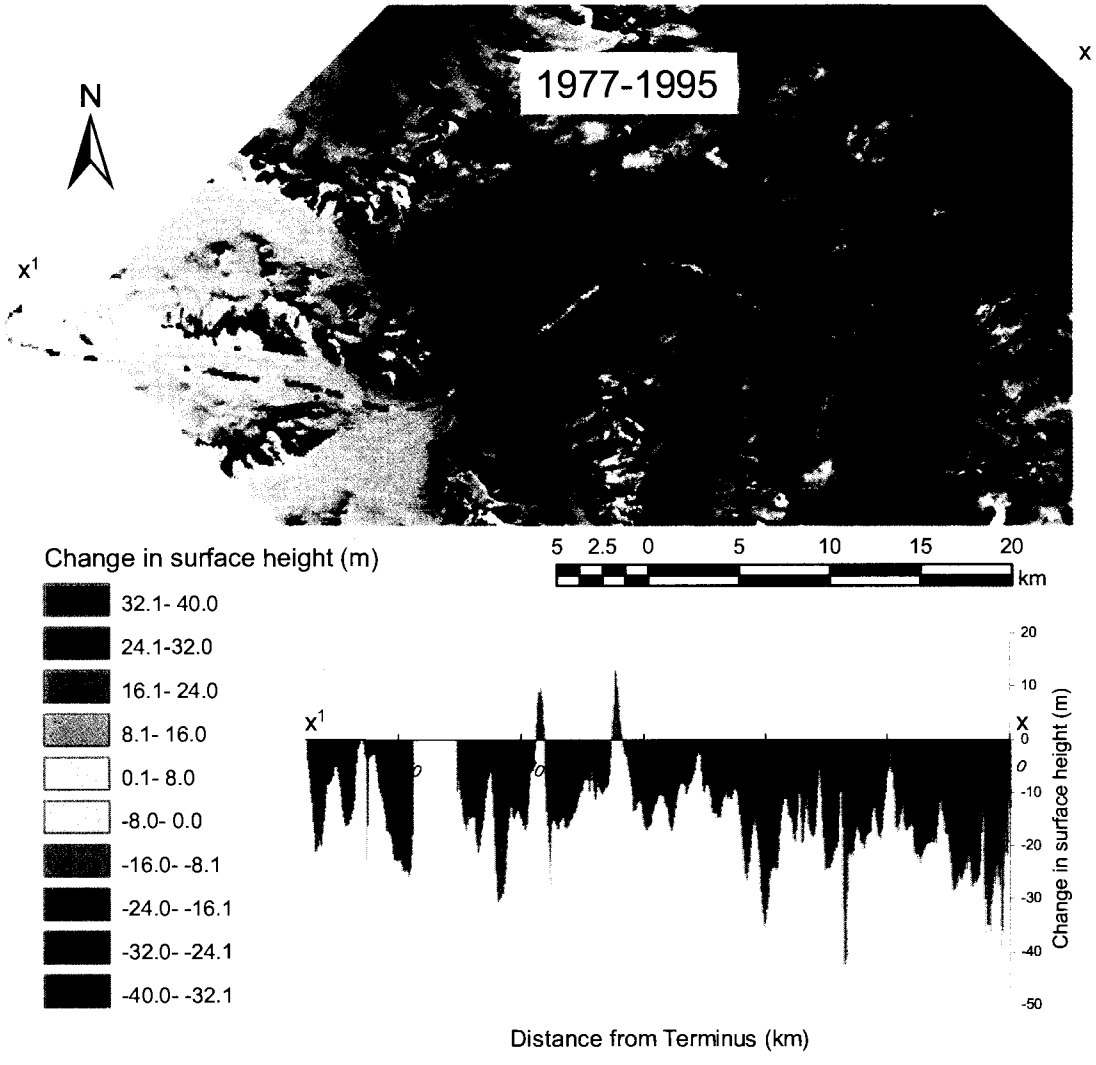

Figure 3.3: Surface elevation changes from 1977-1995 (1977 CDED DEM subtracted from the 1995 LIDAR DEM) displayed over the 2007 SPOT-5 image. The inset graph is a cross-section of the thinning/thickening along the profile (x to x^1).

Table 3.1: Thinning/thickening rates on the Kaskawulsh Glacier measured in this study

	Accumulation area (m)	Ablation area (m)	Full Glacier (m)	Rate (m yr^{-1})
1977-1995	-12.4	-15.6	-14.5	-0.8
1995-2000	-2.7	-5.8	-4.8	-1.0
2000-2007	16.9	0.5	5.7	0.8
Total of individual periods	1.8	-20.9	-13.6	-0.5
1977-2007 Swath Profile	-0.2	-10.2	-5.9	-0.2

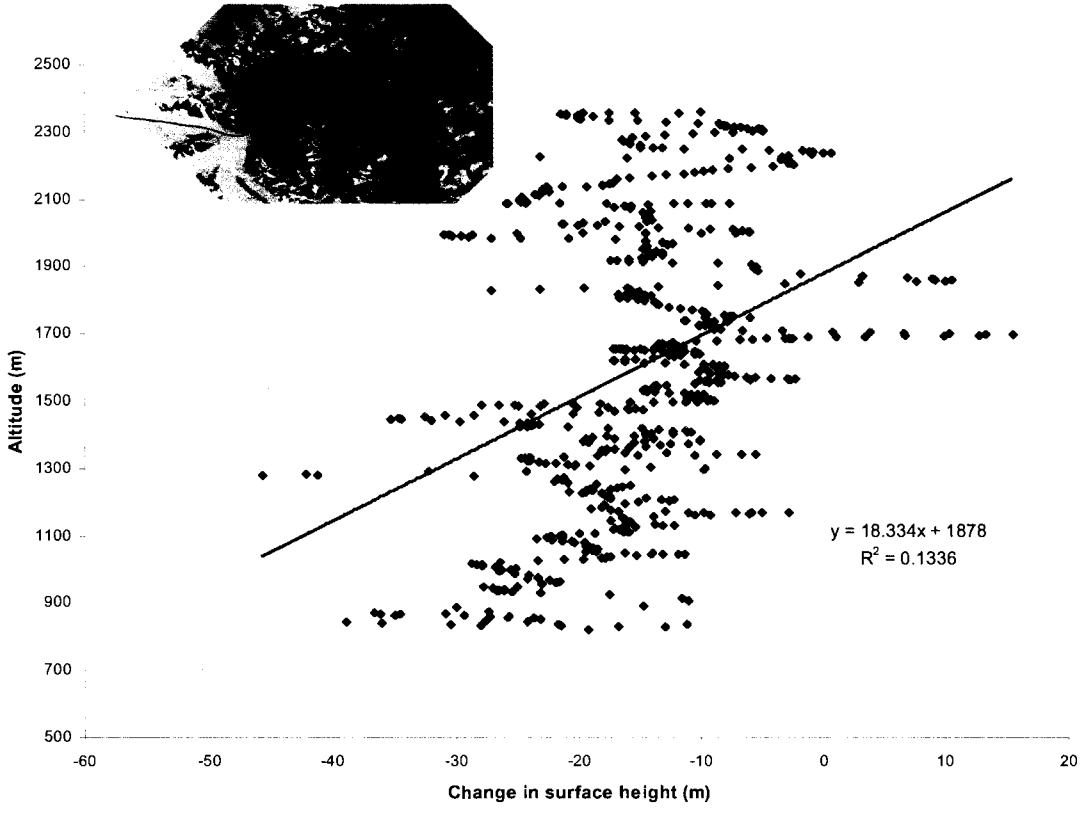

Figure 3.4: Relationship between changes in surface height and altitude (1977-1995) sampled from the profile shown in the inset map.

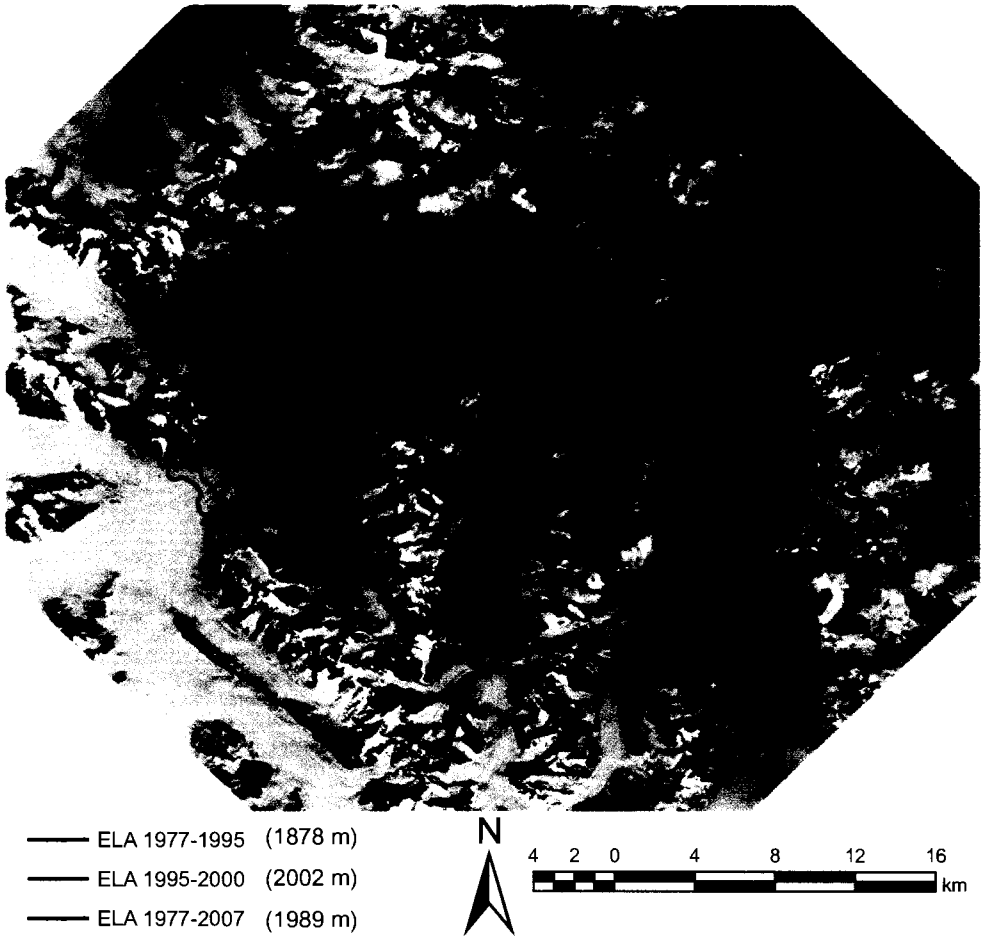

Figure 3.5: Changes in the position of the ELA (1977-2007). ELAs are displayed over the 2007, SPOT-5 image.

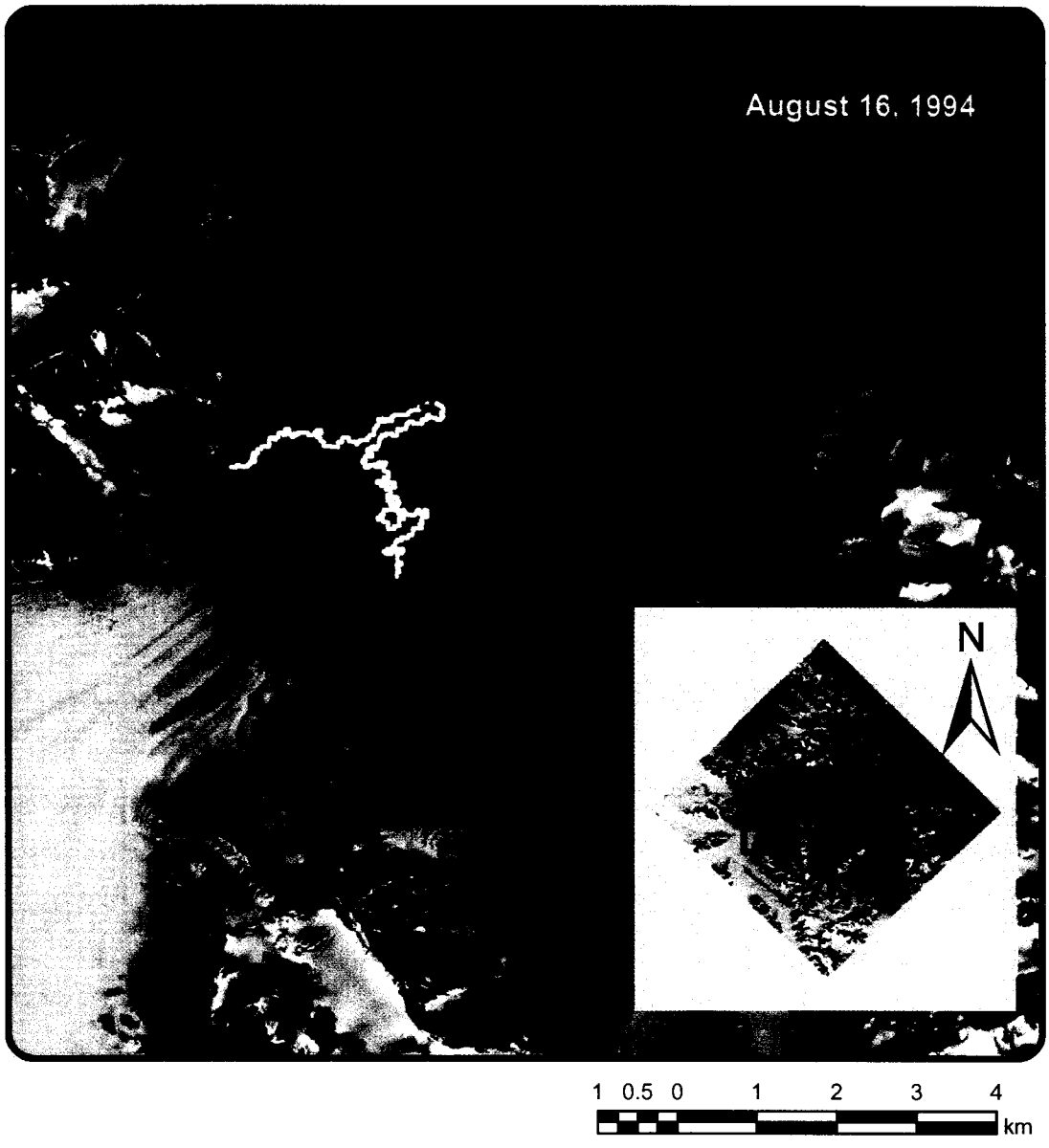

Figure 3.6: Changes in the position of the snowline for September 3, 1977 (1813 m), August 16, 1994 (1852 m), July 19, 2001 (1835 m), and August 28, 2007 (1954 m) digitized from Landsat images (Table 2.1). Late-summer snow lines can be interpreted as the ELA for temperate glaciers (Paterson 1994). ELAs are displayed over the 2007 SPOT-5 image.

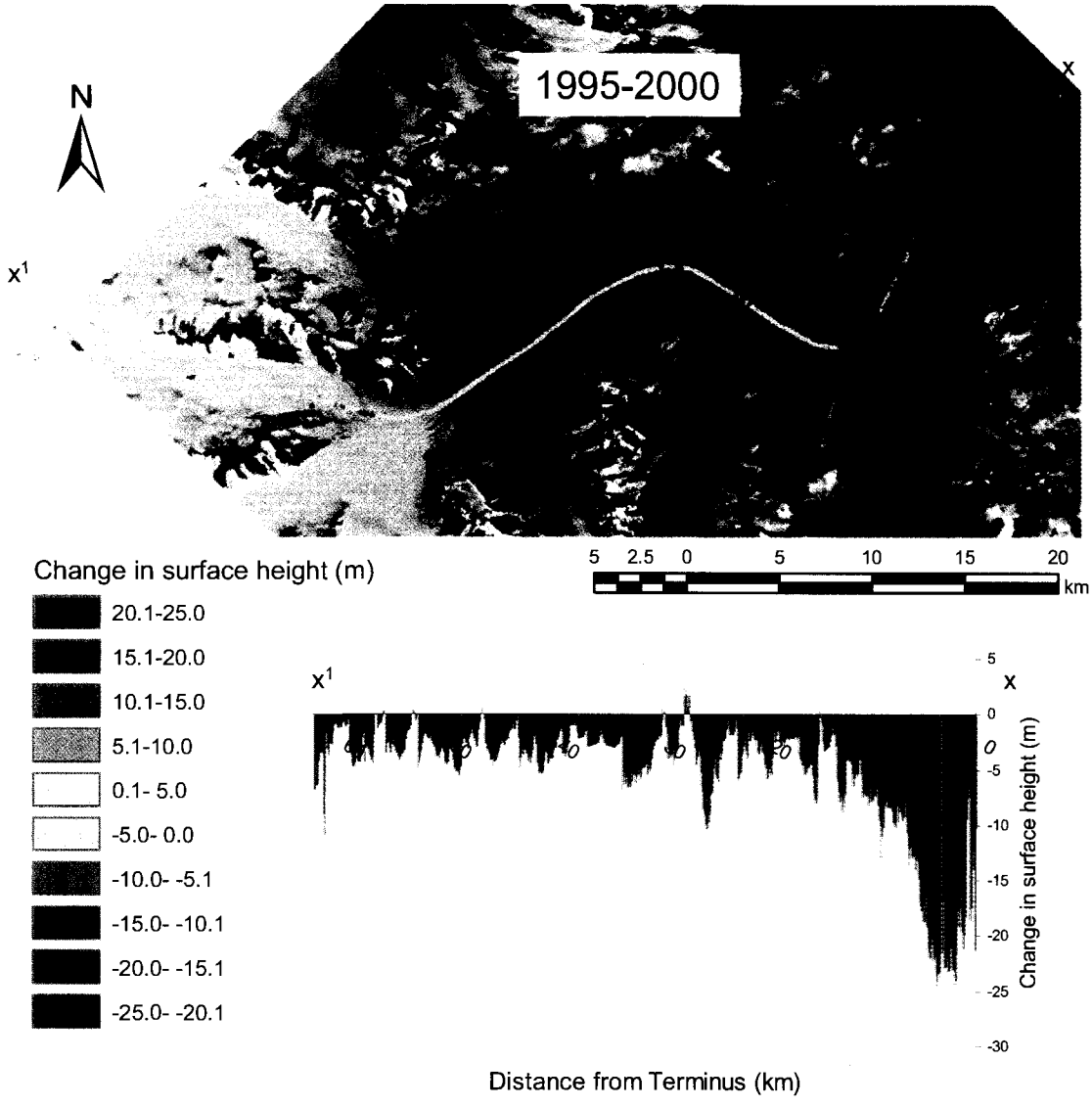

Figure 3.7: Surface elevation changes from 1995-2000 (1995 LIDAR DEM subtracted from the 2000 LIDAR DEM) displayed over the 2007 SPOT-5 image. The inset graph is a cross-section of the thinning/thickening along the profile (x to x^1).

some local areas do undergo thickening of up to 1.7 m. Overall, for the entire glacier length between 1995 and 2000, the mean thinning is 4.8 m, which constitutes a rate of thinning of 0.96 m yr^{-1}.

In general thinning decreases with increasing altitude, with an overall change in surface height of 17.0 m km^{-1} altitude (Figure 3.8). This relationship is statistically significant at the 99.9% confidence interval. The ELA for this period is located at 2002 m (Figure 3.5). Snow lines on the central arm of the glacier for this period (1994-2001) suggest a lower ELA of ~1843 m (Figure 3.6). This ELA may be artificially low, however, as the 2001 ELA is estimated from a Landsat image captured on July 19th that is unlikely to have captured the true end-of-summer snow line.

3.1.4 Elevation changes over 2000-2007

The elevation data for 2000 and 2007 do not overlap throughout most of the ablation zone. Therefore, interpolated data at the terminus is used in conjunction with the raw data in the accumulation zone to monitor change over this interval. Between 2000 and 2007, there is a significant change in the trends observed on the glacier compared to the earlier periods, with the glacier undergoing an average thickening (Figure 3.9). Despite prominent thinning of up to 27 m at the terminus (the lowermost 4 km of the glacier), the lower ablation area (below 1347 m) undergoes an average thickening of 0.5 m. In the accumulation zone, no areas of thinning are observed, and the average thickening is 16.9 m.

The average thickening for the length of the glacier for this period is calculated using a weighted average of the mean thickening in the accumulation and ablation zones, and amounts to 5.7 m. This is heavily biased by the gains in the accumulation area. Extrapolating change values from the terminus to the entire ablation zone is an important source of error over this period because negative changes are generally greatest at the terminus. Therefore this extrapolation would have caused an underestimation of gains over this period.

This 16.9 m surface height gain is a large amount of accumulation over a 7-year period, but we have little reason to discount the data because it compares the DEMs created from laser altimetry flightlines, which are considered to be the most accurate form of elevation data available in the accumulation area of glaciers (Hopkinson et al. 2001).

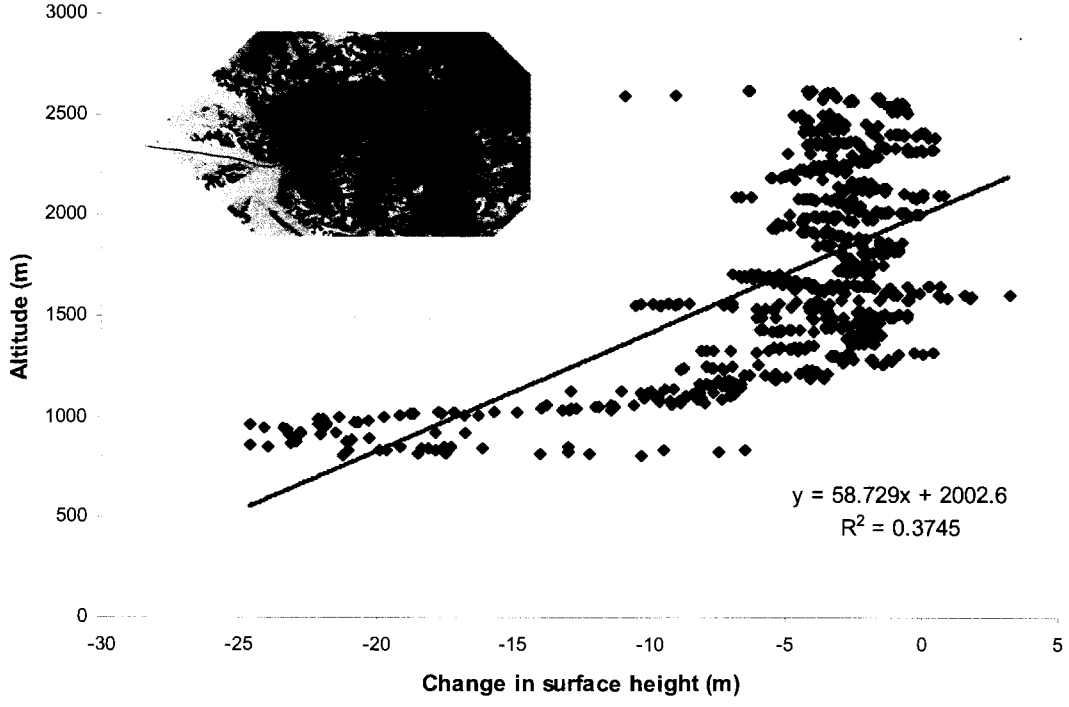

Figure 3.8: Relationship between changes in surface height and altitude (1995-2000) sampled from the profile shown in the inset map.

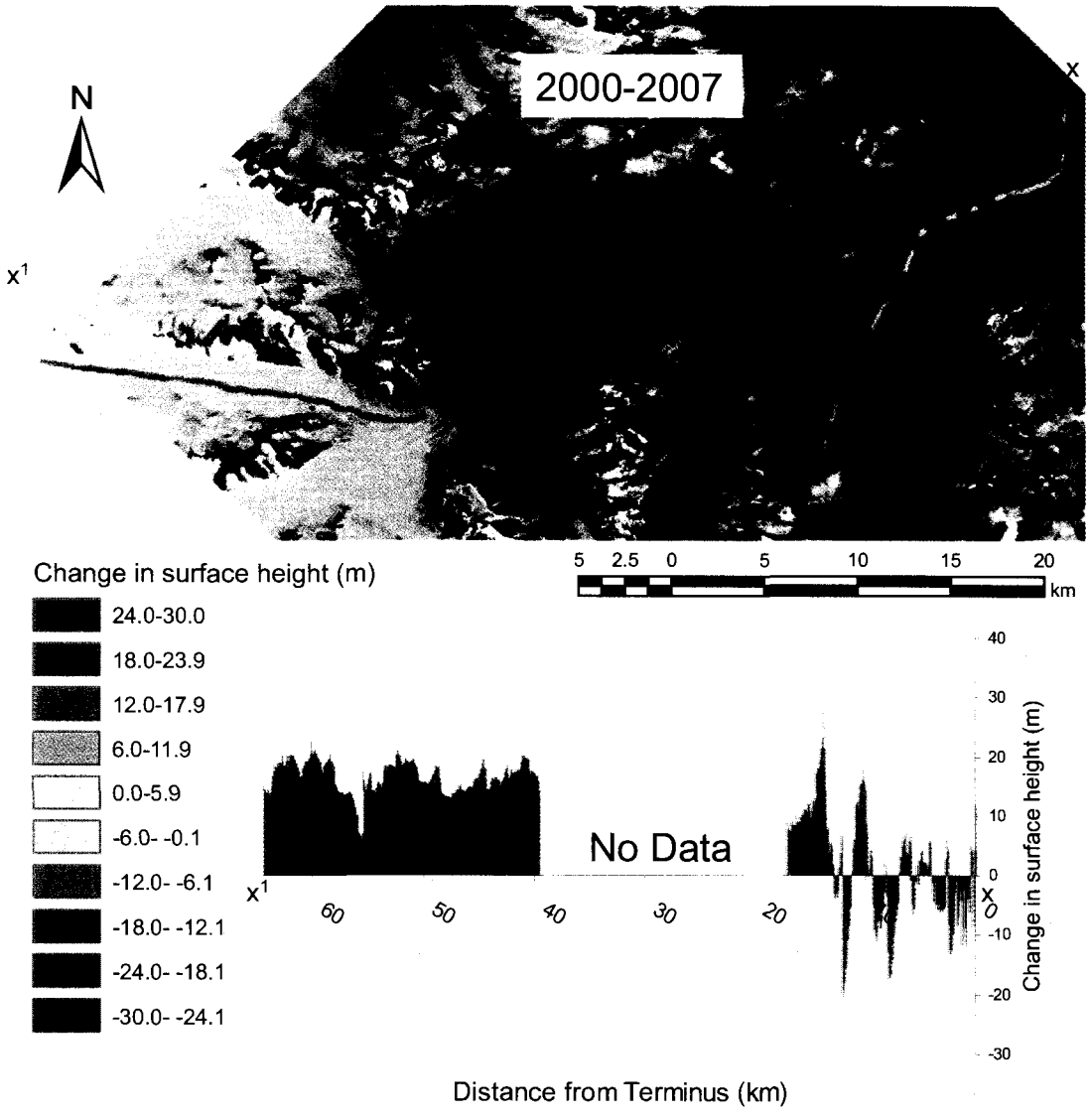

Figure 3.9: Surface elevation changes from 2000-2007; the ablation zone uses the 2000 LIDAR surface subtracted from an interpolated DEM from the 2007 scanning LIDAR data. The accumulation zone uses the 2000 LIDAR DEM subtracted from points sampled in the 2007 LIDAR profile. Changes in surface height are displayed over the 2007 SPOT-5 image. The inset graph is a cross-section of the thinning/thickening along the profile (x to x^1).

Furthermore, comparison against GCPs collected in summer 2008 suggest that the 2007 DEM is extremely accurate (to ~2.5 m vertically).

As a check on the LIDAR data, comparison can be made with data collected by a Campbell Scientific SR-50 ultrasonic snow-depth sounder in the accumulation area of the Kaskawulsh Glacier between 2003 and 2007 (Figure 3.10). This sounder measures the changing distance between the sensor and snow surface daily, and therefore records snow accumulation and ablation at the surface of the glacier. Simultaneously as data is being collected, the entire surface of the accumulation zone is being lowered due ice flow through the glacier system. The snow-depth sounder does not measure this surface depression because it is being lowered along with the glacier surface, although this is likely a minor factor as the SR-50 sensor was located near a drainage divide whose velocities are typically low. Figure 3.10 shows that between 2003 and 2007 there was a net increase in surface height of just over 14 m, or ~3.5 m yr^{-1}. Assuming a similar rate of accumulation between 2000 and 2003 (accumulation data prior to 2003 is not available), an estimated total snow accumulation of 24.5 m occurred between 2000 and 2007. Therefore average thickening of 16.9 m in the accumulation zone is not unreasonable. The remaining 7.6 m of accumulation could be compensated for by vertical ice motion.

Again there is a positive correlation between change in surface height and altitude; during this interval, the change in elevation is 21.6 m km^{-1} altitude (Figure 3.11). The y-intercept occurs at 1283 m. Although one would expect a lower ELA with glacial thickening, this is believed to be artificially low due to the missing data between 1345 m and 1825 m. Visual estimation of the ELA using the late summer snow lines indicates an ELA of ~1885 m for the period 2001-2007 (Figure 3.6).

3.1.5 Elevation changes over 1977-2007

Because the 1977 DEM covers the entire Kaskawulsh Glacier and the 2007 DEM was created using swath mapping, a greater area of the glacier can be compared for thickness change over the period 1977-2007. Using this increased coverage, the ablation zone thinned by an average of 10.2 m (Figure 3.12; Table 3.1). Thinning was particularly extensive across the glacier terminus, with maximum losses (up to 72 m) near the glacier centre. The accumulation zone underwent modest overall thinning of almost 0.2 m, although

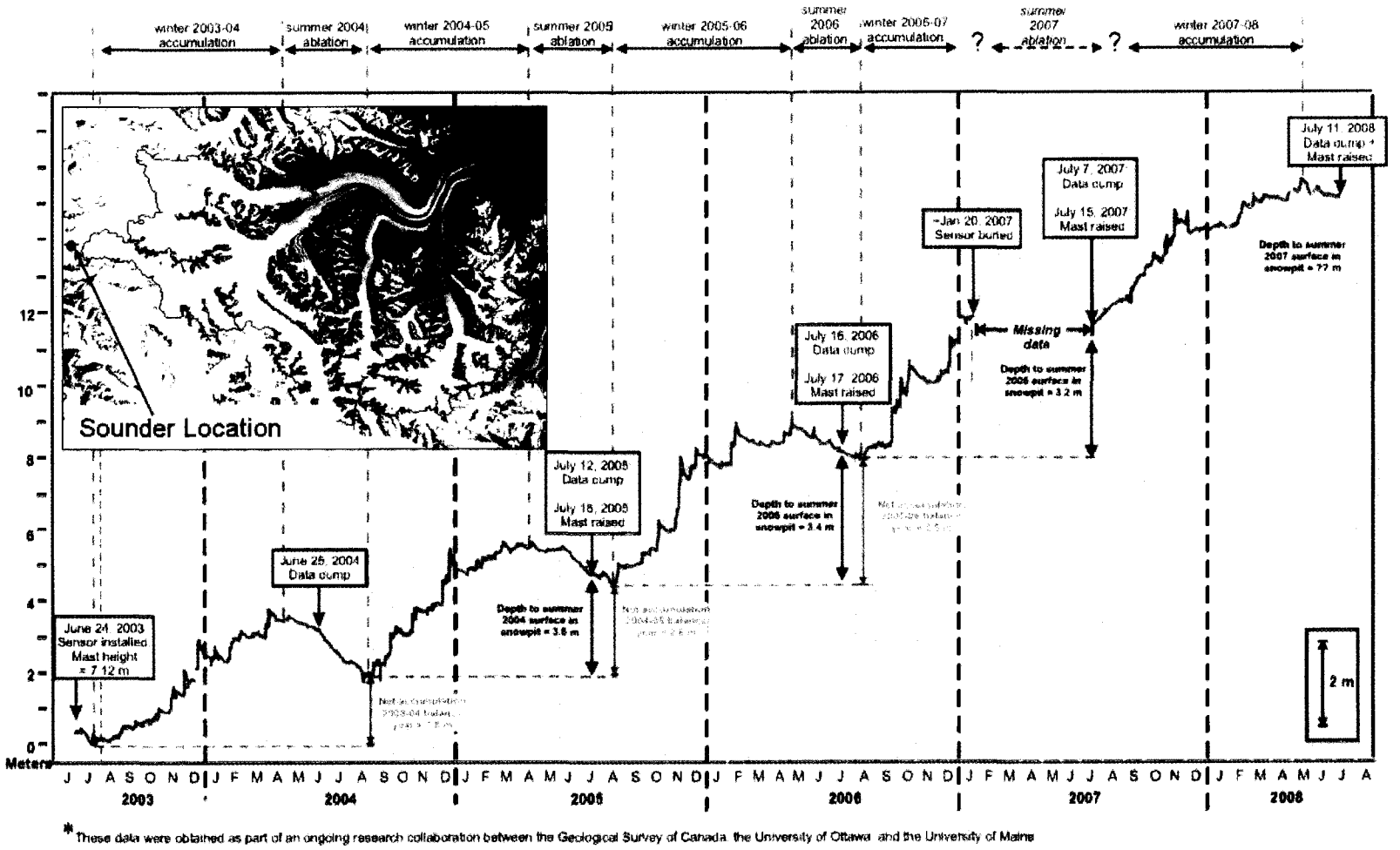

*These data were obtained as part of an ongoing research collaboration between the Geological Survey of Canada, the University of Ottawa, and the University of Maine

Figure 3.10: Snow accumulation at the Divide Station (2003-2007)
(Zdanowicz 2009; unpublished data)

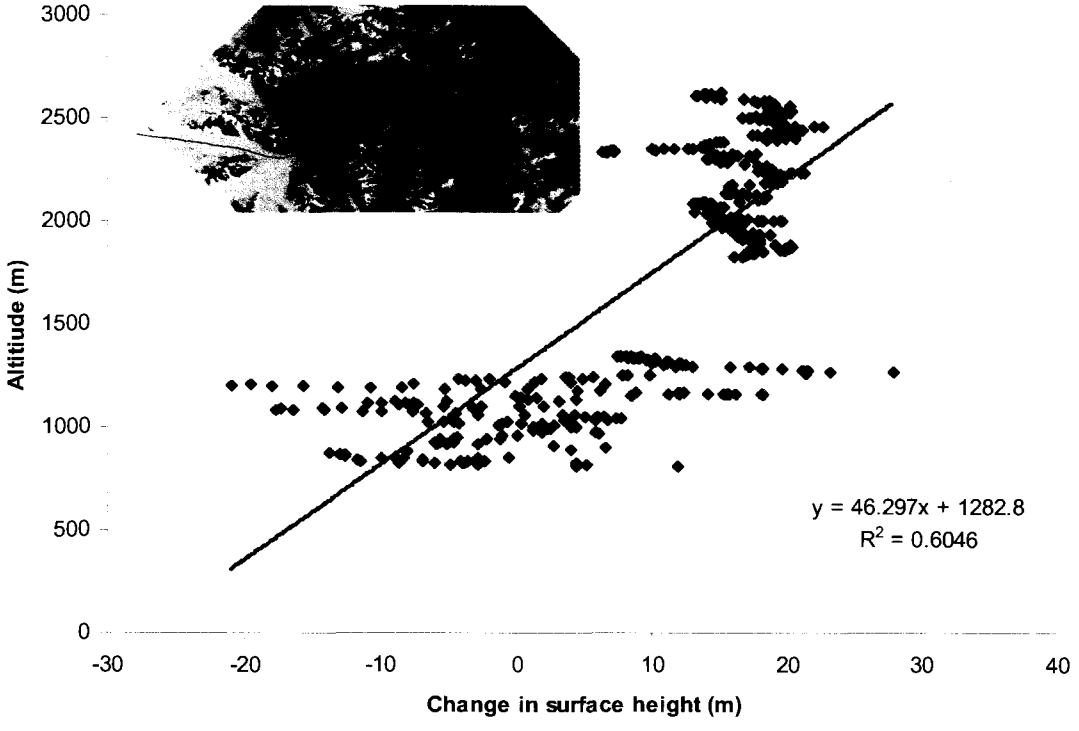

Figure 3.11: Relationship between changes in surface height and altitude (2000-2007) sampled from the profile shown in the inset map; the change in elevation in the ablation zone uses the 2000 LIDAR surface subtracted from an interpolated DEM from the 2007 scanning LIDAR data. The accumulation zone uses the 2000 LIDAR DEM subtracted from points sampled in the 2007 LIDAR profile.

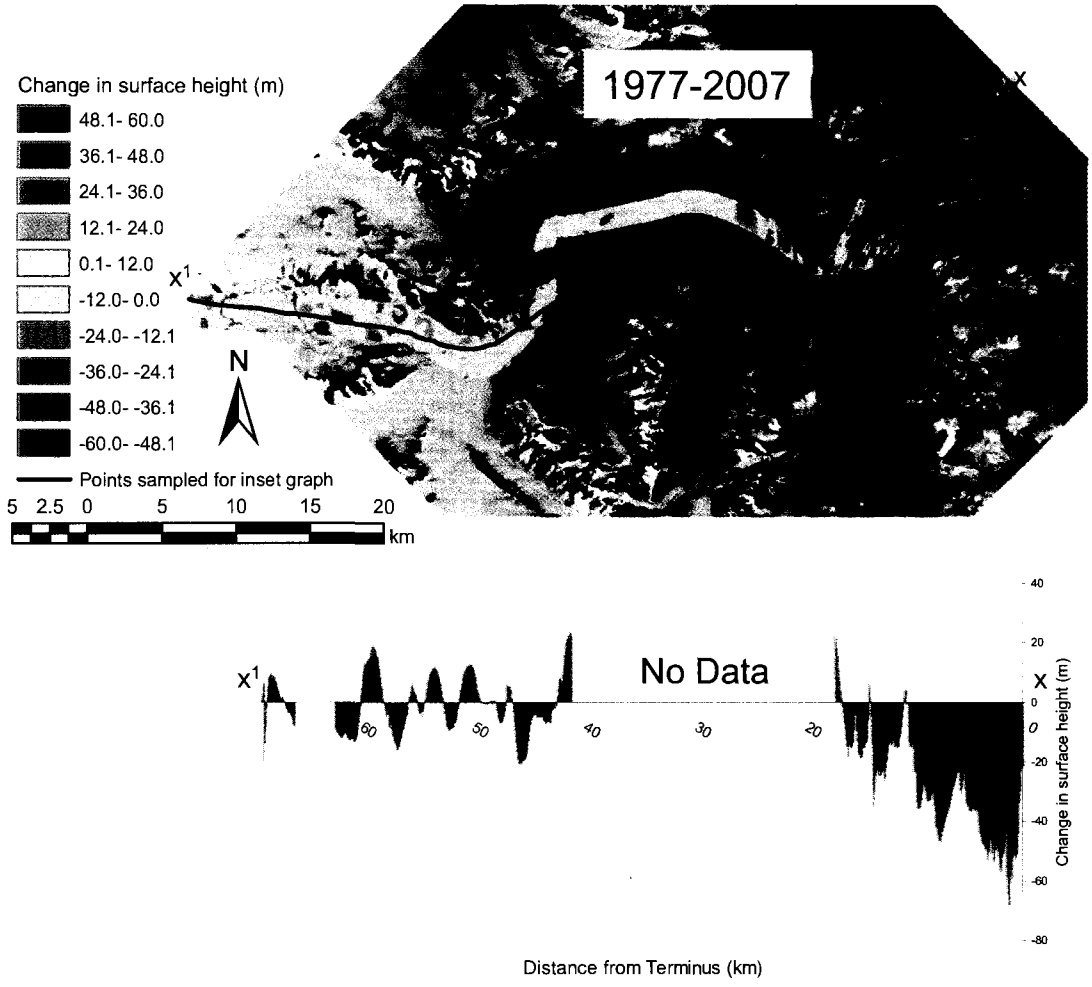

Figure 3.12: Surface elevation changes along the swath profile from 1977-2007 (1977 CDED DEM subtracted from the 2007 scanning LIDAR DEM). Changes in surface height are displayed over the 2007 SPOT-5 image. The inset graph is a cross-section of the thinning/thickening along the central profile (x to x^1) indicated in purple. This graph uses the 1977 CDED DEM subtracted from points sampled from an interpolated DEM from the 2007 scanning LIDAR data in the ablation zone. The accumulation zone uses the 1977 CDED DEM subtracted from points sampled in the 2007 LIDAR profile. The middle reaches of the graph show "No Data" as the centre line profile does not overlap the 2007 DEM in this region.

some areas along the glacier did experience localized thickening. Patches of thickening ice occur not only in the accumulation zone, but also in portions of the ablation zone above 1460 m. Overall the mean thinning on the Kaskawulsh Glacier between 1977 and 2007 is 5.9 m, which translates to a rate of thinning of 0.2 m yr^{-1}.

In general, thinning decreased with increased altitude (Figure 3.13). The rate of change of surface height increases by 46.9 m km^{-1} altitude, a relationship which is statistically significant at the 99.9% confidence interval. The 30-year ELA for the glacier is located at 1989 m (Figure 3.5). The average for this 30-year period as indicated by the snow lines on the central arm of the glacier for 1977, 1990, 1994, 2001, and 2007 is a much lower ELA of ~1859 m (Figure 3.6). This ELA may be artificially low, however, if the years sampled happened to be years with relatively large amounts of snow, and if the images used did not represent the true end-of-summer snow line.

When the individual thickness changes from 1977-1995, 1995-2000 and 2000-2007 are added together the accumulation area is shown to thicken by 1.8 m (Table 3.1). Thinning in the ablation area is calculated at 20.9 m using this method, producing an overall thinning of 13.6 m. These numbers do not agree particularly well with changes measured directly from 1977-2007 because narrow center-line profiles neglect differential thinning across the width of the glacier. Because the changes in thickness at the centre of the glacier arm are assumed to be constant across the width of the glacier for the periods 1977-1995, 1995-2000 and 2000-2007, between 1 and 3 m yr^{-1} of vertical error at the margins of the glacier may have been introduced, with errors likely to be greatest at low elevations (Arendt et al. 2008; Echelmeyer et al. 1996). The error introduced by ignoring this non-uniformity cannot be quantified due to data limitations which prevent data extrapolation across the middle section of the glacier for the period 2000-2007 (described in section 3.1.4). Thus an unquantified margin of error is assumed over the individual periods 1977-1995, 1995-2000, and 2000-2007. The overall changes from 1977-2007 avoids this error because when the wide swath of the 2007 DEM is compared to the full-coverage 1977 DEM, the variable thinning values across the width of the glacier are captured and incorporated into the average.

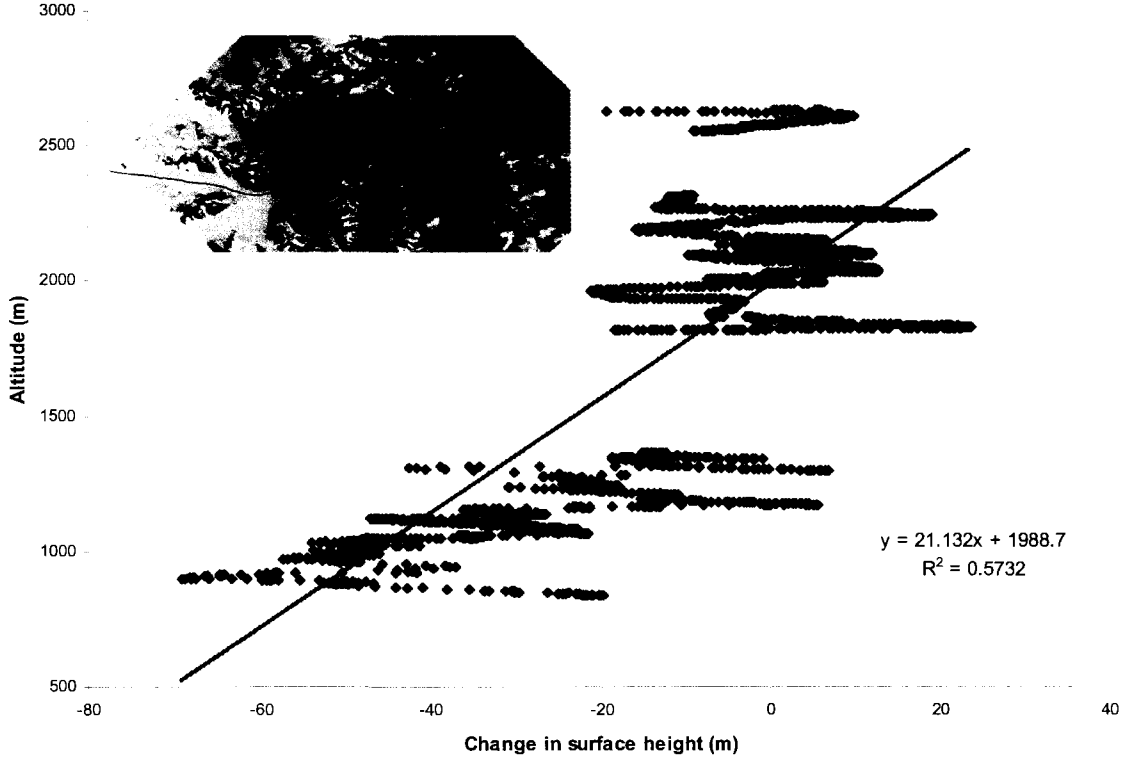

Figure 3.13: Relationship between changes in surface height and altitude (1977-2007) sampled from the profile shown in the inset map. The changes in the ablation zone are based on interpolation of the 2007 DEM differenced from the 1977 DEM. Changes in the accumulation zone represent points sampled in the 2007 LIDAR profile differenced from the 1977 DEM. The middle portion of the glacier is omitted from analysis.

3.1.6 Quantification of errors

There are several sources of error which might have impacted the results of this study. Figures 3.14 through 3.16 show the surface height profile of the glacier, with error bars indicating the amount of error associated with each data set. Figure 3.14 shows that relative changes in surface height fall outside of the error bars for 1977, 1995, and 2000. Therefore the large elevation changes noted at the terminus for these years are considered to be reliable. Some isolated portions of the 2007 profile show relative thickness changes against the 2000 profile that are generally so small compared to the error limits associated with these datasets, that changes noted between 2000 and 2007 fall within error limits. However for most of the profile below 1150m, relative changes from 2000 to 2007 fall outside of error bars. Changes in elevation between 1977 and 2007 are also well outside of the error bars for areas below 1150 m (10 km upglacier from the terminus; Figure 3.14).

Figure 3.15 shows that above 1150 m, relative changes in thickening/thinning become smaller. All changes between 1995 and 2000 fall between error bars. Changes between the 1977 and 1995 DEMs fall between error bars at an altitude of 1500 m. Thus, as altitude increases, relative changes are less distinguishable. Figure 3.16 shows that above 1800 m, the 1959 and 1977 elevation profiles fall between error bars. Changes between 1995 and 2000 are also negligible compared to the error bars indicated by these profiles. The gains noted between 2000 and 2007, however, do fall outside of the error bars. Therefore changes over this period within the accumulation zone are relatively reliable despite general ambiguity in other elevation values in the accumulation area. Errors throughout the glacier are equally as likely to have caused overestimation of thinning as thickening.

Further errors in elevation data are noted due to instrumental error and experimental error. For instance, when the interpolated 2007 DEM for the ablation area is compared to the original 2007 DEM, differences emerge. The interpolated DEM is on average 0.18 m more negative than the original DEM. The error cannot be corrected as it is not constant, although this error is minimal compared to the average changes indicated by this DEM (+0.5 m).

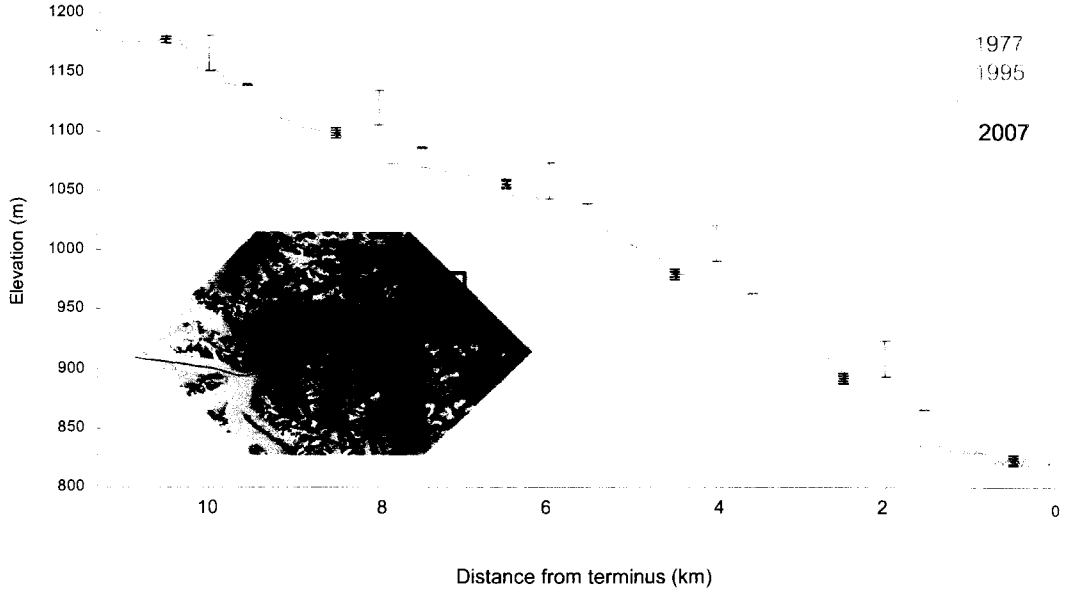

Figure 3.14: Elevation profile along the terminus of the glacier for 1977, 1995, 2000, and 2007. The navy line indicating the elevation of the terminus in 2007 is taken from an interpolation of the glacier surface, while all profiles from 1977, 1995 and 2000 are sampled directly from DEMs. Error bars for each line are indicated. The inset map indicates the location of the points sampled.

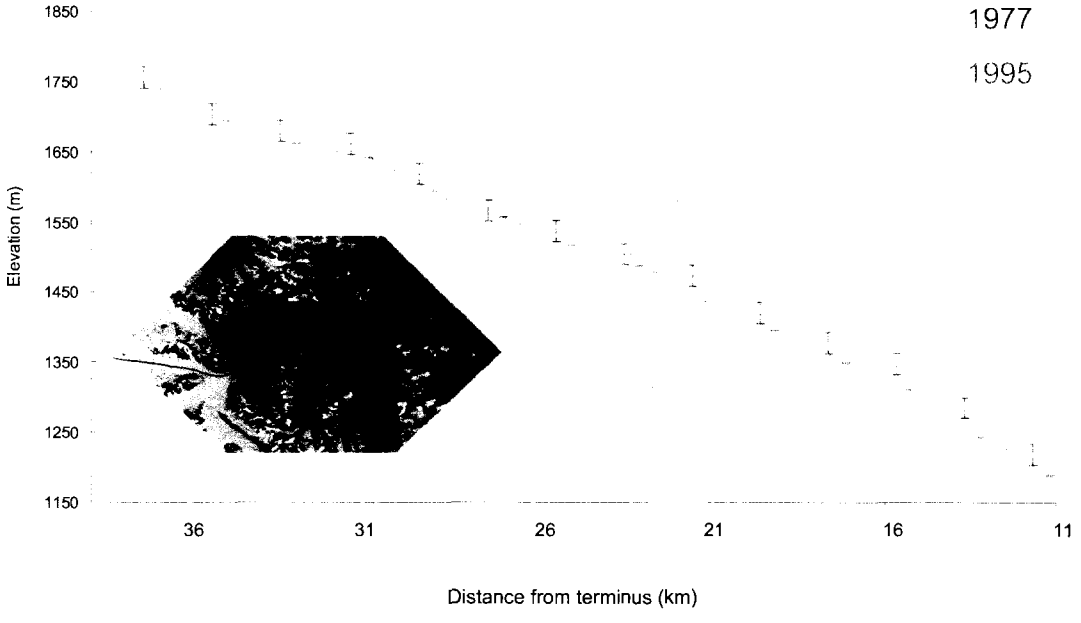

Figure 3.15: Elevation profile along the upper ablation area of the glacier for 1977, 1995, and 2000. Error bars for each line are indicated. The inset map indicates the location of the points sampled.

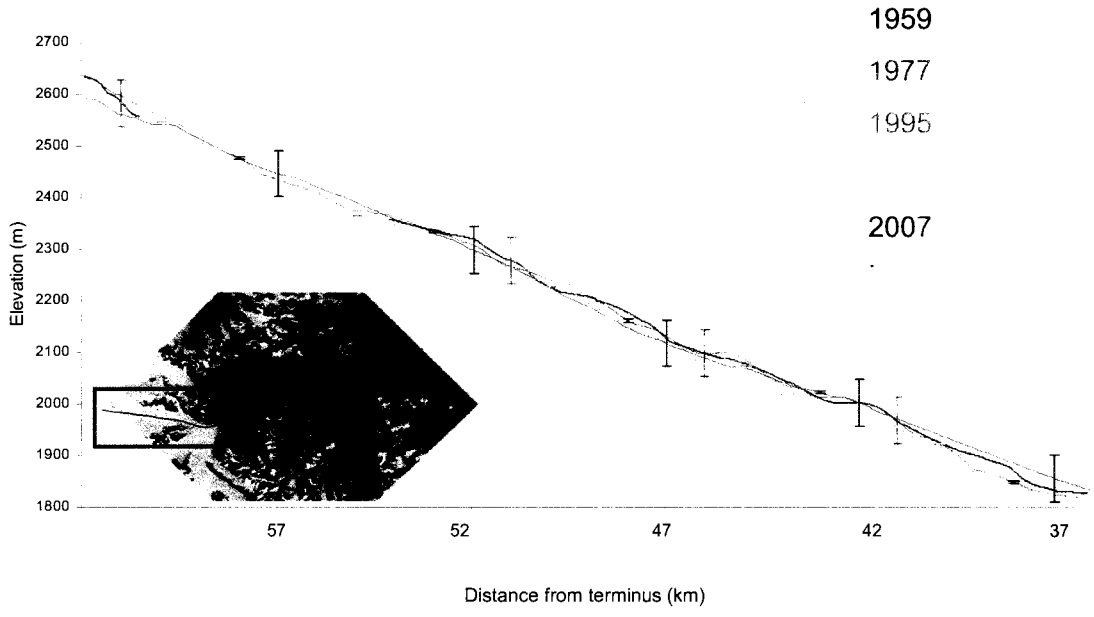

Figure 3.16: Elevation profile along the accumulation zone of the glacier for 1977, 1995, 2000, and 2007. Error bars for each line are indicated. The inset map indicates the location of the points sampled.

3.2 Changes in Area

3.2.1 Terminus area changes

The Kaskawulsh Glacier has been retreating on average since 1836 (Borns and Goldthwait 1966; Reyes et al. 2006; Wiles et al. 2002). Through examination of the terminal position of the glacier since 1956, modern rates of this retreat are quantified. Figures 3.17 and 3.18 show the terminal position of the Kaskawulsh Glacier for 1956, 1977, 1986, 1990, 1994, 2001, 2003, 2006 and 2007. The most current terminal position of the Kaskawulsh Glacier measured for 2007 is located at 138°36'23"W, 60°49'52"N.

Table 3.2 details the average displacement in terminus position, as well as the rate of terminus displacement and the change in ice area, over each time interval. Between 1956 and 2007 the Kaskawulsh Glacier retreated an average of 655 m losing an area of 8.20 km^2. The greatest rate of retreat occurred in the most recent period of 2006-2007, when the glacier receded 79 m yr^{-1}. This accounted for a loss in glacier area of 0.87 km^2, and was accommodated largely by the expansion of terminal lakes on the eastern and western lobes (Figure 3.19). The lake at the front of the eastern lobe of the terminus increased in area by 0.15 km^2 between 2003 and 2007. Meanwhile the lake at the front of western lobe increased in area by 0.82 km^2 between 2003 and 2007. The changes in the area of the lakes appear to have occurred primarily due to retreat of the glacier front rather than a change in drainage morphology at the lake outlets.

Over the 51-yr period, there has been only one brief interval of readvance, and this occurred between 1986 and 1990 when the terminus underwent an advance of 62 m over four years (an average rate of 16 m yr^{-1}), accounting for an increase in glacier area of 0.54 km^2. This advance was partially accommodated by the advance of glacial ice into the terminal lake on the eastern lobe of the glacier (Figure 3.20). This glacial extension appears in 1990 (Figure 3.20c), begins to deteriorate between 2003 and 2006 (Figure 3.19a, Figure 3.19c and Figure 3.19d) but persists until at least 2007 (Figure 3.20d). It appears that this portion of the glacier will soon detach as only a narrow segment (~90 m in width) maintained its connection to the terminus in 2007.

Figure 3.17: Changes in the terminus position (1956-2007) displayed over 1956 air photo mosaic.

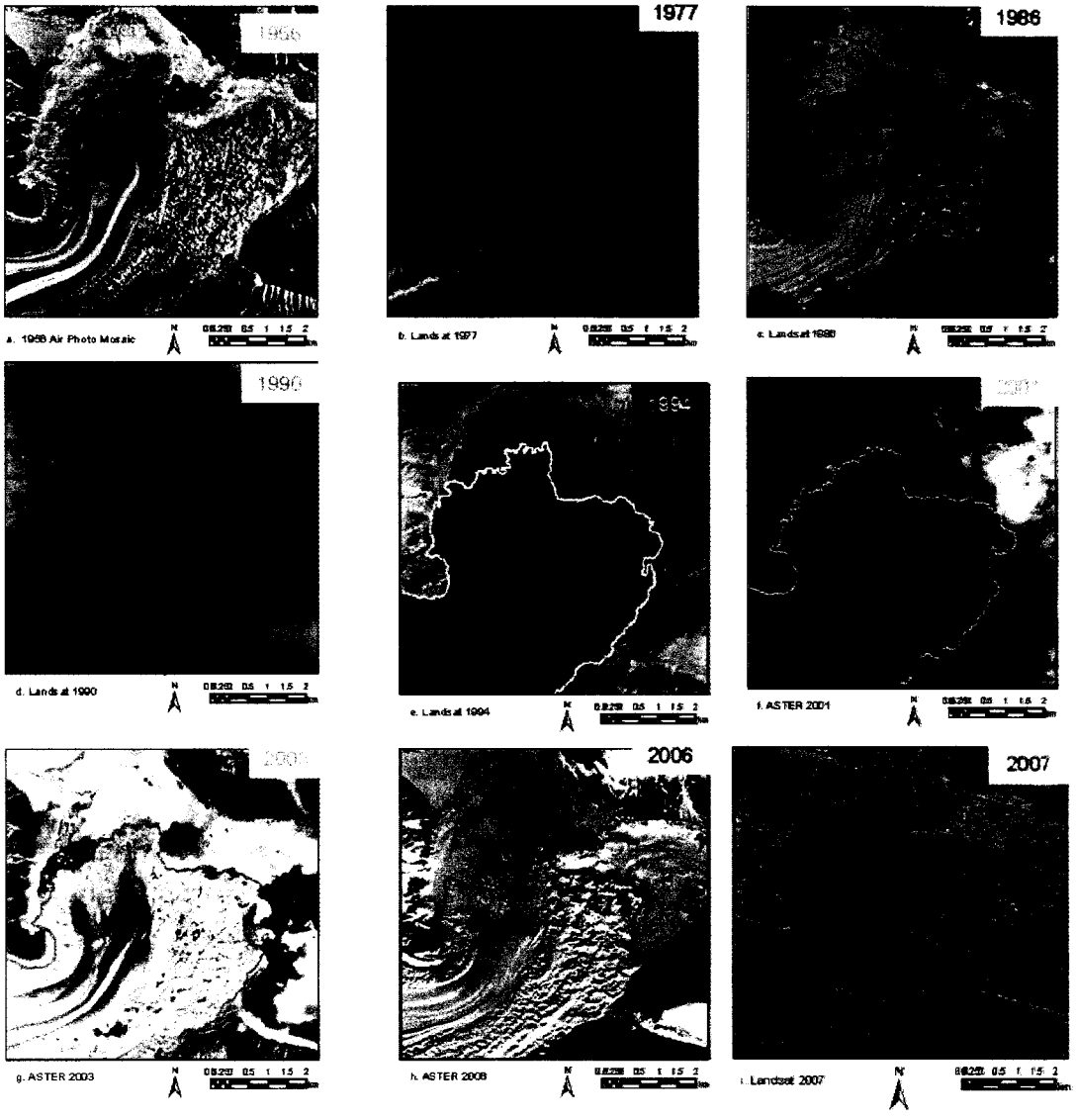

Figure 3.18: Terminus positions in 1956, 1977, 1986, 1990, 1994, 2001, 2003, 2006, and 2007 displayed over source images.

Table 3.2: Change in terminus position for the Kaskawulsh Glacier (1956-2007)

	Average Displacement (m)	Average rate of displacement (m yr^{-1})	Area Change (km^2)
1956-1977	-184	-9	-2.74
1977-1986	-134	-15	-1.82
1986-1990	62	16	0.54
1990-1994	-41	-10	-0.24
1994-2001	-87	-12	-1.05
2001-2003	-32	-16	-0.66
2003-2006	-146	-49	-1.36
2006-2007	-79	-79	-0.87
1956-2007	-655	-13	-8.20

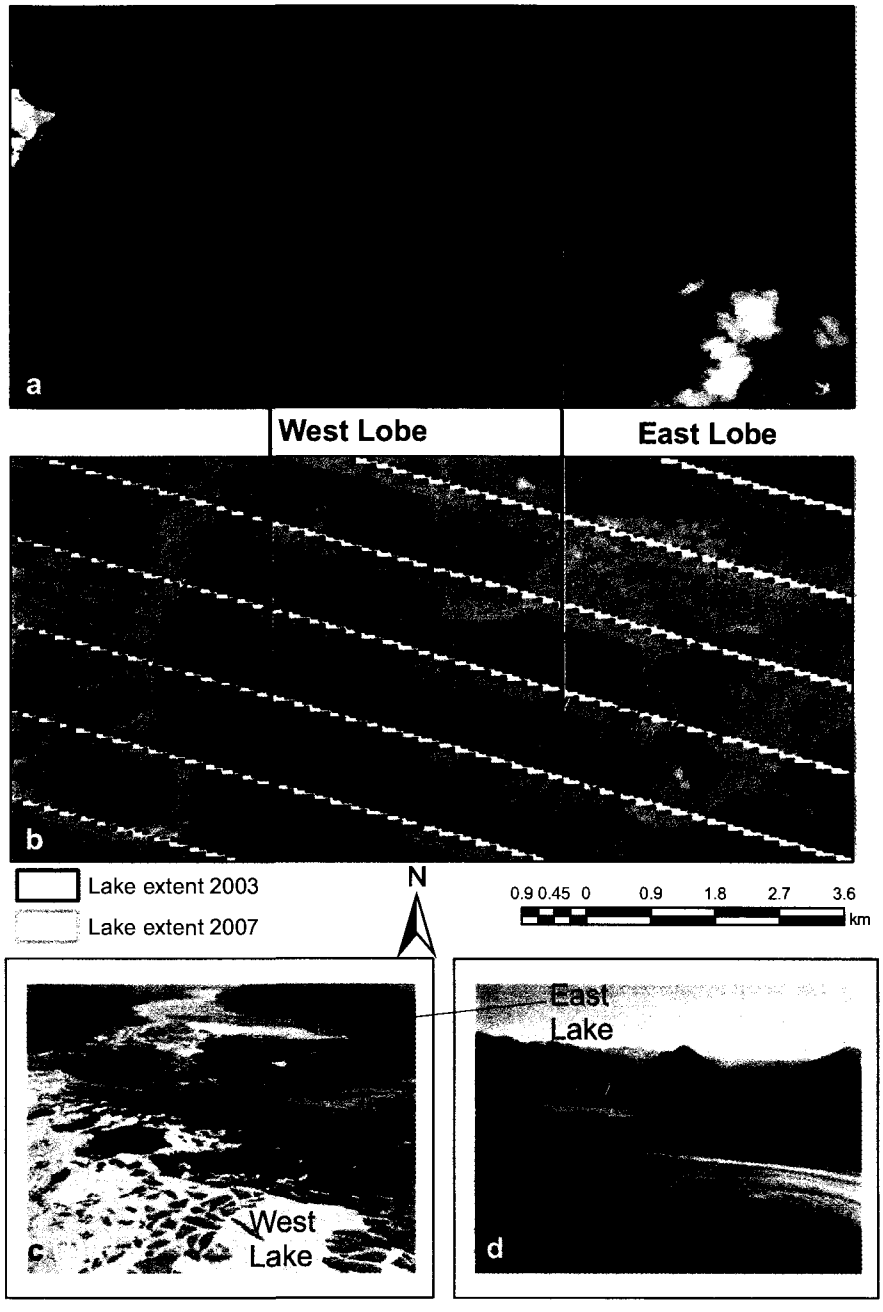

Figure 3.19: Area of lakes at the terminus in 2003 and 2007. Panel A displays the area of the lake at the front of the east lobe in 2003 (1.54 km^2), and of the lake at the front of the west lobe in 2003 (0.94 km^2). Panel B displays the area of the lake at the front of the east lobe in 2007 (1.69 km^2), and of the lake at the front of the west lobe in 2007 (1.76 km^2). Panel C and D show images of the terminal lakes taken from a small aircraft in July 2006.

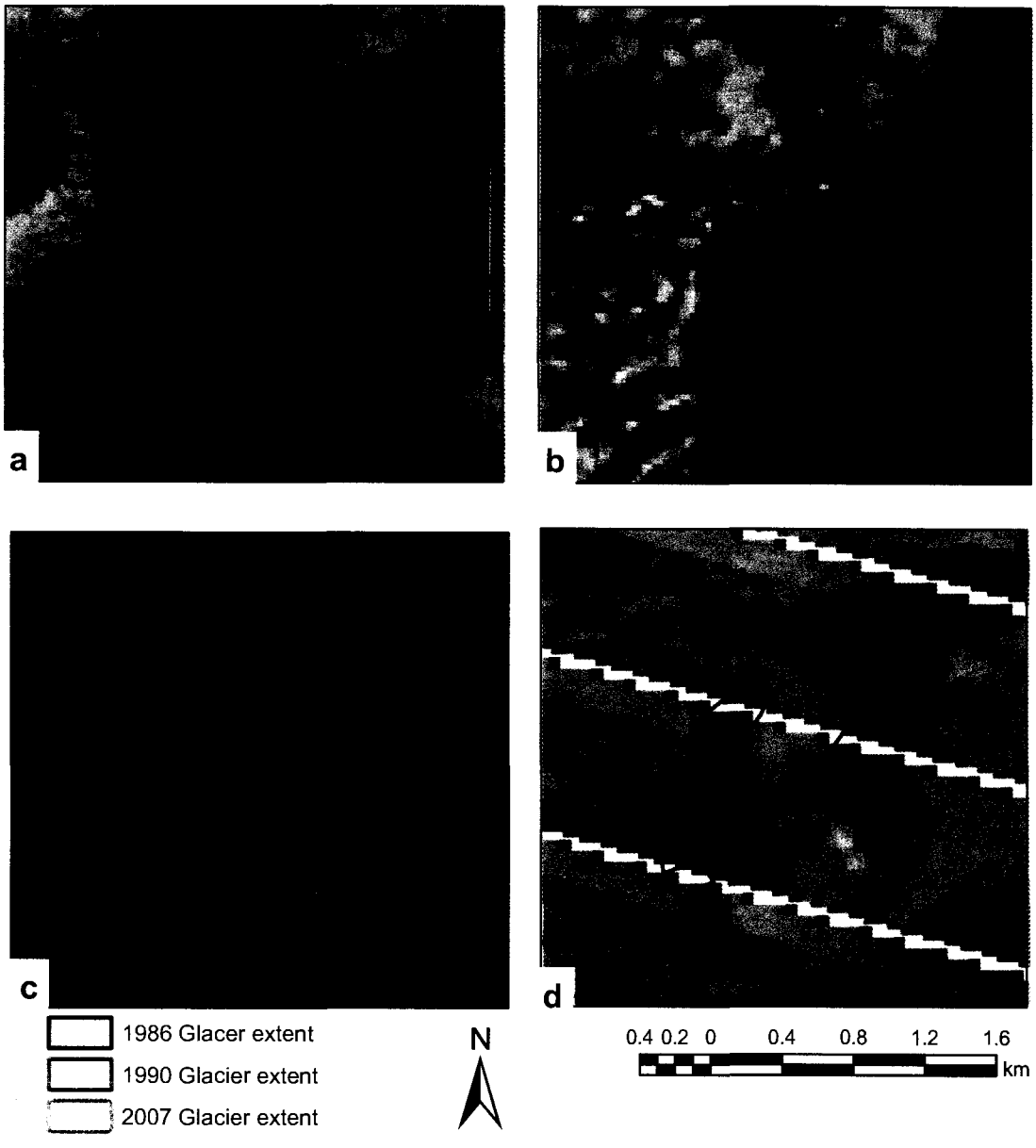

Figure 3.20: Development and persistence of a glacier tongue over a terminal lake on the eastern lobe of the Kaskawulsh Glacier (inset Panel A). Panel B displays a 1986 Landsat image where the tongue is not present. Panel C shows the fully developed tongue on a 1990 Landsat image. Thus the tongue must have developed between 1986 and 1990. Panel D shows a 2007 Landsat image where the tongue appears ready to break away from the terminus.

3.2.2 Area changes in the accumulation zone

Changes in area over the accumulation zone were examined via changes in exposed rock on nunataks. These changes can be used an indicator of general glacier changes in this region because changes in glacier extent would be expected to produce proportional changes in exposed rock area. Areal changes of five representative exposed rock complexes across the accumulation zone were monitored: NA2, NA1, CA2, CA1, and SA (Table 3.3).

Complex NA2 is positioned at the northernmost extent of the glacier's north arm (139°29'40"W; 60°48'12"N, 2731 m asl; Figure 3.21), and is the smallest rock complex examined with an area of 0.25 km^2 in September 1977 (Figure 3.21b). Over the years the exposed rock in this complex increased in area, reaching a maximum of 0.65 km^2 in June 2001 (Figure 3.21d). By September 2007, however, the area of exposed rock at NA2 was 0.51 km^2 (Figure 3.21e). Therefore between September 1977 and September 2007, the area of exposed rock at NA2 more than doubled, representing a local decrease in glacier extent of 0.26 km^2 over a 30-year period.

Complex NA1 (Figure 3.22) is positioned between the north arm and the central arm of the Kaskawulsh Glacier (139°26'01"W; 60°43'39"N, 2615 m asl). In September 1977, the area of this complex was 4.09 km^2 (Figure 3.22b), making it the largest area of exposed rock under examination. By August 1994, the exposed rock had increased to 4.71 km^2 (Figure 3.22c). By June 2001, the area of this complex had decreased to 4.62 km^2 (Figure 3.22d). By June 2007 the area of exposed rock at NA1 decreased further to 4.16 km^2 (Figure 3.22e). Therefore the complex underwent an increase in area of 0.07 km^2, 1.8 % between 1977 and 2007.

Complex CA2 (Figure 3.23) is located just south of NA1, along the central arm of the glacier (139°27'15"W; 60°39'58"N, 2705 m asl). In September 1977, the area of this complex was 1.94 km^2 (Figure 3.23b). By August 1990, the area had decreased to 1.74 km^2 (Figure 3.23c). In 2001, this rock exposure increased in area, reaching its maximum extent of 2.18 km^2 in June 2001 (Figure 3.23d). However by June 2007, its area had decreased to 1.85 km^2 (Figure 3.23e). Over the 30-year period CA2 therefore decreased in area by 0.09 km^2 (4.5%).

Exposed rock complex CA1 (Figure 3.24) is also located on the central arm of the Kaskawulsh Glacier (at 139°22'18"W; 60°34'09"N, 2438 m asl). In September 1977, the

Table 3.3: Change in exposed rock area in the accumulation zone (1956-2007)

	NA2	NA1	CA2	CA1	SA	sum
Year	area (km^2)	area (km^2)	area (km^2)	area (km^2)	area (km^2)	area (km^2)
1956	*n/a*	*n/a*	*n/a*	*n/a*	0.451	*n/a*
1977	0.252	4.087	1.935	1.140	0.520	7.934
1990	0.622	*n/a*	1.739	0.977	*n/a*	*n/a*
1994	0.625	4.708	*n/a*	*n/a*	*n/a*	*n/a*
2001	0.646	4.616	2.183	1.103	0.686	9.234
2007	0.512	4.160	1.847	1.105	0.686	8.309

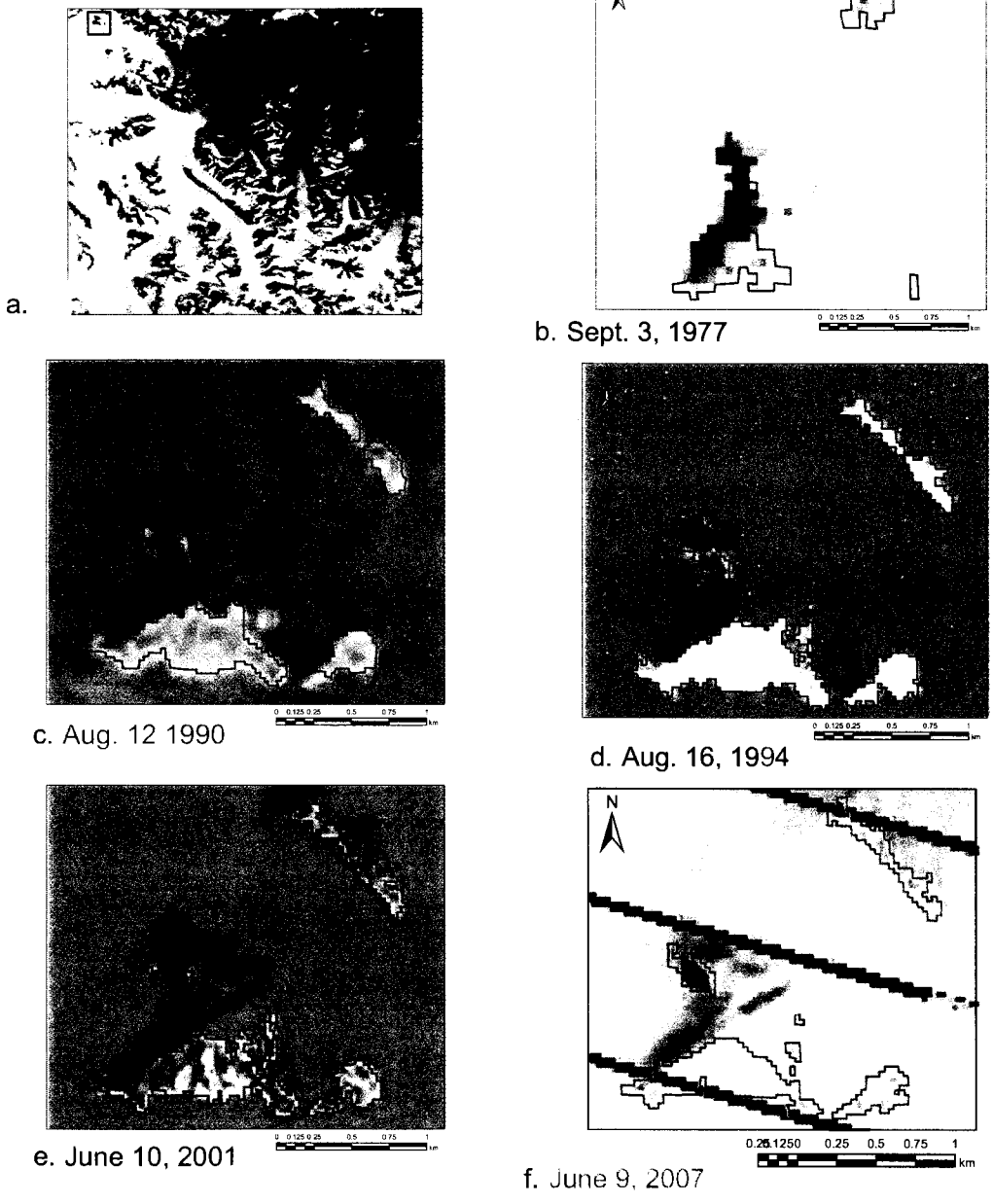

Figure 3.21: Area changes in nunataks on the northern arm of the glacier in the accumulation area (NA2 exposed rock complex). Panel A is the inset map. Panel B shows the area of exposed rock in 1977 (0.252 km^2). Panel C shows the area of exposed rock in 1990 (0.622 km^2). Panel D shows the area of exposed rock in 1994 (0.625 km^2). Panel E shows the area of exposed rock in 2001 (0.65 km^2). Panel F shows the area of exposed rock in 2007 (0.51 km^2).

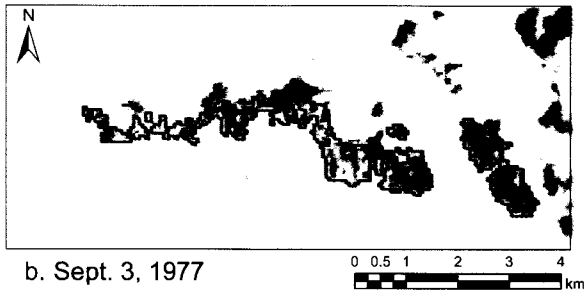

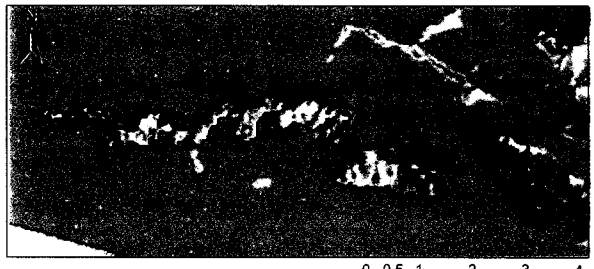

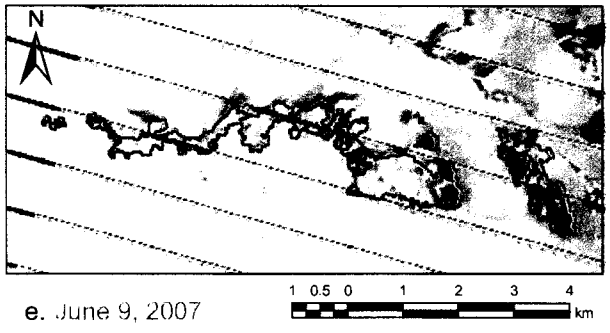

Figure 3.22: Area changes in nunataks on the northern arm of the glacier in the accumulation area (NA1 exposed rock complex). Panel A is the inset map. Panel B shows the area of exposed rock in 1977 (4.09 km^2). Panel C shows the area of exposed rock in 1994 (4.71 km^2). Panel D shows the area of exposed rock in 2001 (4.62 km^2). Panel E shows the area of exposed rock in 2007 (4.16 km^2).

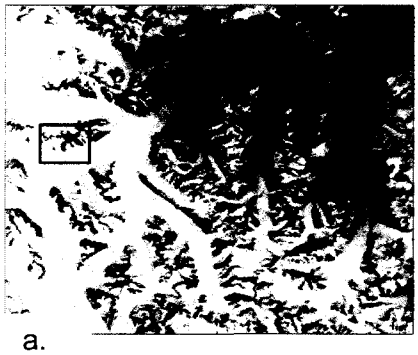

a.

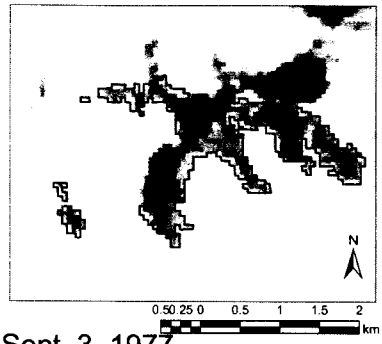

b. Sept. 3, 1977

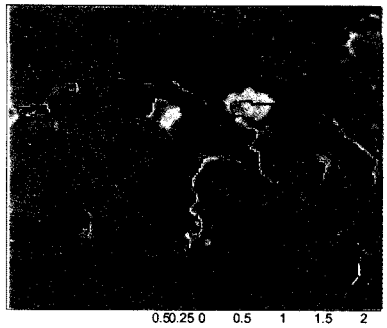

c. Aug. 12, 1990

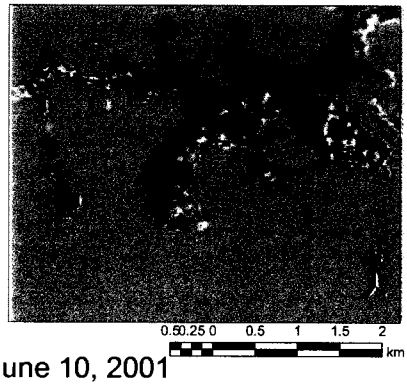

d. June 10, 2001

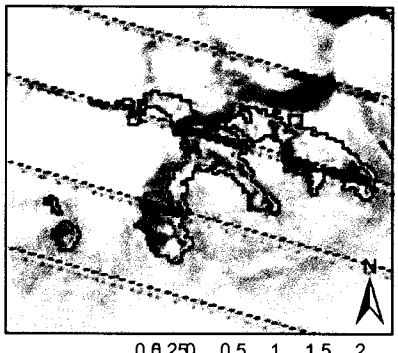

e. June 9, 2007

Figure 3.23: Area changes in nunataks on the central arm of the glacier in the accumulation area (CA2 exposed rock complex). Panel A is the inset map. Panel B shows the area of exposed rock in 1977 (1.94 km^2). Panel C shows the area of exposed rock in 1990 (1.74 km^2). Panel D shows the area of exposed rock in 2001 (2.18 km^2). Panel E shows the area of exposed rock in 2007 (1.85 km^2).

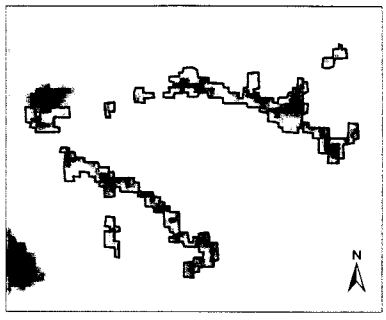

b. Sept. 3, 1977

c. Aug. 12, 1990

d. June 10, 2001

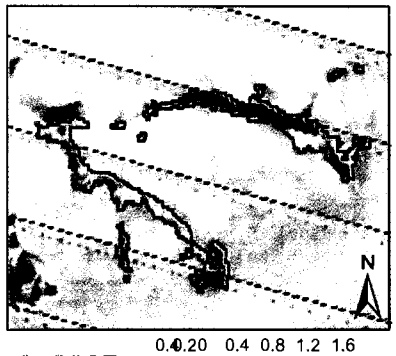

e. June 9, 2007

Figure 3.24: Area changes in nunataks on the central arm of the glacier in the accumulation area (CA1 exposed rock complex). Panel A is the inset map. Panel B shows the area of exposed rock in 1977 (1.14 km^2). Panel C shows the area of exposed rock in 1990 (0.98 km^2). Panel D shows the area of exposed rock in 2001 (1.10 km^2). Panel E shows the area of exposed rock in 2007 (1.10 km^2).

area of exposed rock measured 1.14 km^2 (Figure 3.24b). By August 1990, this had decreased to 0.98 km^2, but by June 2001 most of its area was regained (Figure 3.24d; area = 1.10 km^2). The area of CA1 then stayed relatively constant through June 2007 (Figure 3.24e), when its area was calculated at 1.11 km^2. Thus the area of exposed rock decreased by 0.04 km^2 (3.1%) between 1977 and 2007.

Finally, rock complex SA (Figure 3.25) is located in the accumulation area of the southern arm of the Kaskawulsh Glacier (138°46'7"W; 60°28'31"N; the elevation is unknown as the DEMs used in this study do not extend to this arm). This was the only portion of the accumulation area for which air photo coverage is available from 1956. In September 1956, the area of this complex was 0.45 km^2 (Figure 3.25b). The exposed rock area increased through the period of observation (Figure 3.25c) to its maximum of 0.69 km^2 in June 2001 (Figure 3.25d). This area is maintained through June 2007 (Figure 3.25e). Over this 51-year period, the area of exposed rock increased by a total of 0.24 km^2 (52.1%), while between 1977 and 2007 the increase was 0.17 km^2 (31.9%).

The combined area of the 5 exposed complexes sampled was 7.93 km^2 in 1977. By 2007, the area of exposed rock area had increased by 0.38 km^2 to 8.31 km^2. In 1977, the total area of exposed rock within the accumulation area (all areas located above 1989 m asl, and including the south arm) was calculated at 244.20 km^2. If it is assumed that the 5 complexes are representative of exposed rock throughout the accumulation area of the Kaskawulsh Glacier, then the increase in exposed rock would have been 11.56 km^2 between 1977 and 2007. This represents a rate of ice area decrease of 0.39 $km^2\ yr^{-1}$ (0.05% yr^{-1}).

The rate of area change in the accumulation zone also varies over time. Because data from all 5 rock exposures is available for 2001, the change in area of the accumulation zone between 1977 and 2001 can also be calculated. In 2001, the area of exposed rock for the 5 complexes was 9.23 km^2, which is an increase of 1.30 km^2 since 1977. Extrapolated across the accumulation area, this represents an estimated increase in exposed rock of 40.00 km^2 (16.38%) over the 24-year period. Therefore between 1977 and 2001 the rate of area change was 1.67 $km^2\ yr^{-1}$. Finally between 2001 and 2007 the area of exposed rock in the 5 complexes decreased by 0.93 km^2. Across the accumulation area, this represents a decrease in exposed rock of 24.46 km^2 (8.60%). Thus between 2001 and 2007, the rate of area change was -4.08 $km^2\ yr^{-1}$ (0.50 % yr^{-1}).

a.

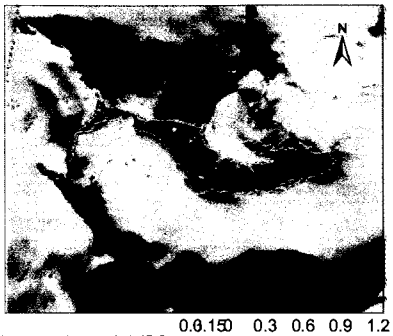

b. Sept 11, 1956

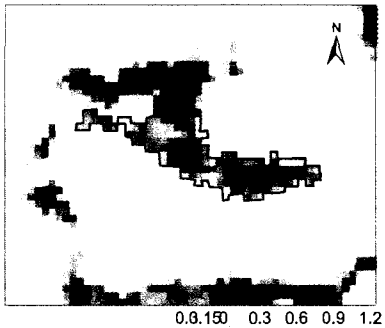

c. Sept. 3, 1977

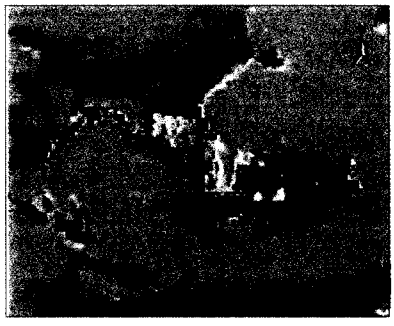

d. June 10, 2001

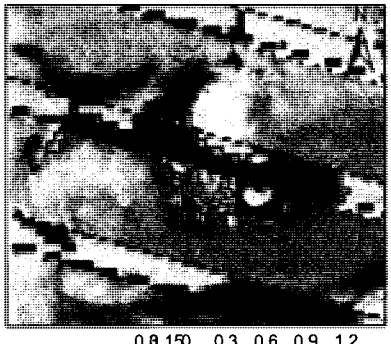

e. June 9, 2007

Figure 3.25: Area changes in nunataks on the south arm of the glacier in the accumulation area (SA exposed rock complex). Panel A is the inset map. Panel B shows the area of exposed rock in 1956 (0.45 km^2). Panel C shows the area of exposed rock in 1977 (0.52 km^2). Panel D shows the area of exposed rock in 2001 (0.69 km^2). Panel E shows the area of exposed rock in 2007 (0.69 km^2).

Changes in area within the accumulation zone are variable not only in time, but also in space (Figure 3.26). On the north arm of the glacier, NA1 and NA2 increase in area between 1977 and 1994. Between 1994 and 2001, while NA1 decreases in area moderately, NA2 increases in area moderately. Finally, between 2001 and 2007 both NA1 and NA2 decrease in area. The two exposures are located ~8 km from one another at similar elevations, therefore are likely influenced by very similar microclimates. NA2 is located at the divide between the Kaskawulsh and Kluane Glaciers. Thus, the Kluane Glacier system may influence the NA2 complex and explain why NA2 increases in area between 1994 and 2001 while NA1 decreases in area.

CA2 is located ~6 km south of NA1, and CA1 is located ~10 km southeast of CA2. Both CA2 and CA1 are at similar elevations and along the central arm of the glacier and thus likely experience similar microclimates. Between 1977 and 1990 both CA1 and CA2 undergo decreases in area. Between 1990 and 2001, both complexes increase in area moderately, and then between 2001 and 2007 CA2 decreases in area while CA1 decreases in area, albeit very slightly.

Rock complex SA is the most geographically isolated exposure, located 68 km SE of its nearest neighbour (CA1). Despite the distance, this complex experiences fluctuations similar to the other exposed rock complexes; between 1977 and 2001, the rock exposure increases in area, and between 2001 and 2007 the area remains steady. Thus, variability in snow accumulation and melt patterns across the accumulation zone of the glacier appears to be relatively low. Despite microclimatic differences, the entire glacier system seems to be governed by the same general climate and would be expected to respond relatively uniformly to climatic perturbations.

3.2.3 Overall area changes

By combining the changes in the accumulation and ablation zones discussed above, the changes in area of the entire Kaskawulsh Glacier can be calculated for 1977, 2001 and 2007 (the years when area data is available for the accumulation zone). In 1977, the area of the glacier was 1111.81 km^2. In 2001, the area had decreased by 42.57 km^2 to 1069.24 km^2. By 2007, the glacier had increased in area by 17.34 km^2, to 1086.59 km^2 largely due to

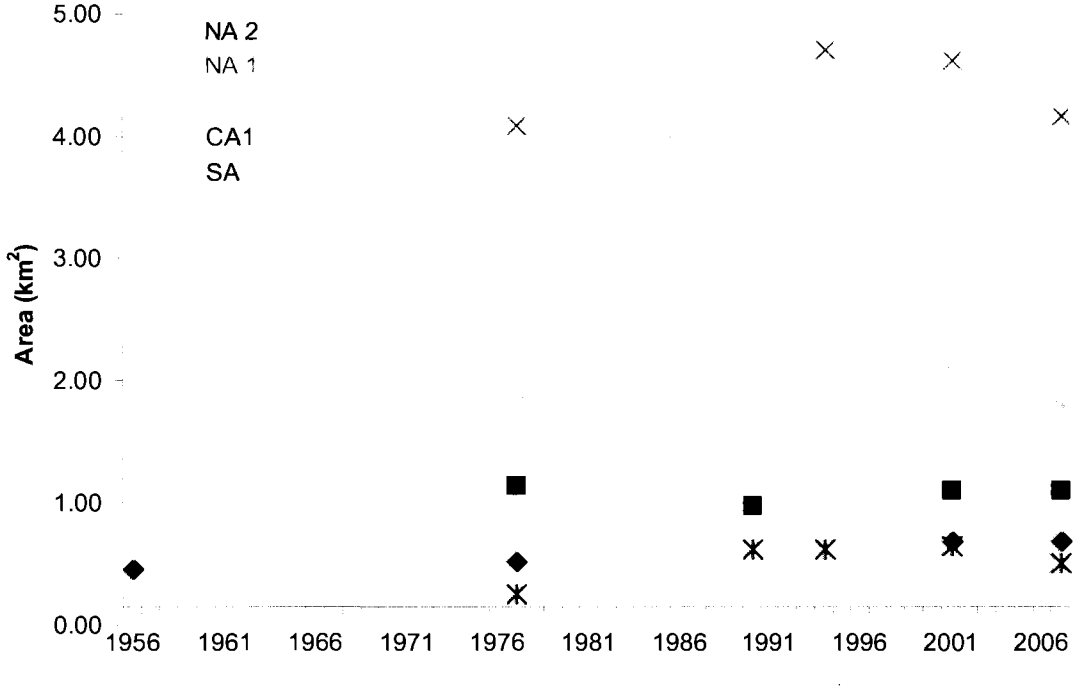

Figure 3.26: Area changes in nunataks across the Kaskawulsh Glacier accumulation area. NA2 and NA1 (the purple and blue series respectively) represent exposed rock complexes on the northern arm of the glacier. CA2 and CA1 (the green and pink series respectively) represent exposed rock complexes on the central arm of the glacier. SA (the navy series) represents exposed rock complexes on the southern arm of the glacier.

increases in the accumulation area. Therefore, over the 30-year period, the glacier decreased in area by 25.22 km^2, or 2.27%.

Errors in the area change calculations largely arise from the fact that measurements of changes along many of the glacier margins could not be made directly, instead having to be interpolated from the changes that occurred at the 5 nunatak complexes. This was mainly due to the presence of shadows and thick moraines that precluded the detection of glacier width changes. Area change calculations were also affected by snowfall in the years for which imagery satellite imagery was available. If the image used was acquired in year of particularly heavy snowfall or directly after a large snowfall event, then the glacier area calculated would be artificially high. Likewise late summer imagery of the glacier was not always available. In some years area was calculated from images acquired as early as June (as in 2001 and 2007). In these years glacier area calculations were likely also artificially high. In addition, the use of area changes as an indicator of glacier health is complicated by the fact that much of the glacier is bordered by steep valley sidewalls that would show little change in glacier area even if there were substantial changes in ice thickness (Figure 3.27).

3.3 Changes in Volume

Given the changes in area and surface height discussed above, the temporal changes in volume of the Kaskawulsh Glacier can be calculated. These changes in volume cannot be directly interpreted as changes in mass balance, however, as at least some of the volume change could be attributed to internal accumulation, particularly in the accumulation zone. Internal accumulation occurs when meltwater from the surface of a glacier filters into the snowpack and glacier interior and refreezes. Although difficult to quantify, internal accumulation can account for between 5 and 100% of annual net accumulation (Kaser et al. 2006).

Table 3.4 shows the changes in volume between 1977 and 2007 for the glacier as a whole, as well as a breakdown for the accumulation and ablation zones. The greatest loss occurred between 1977 and 1995, when the glacier's volume depleted at a rate of 0.82 km^3 yr^{-1} (0.52 km^3 yr^{-1} we). Between 1995 and 2000, volume continued to decrease at a rate of 0.76 km^3 yr^{-1} (0.52 km^3 yr^{-1} we). In contrast, between 2000 and 2007 the volume of the

Figure 3.27: Steep sidewalls bordering the Kaskawulsh Glacier, June 29, 2008; view is upglacier on the north arm from the confluence of the north and central glacier arms, close to the equilibrium line.

Table 3.4: Volume changes on the Kaskawulsh Glacier (1977-2007)

Glacier-wide				
	ΔV (km^3)	**Rate ($km^3 a^{-1}$)**	**ΔV_{we} (km^3)**	**Rate ($km^3 a^{-1}$ we)**
1977-1995	-14.73	-0.82	-9.30	-0.52
1995-2000	-3.82	-0.76	-2.61	-0.52
2000-2007	14.22	2.03	7.30	1.04
Total*	-4.33	-0.14	-4.60	-0.15
Swath 1977-2007**	-3.14	-0.10	-2.76	-0.09

Accumulation Zone						
	a_1 (km^2)	**Δh_1 (m)**	**Δa_2 (km^2)**	**h_2 (m)**	**Δv (km^3)**	**Δv_{we} (km^3)**
1977-1995	788.20	-12.4	-30.00	-12.4	-10.15	-5.17
1995-2000	779.87	-2.7	-8.33	-2.7	-2.13	-1.09
2000-2007	806.65	16.9	26.78	16.9	14.08	7.18
Total*	n/a	1.8	n/a	1.8	1.81	0.92
Swath 1977-2007**	806.65	-0.2	18.45	-0.2	-0.16	-0.08

Ablation Zone						
	a_1 (km^2)	**Δh_1 (m)**	**Δa_2 (km^2)**	**h_2 (m)**	**Δv (km^3)**	**Δv_{we} (km^3)**
1977-1995	291.94	-15.6	-1.66	-15.6	-4.58	-4.12
1995-2000	291.19	-5.8	-0.75	-5.8	-1.69	-1.52
2000-2007	279.94	0.5	-11.25	0.5	0.13	0.12
Total*	n/a	-20.9	n/a	-20.9	-6.14	-5.53
Swath 1977-2007**	279.94	-10.2	-12.00	-10.2	-2.98	-2.68

a_1 is the area of remaining glacier ice, Δh_1 is the change in elevation of the remaining glacier ice, Δa_2 is the change in area of the glacier, and h_2 is the former thickness of the ice that was removed. In the ablation zone, the ice density used to calculate water equivalent change was 0.90 g cm^{-3} (d_2); for changes in the accumulation area, the ice density used was 0.51g cm^{-3} (d_1). Changes are calculated using Calculations 1 and 3 (section 2.4.3 of this paper).

* denotes the cumulative total of changes measured along the central glacier profile between 1977-1995, 1995-2000 and 2000-2007 (Figures 3.3, 3.7, and 3.9)
** denotes changes measured from the swath profile of the glacier between 1977 and 2007 (Figure 3.12)

Kaskawulsh Glacier increased at a rate of 2.03 km^3 yr^{-1} (1.04 km^3 yr^{-1} we). Most of these recent changes can be attributed to gains in the accumulation zone.

Table 3.4 indicates different values calculated for volume change over the entire study period (1977-2007), when compared to the sum of the 3 separate intervals. The total reduction in ice volume calculated by adding together the separate intervals is 4.33 km^3 (-0.14 km^3 yr^{-1}), or a water equivalent decrease of 4.60 km^3 (-0.15 km^3 yr^{-1} we). Losses in volume occur prominently in the ablation zone (-6.14 km^3; -5.53 km^3 we), while volume is gained in the accumulation zone (1.81 km^3; 0.92 km^3 we).

The second set of values is calculated from the overall area changes between 1977 and 2007, and the overall surface height changes between the 1977 DEM and the full 2.3 km wide swath DEM from 2007 (Figure 3.12). These values differ from periodic change values as they account for variability in thinning/thickening across the width of the glacier. This data shows that between 1977 and 2007 the glacier lost a total of 3.14 km^3 (-2.76 km^3 we), at an overall rate of 0.10 km^3 yr^{-1} (0.09 km^3 yr^{-1} we). This data shows minimal volume losses in the accumulation zone (-0.16 km^3; -0.08 km^3 we), and moderate volume losses in the ablation zone (-2.98 km^3; -2.68 km^3 we).

One potential source of error in the volume calculations is that variability in the location of the ELA was not considered when calculating the area of the accumulation and ablation zones for the various periods examined. This is because no accurate ELA could be determined for the period 2000-2007 from the profile measurements. For the sake of methodological consistency, the long-term ELA of 1989 m was used to separate the accumulation and ablation zones for all periods of observation, and ELA variability was ignored in volume calculations. Accounting for ELA variability would have changed the relative area of the accumulation zone and the ablation zone from year to year, and therefore the conversion of volume changes to water equivalent. Between 1977 and 1995, this would have resulted in slightly lower volume changes in water equivalent, while between 1995 and 2000, this would have resulted in slightly greater changes in water equivalent. Overall the difference would be minimal with regards to the measured water equivalent volume changes.

3.4 Development of a Scaling Ratio

To determine whether a ratio exists that relates elevation, extent, and volume in a simple numerical manner, the trends in change of cumulative length, area, surface height and volume are examined for the period 1977-2007 (Figure 3.28 a, b, c, and d respectively). All variables decrease over the period as a whole although the rates of decrease are variable, and the intermittent trends for each variable differ. Between 2000 and 2007 area, surface height and volume all increase. As no terminal advance occurs between 2000 and 2007, terminus displacement is not statistically related to changes in volume. Therefore a ratio relating terminus displacement to volume change cannot be established. This indicates that fluctuation at a glacier's terminus alone cannot always indicate whether a glacier has increased or decreased in volume (Bahr et al. 1997), at least not at this time scale. The response time of a glacier terminus to a perturbation in the accumulation zone of a glacier may be on the order of years, decades, or centuries, but in the St. Elias Mountains tends to be ~40 years (Arendt et al. 2002; Echelmeyer et al. 1996; Larsen et al. 2007; Sapiano et al. 1998). The time intervals under examination (at the sub-decadal to decadal scale) may be too short to capture the changes in volume via changes at the terminus.

Figure 3.29 more closely examines the relationship between changes in area and changes in volume over the period 1977-2007. The variables display a strong positive correlation with an r^2 value of 0.8251. However, with a P-value of 0.09, this relationship is not statistically significant at the 95% confidence level due to the small number of data points. A longer period of observation for changes in area and changes in volume could rectify this problem. However, no conclusive numerical relationship between area and volume can be determined from this study.

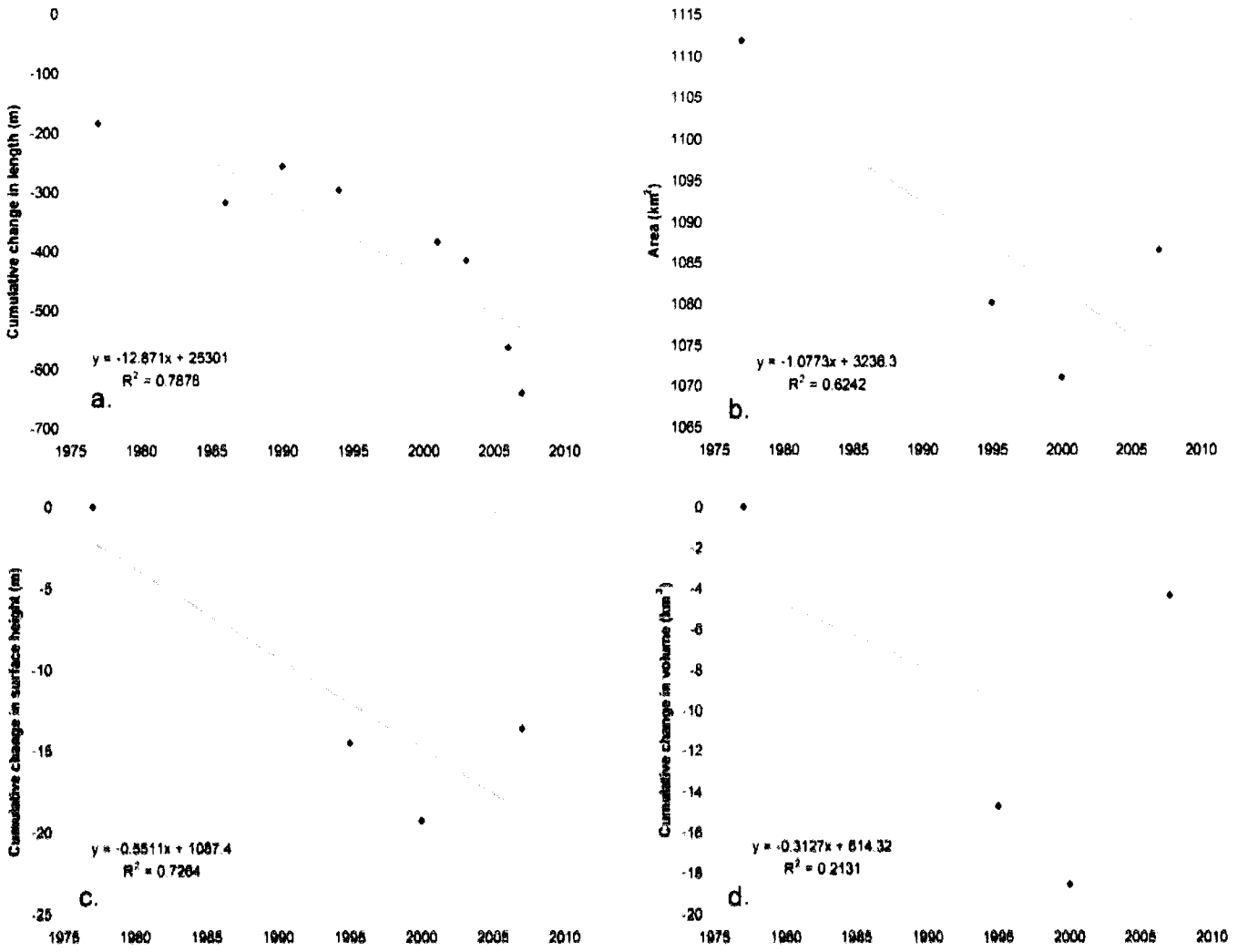

Figure 3.28: Cumulative changes in (a) length (b) area (c) average surface height, and (d) volume (1977-2007)

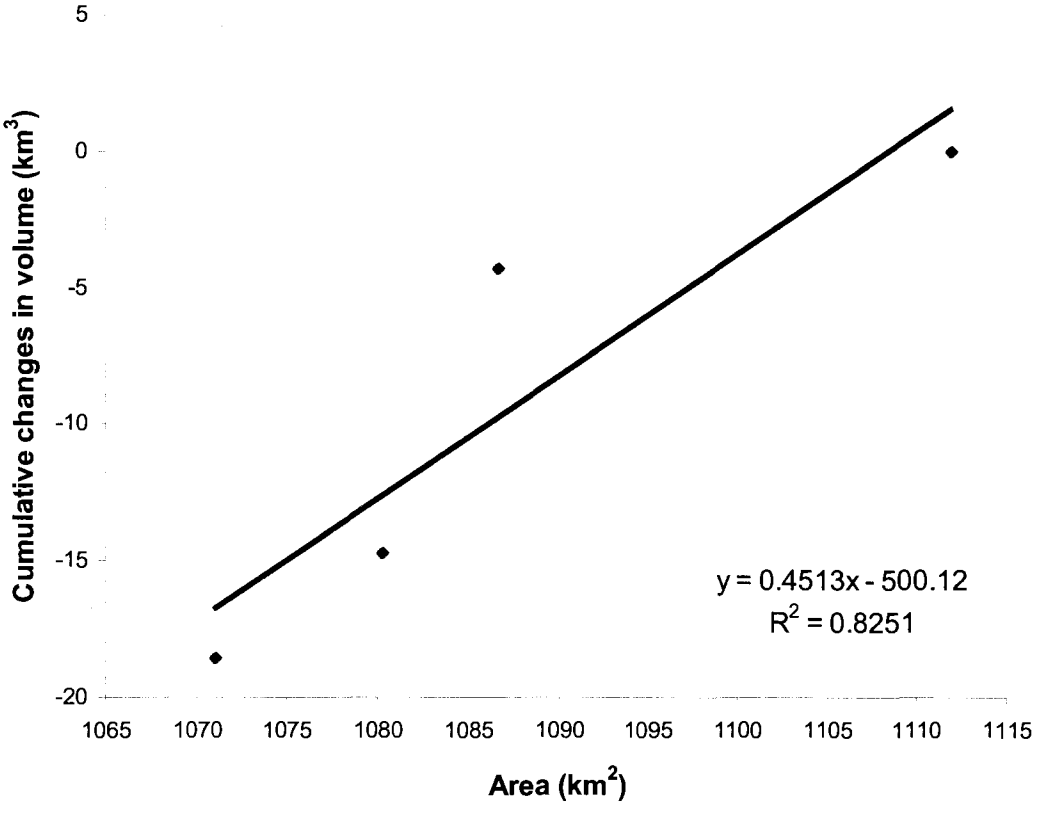

Figure 3.29: Relationship between change in area and change in volume on the Kaskawulsh Glacier (1977-2007).

Chapter 4

4.0 Discussion and Conclusions

4.1 Overall Volume Changes

Between 1977 and 2007, the Kaskawulsh Glacier underwent an overall decrease in volume of between 2.76 km^3 we and 4.60 km^3 we. The rate of volume change over the periods of 1977-1995 and 1995-2007 remained constant at -0.52 $km^3\ yr^{-1}$ we, while between 2000 and 2007, the glacier gained volume at a rate of 1.04 $km^3\ yr^{-1}$ we. Volume losses were prominent within the ablation zone over the period 1977-2007 (between 2.68 km^3 we and 5.53 km^3 we), while volume within the accumulation zone remained relatively constant (between -0.08 km^3 we and +0.92 km^3 we). Concurrently, between 1948 and 2008, the Yukon experienced an increase in mean annual temperatures of 2.0°C (Environment Canada 2009b).

These patterns of glacier change are consistent with changes observed at most glaciers in the Yukon/Alaska region which are thinning and/or retreating (Arendt et al. 2006; Chen et al. 2006a; Larsen et al. 2007; Molnia 2007). For example, Arendt et al. (2002) measured overall glacier losses of 96 $km^3\ yr^{-1}$ we (+/- 35 km^3) in the Gulf of Alaska region between 1955 and 2001 using laser altimetry. Further altimetric study showed that losses in the region may be greater by a factor of two (Arendt et al. 2006; Larsen et al. 2007). Chen et al. (2006) found that the region had lost 101 $km^3\ yr^{-1}$ we (+/- 22 km^3) between 2002 and 2005 according to the GRACE satellite. Luthcke et al. (2008) used surface mass concentration and GRACE satellite data to determine that between 2003 and 2006 glaciers in Alaska shrank by 84 $km^3\ yr^{-1}$ we (+/- 5 km^3). Studies in the Gulf of Alaska region also indicate very large amounts of precipitation in late 2006 and early 2007, which resulted in a less negative balance among the glaciers there in the recent past (Luthcke et al. 2008). Within the St Elias Mountains, Arendt et al. (2008) also used GRACE data in conjunction with satellite laser altimetry to determine mass balance, and found that between 2003 and 2007 these glaciers decreased in volume by between 20.6 $km^3\ yr^{-1}$ we (+/- 3 $km^3\ yr^{-1}$) and 21.2 $km^3\ yr^{-1}$ we (+/- 3.8 $km^3\ yr^{-1}$). These numbers indicate that glaciers of the St. Elias Mountains in general have lost mass at approximately the same rate throughout the past several decades.

Changes in volume of the Kaskawulsh Glacier are largely a function of changes in surface height along the length of the glacier. As such, patterns in glacier thickness change closely reflect the changes in volume previously described. Overall the Kaskawulsh Glacier thinned by an average of 5.9 m to 20.0 m between 1977 and 2007, at a rate of between 0.2-0.7 m yr^{-1}. However, changes in surface height have been variable over time. Between 1977 and 1995 the glacier thinned by 14.5 m (-0.8 m yr^{-1}), while between 1995 and 2000 the overall average thinning was 4.8 m (-1.0 m yr^{-1}). This agrees well with the overall findings of Arendt et al. (2002), who determined that Alaskan glaciers thinned by 0.52 m yr^{-1} between 1955 and 1995 and that this thinning increased to 1.8 m yr^{-1} between 1995 and 2000. However, this does not agree with the rate of thinning measured on the Kaskawulsh Glacier by Arendt et al. (2002). This study found that between 1950 and 1995, the rate of thinning along the glacier was ~1.5 m yr^{-1}, and that between 1995 and 2001, the rate of thinning had decreased to ~0.5 m yr^{-1} (Figure 1.10). The disagreement in these two datasets likely arises because of the differences in periods of observation used (1977-1995 and 1995-2000 for this study, vs. 1955-1995, and 1995-2001 for Arendt et al. (2002)). Furthermore, for the early interval in Arendt's study (1955-1995), direct calculations of change in surface height could only be made for the accumulation zone of the glacier due to limited coverage in the 1955 DEM (Arendt 2009; personal communication). Thus, changes in elevation over the period 1955-1995 would have been skewed. These differences account for disagreement between the two studies.

On the Kaskawulsh Glacier, negative changes have been prominent in the ablation zone (areas below 1989 m asl), with an average thinning of between 10.2 m and 20.9 m between 1977 and 2007. The accumulation zone (areas above 1989 m asl) has experienced minimal change over the study period; average changes in surface height are between -0.2 m and +1.8 m between 1977 and 2007. This is consistent with surface height changes on other glaciers in this region, which have demonstrated slight to no thinning at higher elevations, and increasingly prominent thinning towards the glacier terminus (Arendt et al. 2006, Molnia 2007). In the Western Chugach Mountains, Alaska, at least 23 glaciers display this pattern of surface height change between the 1950s and the early 2000s (Figure 4.1). Changes on these glaciers were measured along centre profiles using DEMs from stereo aerial photographs from the 1950s and LIDAR profile DEMs from the early 2000s.

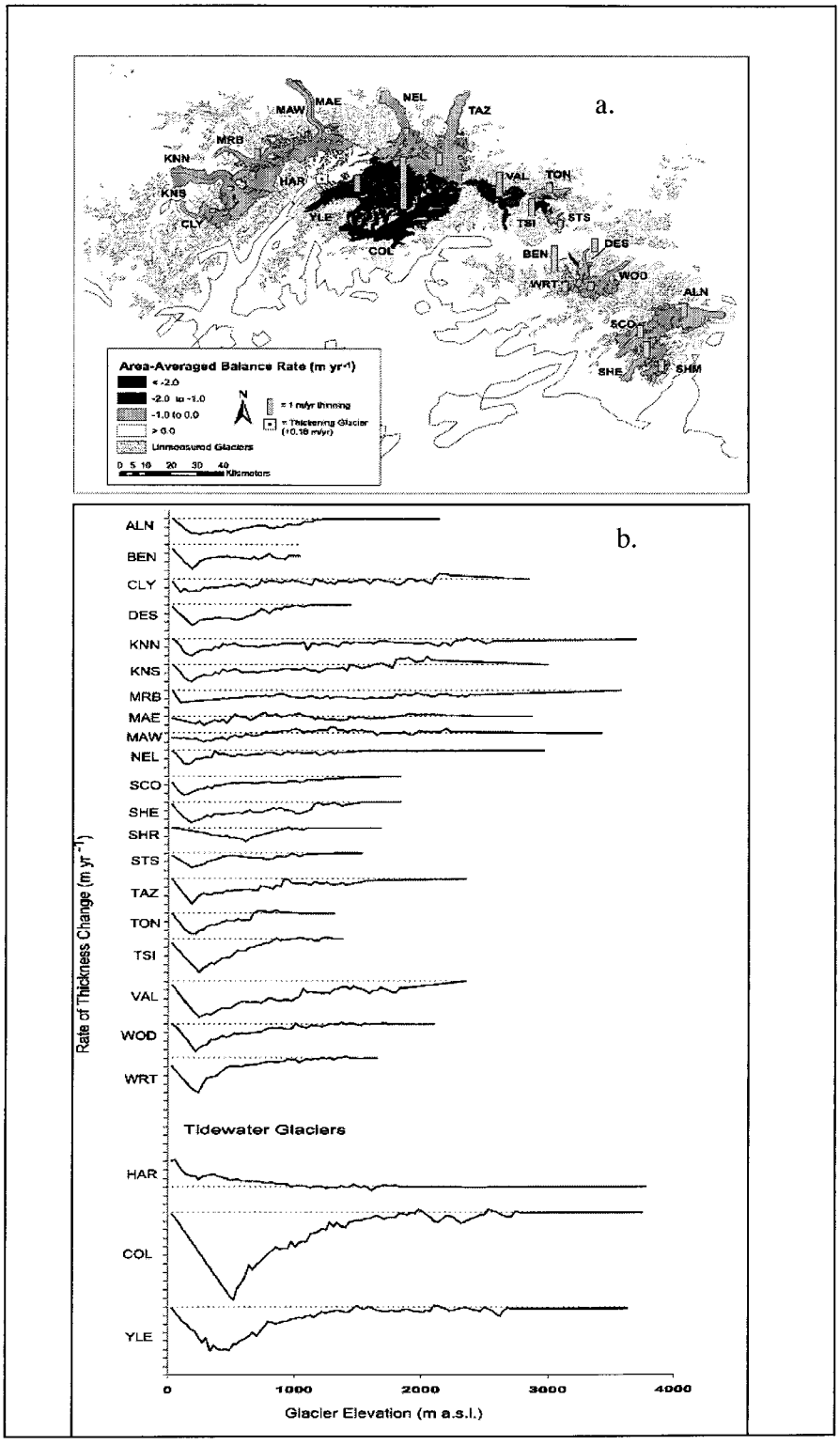

Figure 4.1: Glacier thinning within the Western Chugach Mountains, Alaska (1950/57- 2001/04)
a: Locations of sampled glaciers
b: Time averaged rate of changes in glacier thickness as a function of elevation
Source: Arendt et al. 2006

4.2 Recent Volume Changes

Over the most recent period of 2000-2007, the Kaskawulsh Glacier displays prominent thickening in the accumulation area (+16.9 m) and minor thickening in the ablation area (+0.5 m) with an average thickening of 5.7 m for the glacier as a whole. This thickening is in contrast to the changes being experienced by most other mountain glaciers and ice caps, which thinned on average by ~0.55 m yr^{-1} between 1996 and 2006 (Meier et al. 2007). However, this type of response is not unusual under warming scenarios as a climatic perturbation affects both accumulation and ablation on a glacier (IPCC 2007). Warming at lower elevations causes greater ablation as temperatures warm to well above 0°C and the melt season becomes longer. But at higher elevations, warming may not cause the ambient air temperature to rise above 0°C. Under these conditions, snow and ice does not significantly melt. Rather, in high altitude accumulation zones changes in precipitation would be more likely to result in positive glacier mass balance; warmer climates allow more moisture to be retained in the atmosphere causing an increase in precipitation, and often an increase in snow accumulation on glaciers. Since the 1950s, global mean winter accumulation and summer melting have increased steadily (IPCC 2007). Into the future, this phenomenon coupled with an expected intensification of the Aleutian Low is anticipated to result in an increase in winter precipitation of up to 30% for North America by 2099 (IPCC 2007).

4.3 Comparison with Changes at Other Glaciers

Globally, there are several examples of ice masses that have displayed patterns of thickening at high elevations similar to those observed along the Kaskawulsh Glacier in recent years. Studies in Greenland display that the ice sheet lost mass at an overall rate of -239 km^3 yr^{-1} (+/-23 km^3 yr^{-1}) between 2002 and 2005 (Chen et al. 2006b). However, the breakdown of these changes at different altitudes over 2003-2005 from mascon processing of GRACE satellite data shows that regions of the ice cap above 2000 m asl thickened by 54 km^3 yr^{-1} (+/-12 km^3 yr^{-1}), while regions below 2000 m thinned prominently by 155 km^3 yr^{-1} (+/- 26 km^3 yr^{-1}) (Figure 4.2; Luthcke et al. 2006). Increases at high elevations can be

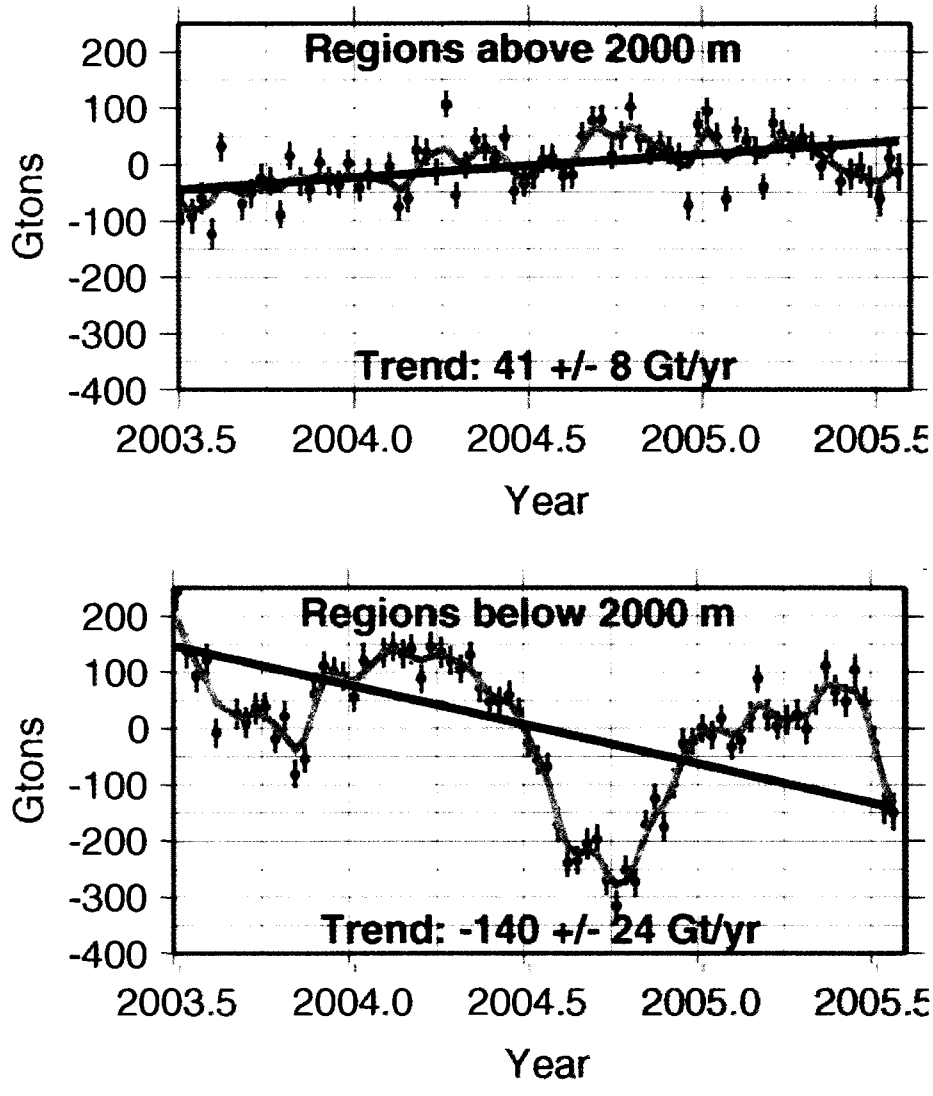

Figure 4.2: Volume trends of the Greenland Ice Sheet observed by the GRACE satellite between mid-2003 and mid-2005.
Source: Luthcke et al. 2006

attributed to increased precipitation resultant from a strongly negative North Atlantic Oscillation (NAO) (Johannessen et al. 2005).

Satellite radar altimetry shows that the Antarctic Ice Sheet also underwent regional thickening over the majority of the eastern ice sheet (up to +0.06 m yr^{-1} for the basin), and over portions of the western ice sheet between 1992 and 2003 (changes in surface height for the basin ranged from -0.10 to +0.19 m yr^{-1}) (Davis et al. 2005). In East Antarctica where thickening was consistent, trends in surface height change correlate statistically with modeled increased snowfall (from the European Centre for Medium-Range Weather Forecasts) for the interior regions (Davis et al. 2005).

Observations of surface height increases at high elevations are not confined to high latitude ice sheets. Mid-latitude mountain environments across the globe also have examples of this phenomenon. Several glaciers that exist in the elevation range between 2300 m and 7000 m in the Karakoram Himalayas displayed thickening and extension between 1997 and 2002 (Hewitt 2005). Inhibition of melt due to the high elevation of these glaciers as well as an increase in winter precipitation is hypothesized to be the cause of the growth in these glaciers, although no statistical relationship has been established.

Glaciers in New Zealand also displayed predominantly positive mass balances between 1980 and 1997 according to annual end-of-summer snowline surveys conducted on 49 index glaciers across the Southern Alps (Chinn 1999). Many glaciers have responded with visible thickening in the upper trunk area, while other, more active glaciers have responded with terminal advances (Chinn 1999). Despite positive mass balance, many glaciers continue to retreat due to response times ranging from 2 years to >21 years. In particular, large glaciers terminating in proglacial lakes continued to recede at the expense of the lake area (Chinn 1999). Studies of the Franz Josef Glacier (one of the 49 glaciers studied by Chinn (1999)), show that precipitation is an important variable in glacier advance in the Southern Alps; comparison of atmospheric flow indices to changes in ELA and glacier length reveal that advance phases of the glacier are influenced by atmospheric circulation featuring greater rates of accumulation, as well as decreased ablation (Hooker and Fitzharris 1999).

Many Scandinavian glaciers have also displayed signs of increased net balance (Figure 4.3). In Svalbard, despite negative mass balance since the 1960s (-4.5 km^3 yr^{-1} we),

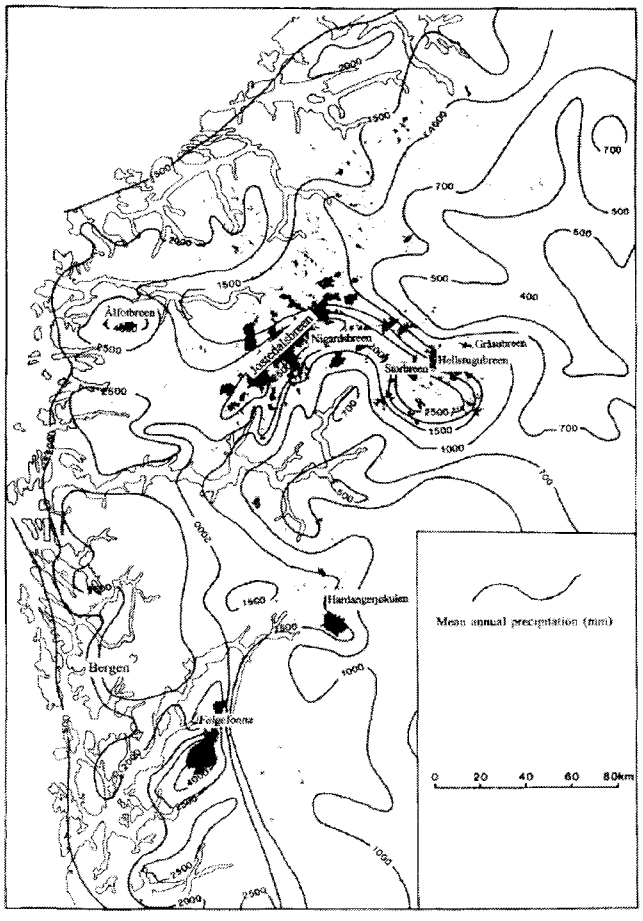

1: Ålfotbreen
2: Hardangerjøkulen
3: Nigardsbreen
4: Engabreen
5: Storglaciären
6: Storbreen
7: Hellstugubreen
8: Gråsubreen
9: Midtre Lovénbreen
10: Austre Brøggerbreen

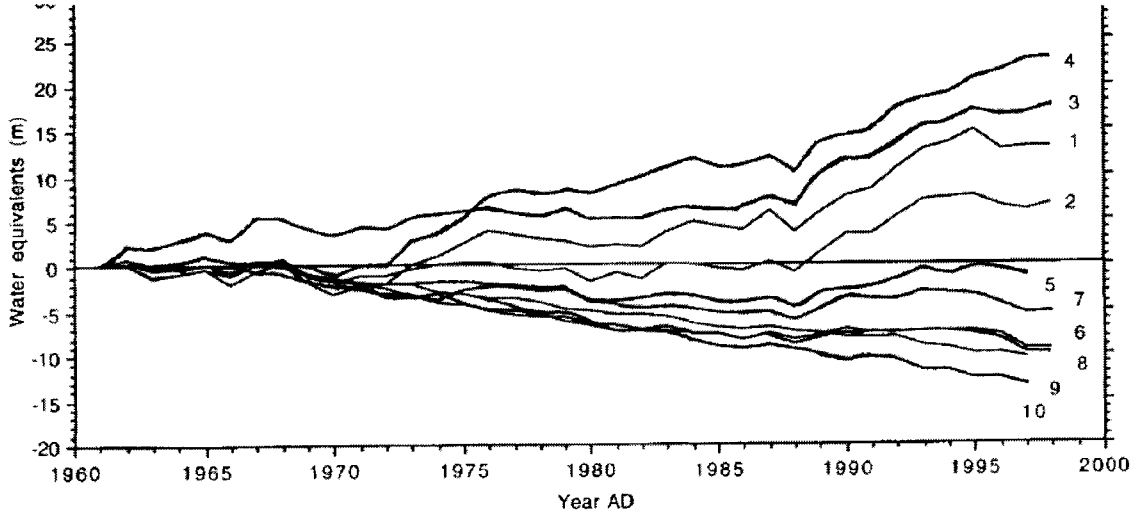

Figure 4.3: Changes in Scandinavian Glaciers (1961-1998)
a: Location of glaciers sampled
b: Cumulative net balance on Norwegian mainland glaciers, Svalbard Glaciers, and Storglaciären in northern Sweden.
Source: Nesje et al. 2000

high altitude surface height increases were measured in the central portions of the Austfonna ice cap (the largest ice cap in the Eurasian Arctic). Using Airborne Topographic Mapper 3 (ATM-3; a scanning LIDAR system developed by NASA) for repeat observations of elevation, a maximum surface height increase of 0.5 m yr^{-1} for 15% of the ice cap was measured over the topographic divides between glacier basins (Bamber et al. 2004). Glacier dynamics cannot explain this thickening since each basin has variable dynamics and the maximum thickening occurs across the individual glacier divides. Therefore, increased precipitation is hypothesized to be the cause of thickening. Observed thickening represents an increase in accumulation of ~40%, and may be associated with a reduction in perennial sea ice cover in the Barents Sea (Bamber et al. 2004).

Maritime glaciers have undergone significant mass increases beginning after 1988 (Nesje et al. 2000). Increases in mean winter air temperatures of 1.2°C correlate well with an increase in winter precipitation (Chinn et al. 2005). In Norway, both continental and maritime glaciers experience years of high winter balance simultaneously, with no spatial variation (Chinn et al. 2005). However the greatest overall accumulation rates in Scandinavia occur in maritime, mountainous regions due to advected moisture from the ocean (Nesje et al. 2000). Correlation analyses show that mass turnover on maritime glaciers shows more correlation with winter balances, while mass turnover on continental glaciers shows more correlation with summer balances, indicating that summer ablation conditions are more influential on continental glaciers than on coastal glaciers (Chinn et al. 2005; Nesje et al. 2000). In Norway, this change in mode occurs ~150 km inland of the coast (Nesje et al. 2000). The accumulation zone of the Kaskawulsh Glacier is situated ~125 km northeast of the Pacific Ocean. It is therefore probable that the maritime climate is an important influence on the accumulation patterns of the glaciers of the St. Elias Mountains as well. An interesting future study would therefore be the relative influence of distance from the ocean on accumulation patterns of glaciers in the Gulf of Alaska region.

Areas of glacier thickening have also been documented in Alaska. Using DEMs created from stereo aerial photography from 1972/73 and DEMs from InSAR (interferometric synthetic aperture radar) from 2000, changes in surface height over the 27 year period were calculated over the Bagley Ice Valley. Above its ELA, the Bagley Ice Valley thickened by an average of 10 m (+/- 7 m) (Muskett et al. 2003). However, the

Bagley Ice Valley is significantly different than the Kaskawulsh Glacier because it feeds the Bering Glacier which is known to surge. Therefore the thickening may be a result of glacier dynamics rather than a result of climatic perturbation. The Hubbard Glacier, which shares an accumulation zone with the Kaskawulsh Glacier also underwent increases in surface elevation between 2003 and 2007 (Figure 4.4). This glacier increased in elevation at a rate of 0.78 m yr^{-1} we (+/- 0.11 m yr^{-1} we) (Arendt et al. 2008). This is extremely similar to the measured rate of surface height increase on the Kaskawulsh Glacier of 0.72 m yr^{-1} we between 2000 and 2007. The close agreement between these two studies gives good confidence in the patterns observed for the area.

Stability in the accumulation zone combined with prominent thinning in the ablation zone and terminus retreat indicates a steepening profile for the Kaskawulsh Glacier (Figure 4.5). This steepening trend would be expected to accelerate ice motion until the glacier approaches a new equilibrium state (Hooke 1995; Larsen et al. 2007). A study of ice velocities on the Kaskawulsh Glacier would be an interesting avenue for future research.

Satellite images from September 3, 2007 show a sharp boundary between bare ice and snow. The snow line is located at ~1954 m (Figure 4.6) which is comparable to the long-term ELA of 1989 m, as well as the estimated ELA for the period of 1961-1969 of between 1950 m and 2000 m (Denton and Stuiver 1969; Macpherson and Krouse 1969; Wagner 1969). This type of snow line is indicative of a period of increased accumulation after several years of negative balance (Paterson 1994), and therefore corroborates the findings of thinning from 1977-2000 followed by large amounts of net accumulation in recent years. This pattern may also be reflective of the increase in accumulation of 0.12 m $decade^{-1}$ (Moore et al. 2002) recorded at high elevations on Mount Logan, although this trend was indicated by a core sampled at a greater elevation than the Kaskawulsh Glacier accumulation zone. Thickening of the Kaskawulsh Glacier must not, however, be considered indicative of overall trends in the Yukon/Alaska region, as regionalization of trends based on measurements from a single glacier can lead to large errors (Arendt et al. 2006; Arendt et al. 2008). Differences in maximum thickness, mass balance, area-altitude distribution, orientation, slope, thermal conditions, rate of terminus melting and distance from the coast will all influence the reaction of a given glacier to a perturbation in climate (Arendt et al. 2002; Kulkarni et al. 2007).

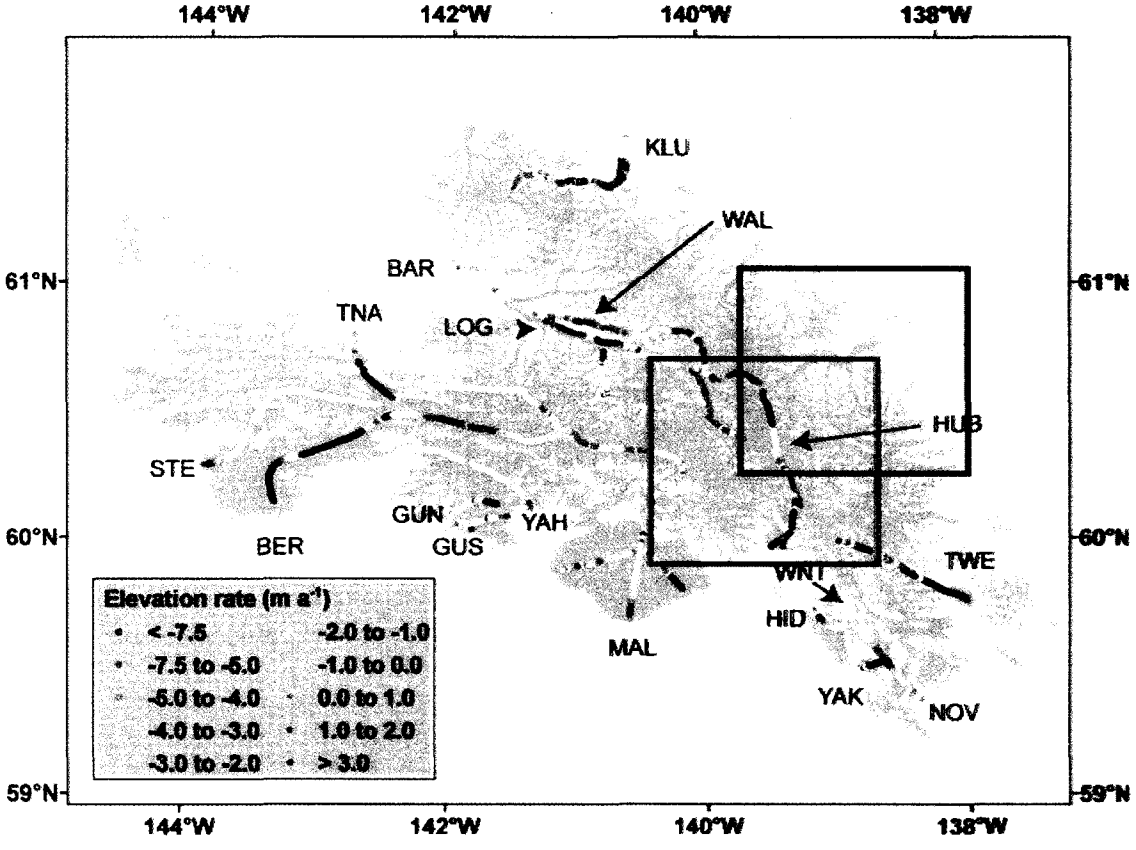

Figure 4.4: Rate of thickness changes of glaciers in the St. Elias Mountains (2003-2007). The green box indicates the location of the Hubbard Glacier. The red box shows the location of the Kaskawulsh Glacier.
Source: Arendt et al. 2008

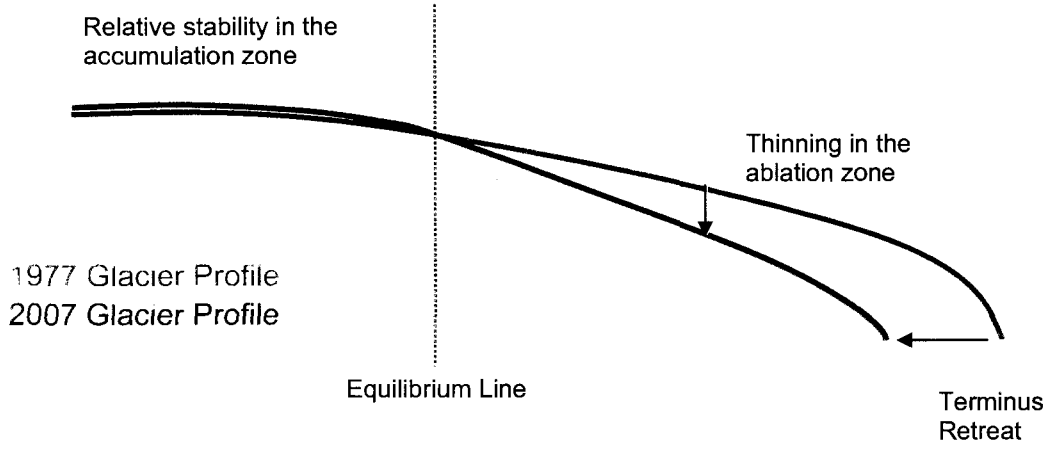

Figure 4.5: Schematic diagram of the steepening profile of the Kaskawulsh Glacier over time

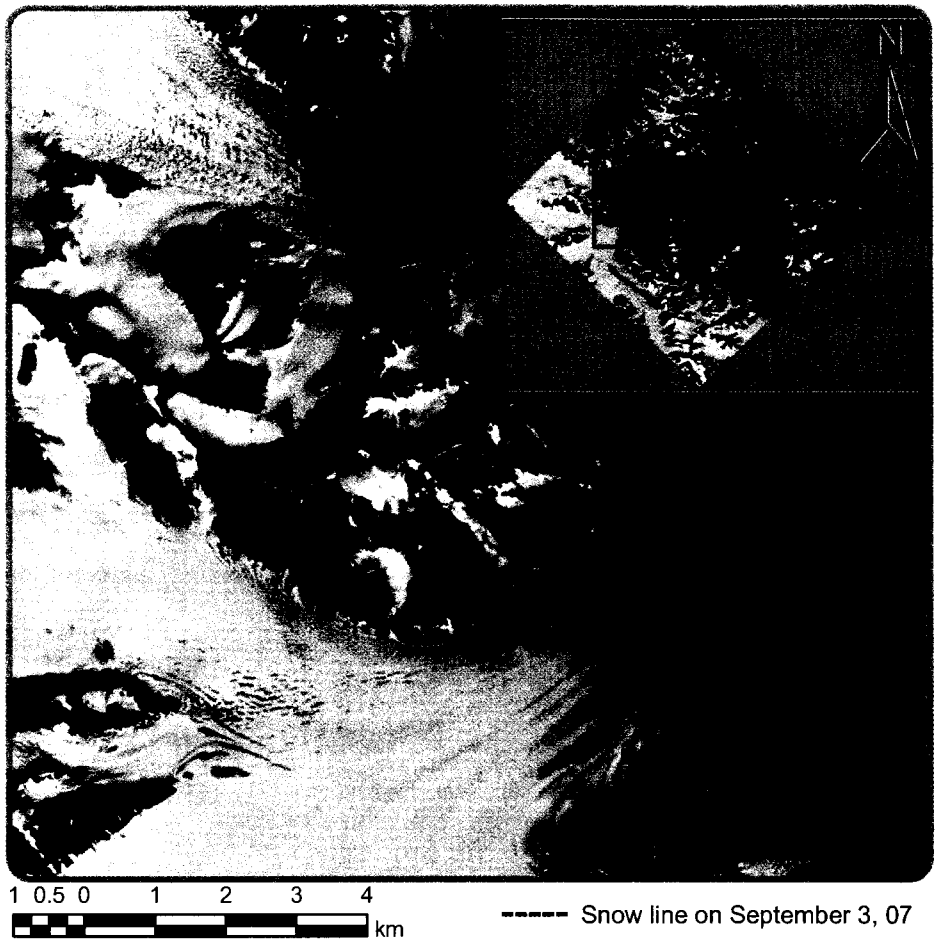

Figure 4.6: Sharp boundary between snow and bare ice on September 3, 2007 (1954 m asl) displayed over the 2007 SPOT-5 image

4.4 Sources of Error

The largest source of error in this study likely arises from not accounting for differential thinning across the width of the glacier arm. This may have caused an overestimate of thinning by up to 1-3 m yr^{-1} along the glacier margins (Arendt et al. 2008; Echelmeyer et al. 1996). Thus volume changes for each period may be artificially large. Data limitations which prevent data extrapolation across the middle section of the glacier for the period 2000-2007 mean that accurate quantification of the error incurred by ignoring differential thinning/thickening across the width of the glacier is not possible. Taking the sum of the ice volume changes for the periods 1977-1995, 1995-2000 and 2000-2007 (all of which use the centre profile of the glacier to calculate average thickness change) yields a number very similar to the volume change measured from 1977-2007 directly using a profile that samples a broad swath encompassing both central portions and marginal portions of the glacier's trunk (2.76 km^3 we vs. 4.60 km^3 we). The similarity between these values shows that the long-term patterns measured are real, and that the intermittent patterns measured along the centre-line of the glacier display reasonable accuracy as well. Future studies of change in glacier volume should nonetheless use a scanning laser altimeter to minimize the errors associated with differential thinning across the glacier width.

4.5 Areal Changes

Areal changes of the Kaskawulsh Glacier are also quantified for 1977 to 2007. In 1977, the total area of the glacier was 1111.8 km^2. By 2001, the area had decreased to 1069.2 km^2. Due to large height increases in the accumulation area between 2001 and 2007, the glacier area in 2007 increased to 1086.6 km^2. Thus, over the 30-year period the glacier lost 2.27% of its area.

Furthermore, the length of the glacier has changed over time. Between 1956 and 2007, an average retreat of 655 m was calculated. The rate of retreat was variable in time, although only one brief period of readvance occurred between 1986 and 1990. Much of the glacier retreat was accommodated by expansion of terminal lakes. Continued terminus retreat could result in the Slims River being pirated by the Kaskawulsh River and a subsequent decrease in the level of Kluane Lake of ~2 m will likely ensue (Bostock 1969;

Brahney et al. 2008a; Brahney et al. 2008b; Bryan 1972; Clague et al. 2006). For this to occur, the terminus of the glacier would have to retreat to the junction of the Kaskawulsh and Slims Rivers, which lies just south of the hill which divides the terminus lobes (Brahney et al 2008a; Bryan 1972) (Figure 4.7). The timing of this hydrological change cannot be determined because the rate of retreat of the Kaskawulsh Glacier fluctuates variably in response to changes in its mass balance. For this reason the glacier displays periodic readvances, such as the one that occurred between 1986 and 1990. One such periodic readvance may be expected in the near future as a response to the recent increases in volume to the accumulation zone (2000-2007).

Finally, because there is a time-lag between a change in volume and response at the glacier terminus a scaling ratio between terminus retreat and volume change cannot be established. The exact time-lag is unknown, although most glaciers in the region have a response time of >40 years (Arendt et al. 2002). A scaling ratio may exist between changes in area and changes in glacier volume, but more data obtained from future altimetric studies would be required to determine this definitively.

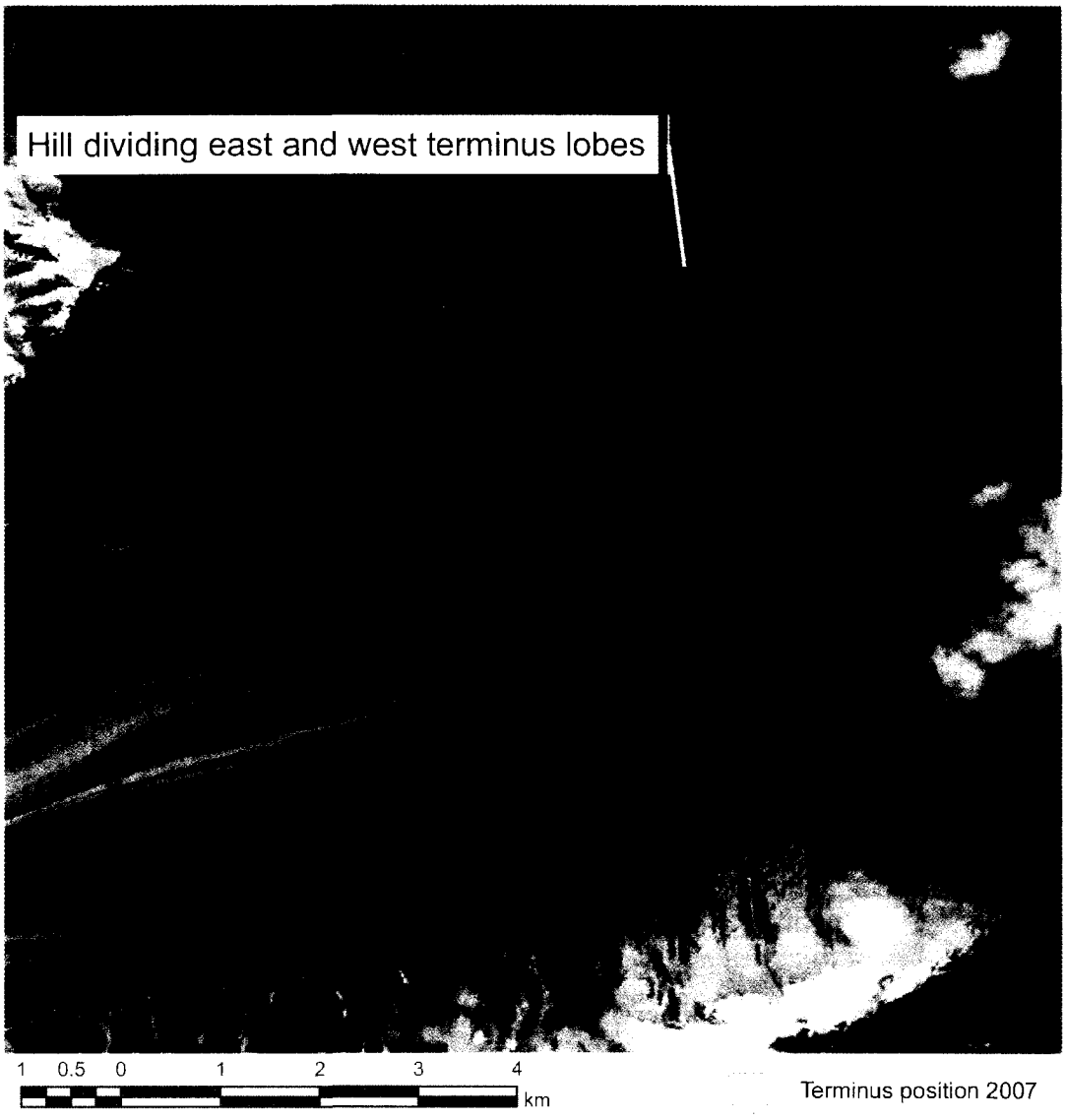

Figure 4.7: Location of hill separating the east and west lobe of the Kaskawulsh Glacier which acts as a critical junction maintaining the current drainage pattern. The location of the 2007 terminus position is indicated overlain on a 2003 ASTER image of the glacier.

5.0 References

Abdalati, W., Drabill, W., Frederick, E., Manizade, S., Martin, C., Sonntag, J., Swift, R., Thomas, R., Yungel, J., and Koerner, R. (2004) Elevation changes of ice caps in the Canadian Arctic Archipelago, Journal of Geophysical Research, 109, F04007, doi: 10.1029/2003JF000045.

ACIA (2004). Impacts of a Warming Arctic- Arctic Climate Impact Assessment, Cambridge, UK: Cambridge University Press, pp.144.

Aguado, E. and Burt, J.E. (2004) Understanding Weather & Climate. Upper Saddle River, New Jersey: Pearson Education, Inc.

Anderson, L., Abbot, M.B., Finney, B.P., and Burns, S.J. (2005) Regional atmospheric circulation change in the North Pacific during the Holocene inferred from lacustrine carbonate oxygen isotopes, Yukon Territory, Canada, Quaternary Research, 64, 21-35.

Alford, D. and Keeler, C. (1969) Stratigraphic studies of the winter snow layer Mount Logan, Saint Elias Range. In V.C. Bushnell & R.H. Ragle (Eds.), Icefield Ranges Research Project; Scientific Results (v. 2) (pp. 37-42). Montreal: Arctic Institute of North America.

Arendt, A., Echelmeyer, K.A., Harrison, W.D., Lingle, C.S., and Valentine, V.B. (2002) Rapid wastage of Alaska glaciers and their contribution to rising sea level, Science, 297 (5580), 382-387.

Arendt, A., Echelmeyer, K., Harrison, W., Lingle, C., Zirnheld, S., Valentine, V., Ritchie, B., and Druckenmiller, M. (2006) Updated estimates of glacier volume changes in the western Chugach Mountains, Alaska, and a comparison of regional extrapolation methods, Journal of Geophysical Research, 111, F03019, doi:10.1029/2005JF00436.

Arendt, A.A., Luthcke, S.B., Larsen, C.F., Abdalati, W., Krabill, W.B., and Beedle, M.J. (2008) Validation of high-resolution GRACE mascon estimates of glacier mass changes in the St. Elias Mountains, Alaska, USA, using aircraft laser altimetry, Journal of Glaciology, 54 (188), 778-786.

Bahr, D.B., Meier, M.F., and Peckham, S.D. (1997) The physical basis of glacier volume-area scaling, Journal of Geophysical Research,102 (B9), 20,355-20,362.

Bamber, J., Krabill, W., Raper, V., and Dowdeswell, J. (2004) Anomalous recent growth of part of a large Arctic ice cap: Austfonna, Svalbard, Geopysical Research Letters, 31, L12402, doi:10.1029/2004GL019667.

Benjey, W. (1969) Upper-air wind patterns in the St. Elias Mountains summer 1965. In V.C. Bushnell & R.H. Ragle (Eds.), Icefield Ranges Research Project; Scientific Results (v. 2) (pp. 3-15). Montreal: Arctic Institute of North America.

Berger, A.L., Spotila, J.A., Chapman, J.B., Pavlis, T.L., Enkelmann, E., Ruppert, N.A., Buscher, J.T. (2008) Architecture, kinematics, and exhumation of a convergent orogenic wedge: A thermochronological investigation of tectonic-climatic interactions within the central St. Elias orogen, Alaska, Earth and Planetary Science Letters, 270, 13-24.

Borns, H.W. and Goldthwait, R.P. (1966) Late-pleistocene fluctuations of Kaskawulsh Glacier, SW Yukon Territory, Canada. American Journal of Science, 264, 600-619

Bostock, H.S. (1969) Kluane Lake: Its drainage and allied problems. In V.C. Bushnell and R.H.Ragle (Eds.) Icefield Ranges Research Project Scientific Results (v.1), pp. 149-160, Montreal: Arctic Institute of North America.

Brahney, J., Clague, J.J., Menounos, B. and Edwards, T.W.D. (2008a) Geochemical reconstruction of late Holocene drainage and mixing in Kluane Lake, Yukon Territory, Journal of Paleolimnology, 40, 489-505.

Brahney, J., Clague, J.J., Menounos, B. and Edwards, T.W.D. (2008b) Timing and cause of water level fluctuations in Kluane Lake, Yukon Territory, over the past 5000 years, Quaternary Research, 70, 213-227.

Bryan, M.L. (1972) Variations in quality and quantity of Slims river water, Yukon Territory, Canadian Journal of Earth Sciences, 9, 1469- 1478.

Carter, B., Shrestha, R., and Slatton, C. (2007) Geodetic laser scanning. Physics Today, 60 (12), 41-47.

Chen, J.L., Tapley, B.D., Wilson, C.R. (2006a) Alaskan mountain glacial melting observed by satellite gravimetry, Earth and Planetary Science Letters, 248, 368-378.

Chen, J.L., Wilson, C.R., and Tapley, B.D. (2006b) Satellite Gravity measurements confirm accelerated melting of Greenland Ice Sheet, Science, 313, 1958-1960.

Chinn, T.J. (1999) New Zealand glacier response to climage change of the past 2 decades, Global and Planetary Change, 22, 155-168.

Chinn, T.J., Winkler, S., Salinger, M.J., and Haakensen, N. (2005) Recent glacier advances in Norway and New Zealand: a comparison of their glaciological and meteorological causes, Geofrasika Annaler, 87, 141-157.

Clague, J.J., Luckman, B.H., Van Dorp, R.D., Gilbert, R., Froese, D., Jensen, B.J.L., and Reyes, A.V. (2006) Rapid changes in the level of Kluane Lake in Yukon Territory over the last millennium, Quaternary Research, 66, 342-355.

Clarke, G.K.C. (1969) Geophysical measurements on the Kaskawulsh and Hubbard Glaciers. In V.C. Bushnell & R.H. Ragle (Eds.), Icefield Ranges Research Project; Scientific Results (v. 1) (pp. 89-106). Montreal: Arctic Institute of North America.

Danby, R.K., Hik, D.S., Slocombe, D. S., and Williams, A. (2003).
Science and the St Elias: an evolving framework for sustainability in North America's highest mountains. The Geographical Journal, 169 (3), 191-204.

Davis, C.H., Li, Y., McConnell, J.R., Frey, M.M., and Hanna, E. (2005) Snowfall-driven growth in East Antarctic ice sheet mitigates recent sea-level rise, Science, 308, 1898-1901.

Denton, G.H. and Stuiver, M. (1969) Late Pleistocene glacial stratigraphy and chronology, northeastern St. Elias Mountians. In V.C. Bushnell and R.H. Ragle (Eds.) Icefield Ranges Research Project Scientific Results (v.1) pp.197-217, Montreal: Arctic Institute of North America.

Dewart, G. (1969a) Moulins on Kaskawulsh Glacier. In V.C. Bushnell and R.H.Ragle (Eds.) Icefield Ranges Research Project Scientific Results (v.1) pp.145-146, Montreal: Arctic Institute of North America.

Dewart, G. (1969b) Seismic investigation of ice properties and bedrock topography at the confluence of the north and central arms of the Kaskawulsh Glacier. In V.C. Bushnell & R.H. Ragle (Eds.), Icefield Ranges Research Project; Scientific Results (v. 2) (pp. 77-102) Montreal: Arctic Institute of North America.

Dyurgerov, M.B. (2002) Glacier Mass Balance and Regime: Data of Measurements and Analysis, INSTAAR Occasional Paper 55: University of Colorado.

Echelmeyer, K.A., Harrison, W.D., Larsen, C.F., Sapiano, J., Mitchell, J.E., DeMallie, J., Rabus, B., Adalgeirsdottir, G. and Sombardier, L. (1996) Airborne surface profiling of glaciers: a case-study in Alaska. Journal of Glaciology, 42, 538-547.

Environment Canada (2009a) Canadian Climate Normals 1971-2000: Burwash A, Yukon Territory. http://www.climate.weatheroffice.ec.gc.ca/climate_normals (electronic resource) Accessed: February 26 2009.

Environment Canada (2009b) Climate Trends and Variations Bulletin. http://www.msc-smc.ec.gc.ca/ccrm/bulletin/annual08/national_e.cfm (electronic resource) Accessed: February 26 2009.

Etzelmüller, B. (2000) On the quantification of surface changes using grid-based digital elevation models (DEMs). Transactions in GIS, 4 (2), 129-143.

Ewing, K., Loomis, S., and Lougeay, R. (1969) Water-spout on Kaskawulsh Glacier. In V.C. Bushnell and R.H.Ragle (Eds.) Icefield Ranges Research Project Scientific Results (v.1) pp.147-148, Montreal: Arctic Institute of North America.

Fujisada, H., Bailey, G.B., Kelly, G.G., Hara, S., and Abrams M.J. (2005) ASTER DEM performance. IEEE Transactions on Geoscience and Remote Sensing, 43 (12), 2707- 2714.

Grew, E. and Mellor, M. (1969) High snowfields of the St. Elias Mountains. In V.C. Bushnell & R.H. Ragle (Eds.), Icefield Ranges Research Project; Scientific Results (v. 1) (pp. 75-87). Montreal: Arctic Institute of North America.

Hartmann, B., and Wendler, G. (2005) The significance of the 1976 Pacific climate shift in the climatology of Alaska. Journal of Climate, 18, 4824-4839.

Havens, J.M and Saarela, D.E. (1969) Exploration meteorology in the St. Elias Mountains. In V.C. Bushnell and R.H.Ragle (Eds.) Icefield Ranges Research Project Scientific Results (v.1) pp.17-22, Montreal: Arctic Institute of North America.

Hewitt, K. (2005) The Karakoram Anomaly? Glacier expansion and the 'elevation effect', Karakoram Himalaya, Mountain Research and Development, 25 (4), 332-340.

Hooke, R.B. (2005) Principles of Glacier Mechanics (2nd ed.). Cambridge: Cambridge University Press.

Hooker, B.L., and Fitzharris, B.B. (1999) The correlation between climatic parameters and the retreat and advance of Franz Josef Glacier, New Zealand, Global and Planetary Change, 22, 39-48.

Hopkinson, C., Demuth, M, Sitar, M, and Chasmer, L. (2001) Applications of airborne LiDAR mapping in glacierized mountainous terrain. International Geoscience and Remote Sensing Symposium, 2, 949-951.

IPCC (2007) Climate Change 2007: The Physical Science Basis. Contribution of Working Group I to the Fourth Assessment Report of the Intergovernmental Panel on Climate Change [Solomon, S., D. Qin, M. Manning, Z. Chen, M. Marquis, K.B. Averyt, M. Tignor and H.L. Miller (eds.)]. Cambridge UK and New York NY, USA: Cambridge University Press, pp. 996.

Johannessen, O.M., Khvorostovsky, K., Miles, M.W., and Bobylev, L.P. (2005) Recent ice-sheet growth in the interior of Greenland, Science, 310, 1013-1016.

Johnson, P. (1985) Implications of Holocene palaeoclimatic changes for the glacier hydrology of the Southwest Yukon. Zeitschrift fur Gletscherkunde und glazialgeologie, 21, 165-174.

Johnson, P. (1986) Holocene paleohydrology of the St. Elias Mountains, British Columbia and Yukon, Geographie physique et Quaternaire, 40 (1), 47-53.
Kääb, A. (2002) Monitoring high-mountain terrain deformation from repeated air- and spaceborne optical data: examples using digital aerial imagery and ASTER data. ISPRS Journal of Photogrammetry & Remote Sensing, 57, 39-52.

Kaser, G., Cogley, J.G., Dyurgerov, M.B., Meier, M.F., and Ohmura, A. (2006) Mass balance of glaciers and ice caps: Consensus estimates for 1961-2004, Geophysical Research Letters, 33, L19501, doi: 10.1029/2006GL027511.

Keeler, C.M. (1969) Snow accumulation on Mount Logan. In V.C. Bushnell and R.H.Ragle (Eds.) Icefield Ranges Research Project Scientific Results (v.2) pp. 33-36, Montreal: Arctic Institute of North America.

King, M., Moore, P., and Lavallee, D. (2006) Choice of optimal averaging radii for temporal GRACE gravity solutions, a comparison with GPS and satellite altimetry. Geophysical Journal International, 166, 1-11.

Kulkarni, A.V., Bahuguna, I.M., Rathore, B.P., Singh, S.K., Randhawa, S.S., Sood, R.K., and Dhar, S. (2007) Glacial retreat in Himalaya using Indian remote sensing satellite data. Current Science, 92 (1), 69-74.

Larsen, C.F., Motyka, R.J., Arendt, A.A., Echelmeyer, K.A., and Geissler, P.E. (2007) Glacier changes in southeast Alaska and northwest British Columbia and contribution to sea level rise. Journal of Geophysical Research, 112, F01007,doi:10.1029/2006JF000586.

Larsen, C.F., Motyka, R.J., Freymueller, J.T., Echelmeyer, K.A. and Ivins, E.R. (2005) Rapid viscoelastic uplift in southeast Alaska caused by post-Little Ice Age glacial retreat. Earth and Planetary Science Letters, 237, 548-560.

Lipovsky, P.S., Evans, S.G., Clague, J.J., Hopkinson, C., Couture, R., Brobowsky, P., Ekström, G., Demuth, M.N., Delaney, K.B., Roberts, N.J., Clarke, G., and Schaeffer, A. (2008) The July 2007 rock and ice avalanches at Mount Steele, St. Elias Mountains, Yukon, Canada. Landslides, 5, 445-455.

Luthcke, S.B., Arendt, A.A., Rowlands, D.D. McCarthy, J.J., and Larsen, C.F. (2008a) Recent glacier mass changes in the Gulf of Alaska region from GRACE mascon solutions. Journal of Glaciology, 54 (188), 767-777.

Luthcke, S.B., Zwally, H.J., Abdalati, W, Rowlands, D.D. Ray, R.D., Nerem, R.S., Lemoine, F.G., McCarthy, J.J., and Chinn, D.S. (2006) Recent Greenland ice mass loss by drainage system from satellite gravity observations, Science, 314, 1286-1289.

Macpherson, D.S. and Krouse, H.R. (1969) O^{18}/O^{16} Ratios in snow and ice of the Hubbard and Kaskawulsh Glaciers. In V.C. Bushnell and R.H.Ragle (Eds.) Icefield Ranges Research Project Scientific Results (v.1), pp. 63-73, Montreal: Arctic Institute of North America.

Marcus, M.G., and Ragle, R.H. (1970). Snow accumulation in the Icefield Ranges, St. Elias Mountains, Yukon. Arctic and Alpine Research, 2 (4), 277-292.

Meier, M.F., and Dyurgerov, M.B. (2002) How Alaska affects the world. Science, 297 (5580), 350-351.

Meier, M.F., Dyurgerov, M.B., Rick, U.K., O'Neel, S., Pfeffer, W.T., Anderson, R.S., Anderson, S.P., and Glazovsky, A.F. (2007) Glaciers dominate eustatic sea-level rise in the 21st century. Science, 317 (1064), doi:10.1126/science.1143906.

Meigs, A., and Sauber, J. (2000). Southern Alaska as an example of the long-term consequences of mountain building under the influence of glaciers. Quaternary Science Reviews,19, 1543-1562.

Molnia, B.F. (2007) Late nineteenth to early twenty-first century behaviour of Alaskan glaciers as indicators of changing regional climate, Global and Planetary Change, 56, 23-56.

Moore, G.W.K., Holdsworth, G., and Alverson, K. (2001) Extra-tropical response to ENSO as expressed in an ice core from the Saint Elias Mountain Range. Geophysical Research Letters, 28 (18), 3457-3460.

Moore, G.W.K., Holdsworth, G., and Alverson, K. (2002) Climate change in the North Pacific region over the past three centuries, Nature, 420, 401-403.

Muskett, R.R., Lingle, C.S., Sauber, J.M., Rabus, B.T., and Tangborn, W.V. (2008) Acceleration of surface lowering on the tidewater glaciers of Icy Bay, Alaska, U.S.A. from InSAR DEMs and ICESat altimetry. Earth and Planetary Science Letters, 265, 345-359.

Muskett, R.R., Lingle, C.S. Tangborn, W.V., Rabus, B.T. (2003) Multi-decadal elevation changes on Bagley Ice Valley and Malaspina Glacier, Alaska. Geophysical Research Letters, 30 (16), 1857, doi:10.1029/2003GL017707.

Nesje, A., Lie, Ø., and Dahl, S.O. (2000) Is the North Atlantic Oscillation reflected in Scandinavian glacier mass balance records? Journal of Quaternary Science, 15 (6), 587-601.

Paterson, W.S.B. (1994). The Physics of Glaciers (3rd ed.).Tarrytown, New York: Pergamon.

Reyes, A.V., Luckman, B.H., Smith, D.J., Clague, J.J., and Van Dorp, R.D. (2006) Tree-ring dates for the maximum Little Ice Age advance of Kaskawulsh Glacier, St. Elias Mountains, Canada, Arctic, 59 (1), 14-20.

Sapiano, J.J., Harrison, W.D., and Echelmeyer.K.A. (1998) Elevation, volume and terminus changes of nine glaciers in North America. Journal of Glaciology, 44 (146), 199-135.

Sauber, J.M., and Molnia, B.F. (2004) Glacier ice mass fluctuations and fault instability in tectonically active Southern Alaska. Global and Planetary Change,42, 279-292.

Sheaf, M.A., Serpa, L., and Pavlis, T.L. (2003) Exhumation rates in the St. Elias Mountains, Alaska. Tectonophysics, 367, 1-11.

Spotila, J.A., Buscher, J.T., Meigs, A.J., Reiners, P.W. (2004) Long-term glacial erosion of active mountain belts: Example of the Chugach-St Elias Range, Alaska. Geology, 32 (6), 501-504.

Swenson, S. and Whar, J. (2002) Methods for inferring regional surface-mass anomalies from Gravity Recovery and Climate Experiment (Grace) measurements of time-variable gravity. Journal of Geophysical Research, 107 (B9) doi:10.1029/2001JB000576

Taylor-Barge, B. (1969) The summer climate of the St. Elias Mountains Region. In V.C. Bushnell and R.H. Ragle (Eds.), Icefield Ranges Research Project; Scientific Results (v.1) (pp. 33- 49). Montreal: Arctic Institute of North America.

Toutin, T. (2008) ASTER DEMs for geomatic and geoscientific applications: a review. International Journal of Remote Sensing, 29 (7), 1855-1875.

Wagner, W.P. (1969) Snow facies and stratigraphy on the Kaskawulsh Glacier. In V.C. Bushnell & R.H. Ragle (Eds.), Icefield Ranges Research Project; Scientific Results (v. 1) (pp. 55-62). Montreal: Arctic Institute of North America.

Wake, P.C., Yalcin, K., and Gundestrup, N.S. (2002) The climate signal recorded in the oxygen-isotope, accumulation and major-ion time series from the Eclipse ice core, Yukon Territory, Canada. Annals of Glaciology, 35, 416-422.

Ward, B.C., Bond, J.D., and Gosse, J.C. (2007) Evidence for a 55-50 ka (early Wisconsin) glaciation of the Cordilleran ice sheet, Yukon Territory, Canada. Quaternary Research , 68, 141-150.

Wiles, G.C., Jacoby, G.C., Davi, N.K., and McAllister, R.P. (2002) Late Holocene glacier fluctuations in the Wrangell Mountains, Alaska. Bulletin of the Geological Society of America, 114 (7), 896-908.

Yalcin, K. and Wake, C.P. (2001). Anthropogenic signals recorded in an ice core from Eclipse Icefield, Yukon Territory, Canada. Geophysical Research Letters, 28(23), 4487-4490.

Yalcin, K., Wake, C.P., Kreutz, K.J., Germani, M.S., and Whitlow, S.I. (2007) Ice core paleovolcanic records from the St. Elias Mountains, Yukon, Canada. Journal of Geophysical Research, 112, D08102, doi:10.1029/2006JD007497